

---

Theses and Dissertations

---

Spring 2018

## Photochemical transformations of dichloroacetamide safeners

Andrew Kral  
*University of Iowa*

Follow this and additional works at: <https://ir.uiowa.edu/etd>



Part of the [Civil and Environmental Engineering Commons](#)

Copyright © 2018 Andrew Kral

This thesis is available at Iowa Research Online: <https://ir.uiowa.edu/etd/6164>

---

### Recommended Citation

Kral, Andrew. "Photochemical transformations of dichloroacetamide safeners." MS (Master of Science) thesis, University of Iowa, 2018.

<https://doi.org/10.17077/etd.f5ku19pc>

---

Follow this and additional works at: <https://ir.uiowa.edu/etd>



Part of the [Civil and Environmental Engineering Commons](#)

PHOTOCHEMICAL TRANSFORMATIONS OF DICHLOROACETAMIDE  
SAFENERS

by

Andrew Kral

A thesis submitted in partial fulfillment  
of the requirements for the Master of Science  
degree in Civil and Environmental Engineering in the  
Graduate College of  
The University of Iowa

May 2018

Thesis Supervisor: Associate Professor David Cwiertny

Copyright by

Andrew Kral

2018

All Rights Reserved

Graduate College  
The University of Iowa  
Iowa City, Iowa

CERTIFICATE OF APPROVAL

---

MASTER'S THESIS

---

This is to certify that the Master's thesis of

Andrew Kral

has been approved by the Examining Committee for  
the thesis requirement for the Master of Science degree  
in Civil and Environmental Engineering at the May 2018 graduation.

Thesis Committee:

\_\_\_\_\_  
David Cwiertny, Thesis Supervisor

\_\_\_\_\_  
Greg LeFevre

\_\_\_\_\_  
Hans-Joachim Lehmler

## **Acknowledgements**

I'd like to thank my advisor, David Cwiertny, for his invaluable help in completing this project. I'd also like to thank all past and present members of the Cwiertny lab—especially Nick Pflug and Monica McFadden—for their incredible help conducting experiments and analyzing data.

## Abstract

Safeners are widely used ingredients in commercial herbicide formulations, but their environmental fate has garnered relatively little scrutiny because of their classification as “inert” by the US EPA. Here, we investigated the photolysis of one popular class of safeners, dichloroacetamides, to better understand their persistence and formation potential for bioactive transformation products in surface waters. Of four commonly used dichloroacetamide safeners only benoxacor underwent direct photolysis under simulated natural sunlight ( $\lambda > 305$  nm). Benoxacor had a half-life of  $\sim 8$  min and produced several more polar photoproducts when irradiated under environmentally relevant conditions (pH 5-9), thus direct photolysis will likely be an important fate pathway for benoxacor in surface waters. Other dichloroacetamide safeners AD-67, dichlormid, and furilazole, were resistant to direct photolysis at  $\lambda > 305$  nm but were slowly degraded during indirect photolysis in the presence of common photosensitizers generating ROS (e.g., humic acid, nitrate). These three safeners also photolyzed under  $\lambda > 250$  nm—commonly applied during UV disinfection of drinking water—to generate new photoproducts. Where possible, we identified photoproducts using NMR and high-resolution mass spectrometry. Only benoxacor photolysis yielded identifiable transformation products. These products were generally more polar and often dechlorinated suggesting they are likely to have a bioactivity different to that of benoxacor. Overall, photolysis of safeners appears to be an important and previously unreported fate pathway for the widely used dichloroacetamide safeners.

## Public Abstract

In the United States, nearly a billion kilograms of commercial herbicide mixtures are applied to crops every year. Because herbicide mixtures are so extensively applied to our fields, chemicals from these mixtures can and do migrate from farmland to waterways. The release of these chemicals into waterways threatens plant, animal, and human life. Not only are these applied chemicals toxic, but they can react in the environment in ways which might produce more dangerous chemical compounds. The degradation of herbicides, which comprise the bulk of herbicide mixtures (~80%), has been extensively studied, but the degradation of other chemical ingredients in the commercial herbicide mixtures have not received much attention. One major ingredient in herbicide mixtures, dichloracetamides, also known as “safeners” has shown disconcerting evidence of degradation into more toxic, herbicide-like chemicals.

Safeners are mixed into herbicides to protect crops from the lethal effects herbicides have on target species (i.e., weeds). Safeners are not the main ingredient of herbicide formulas, and are therefore considered inert by the EPA. Because safeners have been labeled as inert, they receive minimal regulatory attention. Little has been done to understand how they interact in the environment despite having the same potential to react with unintended targets (e.g., plants, animals, humans) and undergo chemical changes in the environment as demonstrated by herbicides and countless other chemicals. Since herbicide mixtures are used so extensively, the total amount of safeners used per year in the United States is significant. Thus, understanding how these chemicals behave is critical.

## Table of Contents

List of Tables .....	viii
List of Figures .....	ix
Chapter 1 Introduction .....	1
1.1. Safeners: Widely Used but Overlooked.....	1
1.2. Current Literature: Environmental Fate of Safeners.....	6
1.2.1. Safener Adsorption and Aqueous Mobility .....	6
1.2.2. Safener Reduction on Iron Minerals .....	8
1.2.3. Safener Direct Photolysis.....	9
1.2.4. Safener Indirect Photolysis .....	11
1.3. Research Goals and Hypothesis.....	12
Chapter 2 Materials and Methods .....	19
2.1. Chemicals.....	19
2.2. Photolysis Experiments.....	20
2.2.1. Direct Photolysis Experiments.....	20
2.2.2. Quantum Yield.....	21
2.2.3. Indirect Photolysis Experiments .....	23
2.3.4. Photoproduct Identification .....	23
2.3. Analytical Methods.....	24



Chapter 3 Direct Photolysis of Benoxacor and Identification of Transformation	
Products.....	29
3.1. Introduction.....	29
3.2. Timescale for Benoxacor Direct Photolysis .....	31
3.3. Influence of Aquatic Matrix on Benoxacor Photolysis.....	34
3.4. The Role of Water in Photoproduct Formation .....	36
3.5. Long-Term Photolysis Experiments .....	38
3.6. Identifying Photoproducts.....	39
3.6.1. Identifying [PE] .....	39
3.6.2. Identifying [PA], [PB], and [PC] .....	42
3.6.3. Identifying [PD].....	44
3.6.4. Identifying [PF].....	44
3.7. Conclusions.....	47
Chapter 4 Photolysis of AD-67, Dichlormid, and Furilazole .....	75
4.1. Introduction.....	75
4.2. Safener Photolysis in the Presence of Dissolved Organic Matter.....	78
4.3. Safener Photolysis in Nitrite and Nitrate .....	79
4.4. UVC Photolysis of AD-67, Dichlormid, and Furilazole.....	81
4.5. Conclusions.....	82
Chapter 5 Conclusions .....	97

Literature Cited ..... 100

## List of Tables

Table 1 Dichloroacetamide safeners adjacent to the chloroacetamide herbicides and crops with which they are commercially mixed and applied.....	18
Table 2 HPLC solvent gradient.....	28
Table 3 Observed first order rate constants and half lives for benoxacor photolysis across pHs 5, 7, and 9. ....	73
Table 4 The table shows product ID and corresponding HPLC retention time and absorbance maxima for major products of benoxacor photolysis. ....	74
Table 5 First order rate constants and half-lives for indirect photolysis systems. ....	95
Table 6 Safener photolysis at $\lambda \geq 250$ nm and associated first order decay constants and half-lives.....	96

## List of Figures

Figure 1 Preliminary usage (lbs mile <sup>-2</sup> ) of the herbicides acetochlor and metolachlor in 2015.....	14
Figure 2 UV-Vis absorbance of four dichloroacetamide safeners plotted against solar irradiance.....	15
Figure 3 Occurrence of the commonly used dichloroacetamide safeners in select Iowa and Illinois creeks from Woodward et al.....	16
Figure 4 Reactions of benoxacor and dichlormid in Fe (II) amended goethite slurries. MB represents the chloroacetamide analogue of benoxacor reduction; CDAA, I, and II represent the chloroacetamide analogues of dichlormid reduction.....	17
Figure 5 Irradiance spectrum of 1000 W Newport Xe lamp equipped with 305 nm cut-on filter (a) and a SunTest CPS+ solar simulator at 750 W m <sup>-2</sup> output (b). Output over 300-400 nm is 8.81 x 10 <sup>-3</sup> W cm <sup>-2</sup> (a) and 1.26 x 10 <sup>-2</sup> W cm <sup>-2</sup> (b). ....	26
Figure 6 First order integrated rate laws for PNA-pyr actionmeter (R <sup>2</sup> = 0.999) and benoxacor in 5 mM pH 7 potassium phosphate buffer (R <sup>2</sup> = 0.999).....	27
Figure 7 Solid blue line shows UV-vis absorbance spectrum of benoxacor. Dashed line represents typical solar irradiance near sea-level. Maximum absorbance peaks were found at 216, 258, and 290 nm. ....	49
Figure 8 Benoxacor photolysis at pH 7 using simulated sunlight from a 1000 W Xe lamp ( $\lambda \geq 305$ nm; AM 1.5 filter; Irradiance: 8.81 x 10 <sup>-3</sup> W cm <sup>-2</sup> ). Benoxacor decay was modeled as a first order process, with exponential decay model fit shown (solid black line; $k_{obs}=0.093$ , R <sup>2</sup> = 0.9999). At a detection wavelength of 220 nm, three major photoproducts (defined as Products A, B, and C) and one minor product (Product E) were observed (where dashed lines are not model fits but simply shown to help illustrate the concentration profile of products over time).....	50
Figure 9 Absorbance spectra of benoxacor photoproducts.....	51

Figure 10 Benoxacor rate of decay shows little variance across pH 5 (10a), 7 (10b), and 9 (10c). However, at pH 9, product D (denoted by orange squares) has a significant peak area. ....	52
Figure 11 HPLC traces of benoxacor reactions mixtures after 15 min of photolysis at pH 7 (5a), 60 min of photolysis at pH 7 (5b), and 60 min of photolysis at pH 9 (5c) (monitored at 220 nm). ....	53
Figure 12 Conversion of benoxacor photoproducts at pH 5, 7, 9 and in acetonitrile. Product peaks at a given percent conversion are normalized to the initial benoxacor starting peak area. ....	54
Figure 13 Benoxacor photolyzed in Iowa City river water (pH = 8.5). Similar to benoxacor photolysis at pH 9, product D is a major product at pH 8.5. This figure shows benoxacor photolyzes the same way in environmentally as it does in simulated natural aquatic systems. ....	55
Figure 14 Integrated first-order rate of benoxacor photolysis in pH 7 buffer in 0, 10, and 100 uM metolachlor. ....	56
Figure 15 Benoxacor product yield plots in 0, 10, and 100 uM metolachlor. ....	57
Figure 16 500 uM benoxacor photolysis in acetonitrile for 60 minutes. Subsequently, a 2 mL aliquot is spiked into pH 7 buffer where photolysis continued. Products C, D, and E accumulate in acetonitrile, but when photolysis is continued in water product E (pink diamonds) decays and products A and B (red squares and green triangles, respectively) begin to accumulate. ....	58
Figure 17 100 uM benoxacor photolysis in acetonitrile for 60 minutes. Subsequently, a 2mL aliquot is spiked into 20 mL pH 7 buffer where the solution is placed in the dark and photolysis is stopped. Products C, D, and E are stable over this time period, as is the parent compound benoxacor. Formation of products A and B is not observed. ....	59
Figure 18 Plots show continued photolysis of acetonitrile aliquots in pH 5 and pH 9 buffer (photolysis in acetonitrile not shown). Product E (orange squares) continues to accumulate during pH 9 photolysis. It does not continue to accumulate during pH 5 photolysis, however it also does not decay. ....	60

Figure 19 PNA-pyr actinometer and benoxacor molar absorptivity compared to irradiance of 1000 W Xe lamp with 305 nm cut-on filter and AM 1.5 filter. Quantum yield was calculated between 300 and 400 nm.....	61
Figure 20 Long-term photolysis of benoxacor reveals [PA] and [PB] are directly photolyzed and a sixth and significantly less polar major product, [PF], begins to accumulate. ....	62
Figure 21 GC-MS spectrum of [PE]. ....	63
Figure 22 Mechanism for the formation of [PE] via benoxacor direct photolysis. ....	64
Figure 23 Proposed mechanism for photolysis of metolachlor under UV light [6]. ....	65
Figure 24 Proposed mechanism for photolysis of acetochlor under UV light [9]. ....	66
Figure 25 High resolution mass spectrum of [PA] obtained through LC-HRMS. ....	67
Figure 26 High resolution mass spectrum of [PB] obtained through LC-HRMS.....	68
Figure 27 High resolution mass spectrum of [PC] obtained through LC-HRMS.....	69
Figure 28 Proposed mechanism for the formation of [PA], [PB], and [PC] from benoxacor and intermediate [PE] via direct photolysis. ....	70
Figure 29 Formation of [PF] during long-term benoxacor photolysis.....	71
Figure 30 Direct injection high resolution mass spectrometry results for [PF]. Parent mass [M+H] <sup>+</sup> is shown at 178.1.....	72
Figure 31 Pathways for indirect photolysis, where <i>i</i> denotes the compound of interest (i.e., safener) and UC represents the photoactive compound. ....	84
Figure 32 Photolysis schemes for nitrite (above) and nitrate (below). ....	85

Figure 33 Indirect photolysis of safeners in 5 mg L <sup>-1</sup> SRHA (a) and 10 mg L <sup>-1</sup> PPHA (b) Observed first order rate constants and half-lives are shown in Table 5. ....	86
Figure 34 Yield plots for the product observed during furilazole indirect photolysis in NO <sub>2</sub> <sup>-</sup> (a), NO <sub>3</sub> <sup>-</sup> (b), PPHA (c), and SRHA (d).....	87
Figure 35 Indirect photolysis quenching experiments were used to eliminate ROS like <sup>1</sup> O <sub>2</sub> (azide) and •OH (isopropyl alcohol, or IPA) to probe their role in safener transformation. ....	88
Figure 36 Absorbance spectra for the products generated during furilazole and dichlormid indirect photolysis. ....	89
Figure 37 Safener photolysis in nitrite (a) and nitrate (b). Observed first order rate constants and half-lives are shown in Table 5. ....	90
Figure 38 Product conversion plots for indirect photolysis in nitrite of dichlormid photoproduct (a) and furilazole photoproduct (b).....	91
Figure 39 Safeners photolyzed by $\lambda \geq 250$ nm in pH 7 buffer free of photosensitizers. First order exponential decay constants, fits, and half-lives are shown below (see Table 6). ....	92
Figure 40 Formation of photoproducts during safeners photolysis at $\lambda \geq 250$ nm. While these products were observed via HPLC analysis, they were not observed during HR-ESI-TOFMS analysis.....	93
Figure 41 Proposed photolysis pathway of dichlormid by Abu-Qare et al. under 254 nm light. Dechlorination product is CDAA, a formerly used herbicide. ....	94

## Chapter 1 Introduction

### 1.1. Safeners: Widely Used but Overlooked

Every year, nearly one billion kilograms of commercial herbicide mixtures are applied to crops across the US in an effort to increase yields [1]. Because these potent chemical mixtures are employed so widely—in both total mass and area—they can and do migrate from farmlands to waterways [2]. Chronic and widespread release of chemicals from agricultural land to surface waters threatens plant, animal, and human life [1, 3, 4]. Not only are the applied mixtures harmful (e.g., glyphosate based herbicides are known to be endocrine disruptors in human cell lines at 0.5 ppm concentrations within 24 h [3]), but the chemical components can themselves react in the environment to produce new and potentially more harmful compounds than initially present [1, 5]. The degradation of herbicides, which comprise the bulk of commercial herbicide *formulations* (~80% by mass) and are considered “active” ingredients, has been extensively studied [6-9]. Yet, the degradation of other chemical ingredients in commercial herbicide formulations has not received much attention [1]. In commercial formulations, herbicides are mixed with any number of chemical additives such as safeners, co-solvents, surfactants, anti-foaming agents, preservatives, emulsifiers, antifreeze, dyes, etc. [10]. The environmental fate of these added compounds is often not well understood. Specifically, the additives known as safeners constitute a widely used class of herbicide ingredients; however, their environmental fate largely remains a mystery [1].

Safeners are mixed into commercial herbicides to protect crops (e.g., maize, rice) from the lethal effects of the active herbicide have on pests (e.g., weeds). They typically constitute 10-15% of the active ingredient's (i.e., the herbicide's) mass [1, 2]. Thus,



although safeners and other chemical additives are not the *main* ingredient of commercial herbicides, the environmental fate (i.e., transformation, degradation) of safeners and other components may be significant when considering the enormous scale on which these commercial formulations are used (Figure 1).

One class of commonly used safeners—dichloroacetamides—has shown disconcerting evidence of degradation into more toxic, herbicide-like chemicals [5, 11]. Dichloroacetamide safeners (Table 1) are added to herbicide formulations containing a chloroacetamide herbicide as the active ingredient. Structurally, dichloroacetamide safeners are very similar to their chloroacetamide herbicide co-formulates (see Table 1). The four most commonly used dichloroacetamide safeners are benoxacor, dichlormid, furilazole, and AD-67 (see Table 1). These safeners are generally pre-mixed in herbicides by manufacturers such as Dow Agro-Sciences (dichlormid), Monsanto (furilazole), and Syngenta (benoxacor) [1]. AD-67, generally used as a safener for pesticides applied to rice in China, is sold separately and is either mixed with the herbicide or pre-sprayed by the applicator [1]. Because safeners are added as one of many “inert” ingredients alongside the “active” herbicide in commercial formulations (which comprises the bulk of the herbicide formula), government and industry don’t specifically track commercial safener usage. Rather, active ingredients (i.e., herbicides) are generally monitored while inert ingredient information is not compiled, largely due to logistical considerations and a lack of enforcement in US code. Thus, annual usage for dichloroacetamide safeners must be estimated based on usage data for the active chloroacetamide herbicide (see Figure 1). As safeners typically are present at 10-15% of the active herbicide’s mass, we estimate safeners use likely exceeds  $2 \times 10^6$  kg year<sup>-1</sup> in the United States [1].

Dichloroacetamide safeners work by promoting transformation of herbicides *in vivo* through activation of the enzyme glutathione S-transferase [12]. The enzymatic transformation products have significantly less herbicidal activity than the parent herbicide; indeed, in most cases, the *in vivo* products' herbicidal activity is negligible [13]. In fact, the enzyme expression safeners elicit and the resulting protection offered by safeners is comparable to the herbicide protection found in genetically modified organism (GMO) phenotypes resistant to several classes of herbicides [14]. In most cases there is no comparable detoxification in common weed species, though the mechanisms of safeners in weeds are poorly understood and largely remain unstudied [15]. Thus, enzymatic detoxification of herbicides with dichloroacetamide safeners allows for selective protection of crops without diminishing the herbicide's effectiveness on weeds. Market forces show consumers' preference for non-GMO foods continues to increase [16], thus we anticipate the use of safeners is likely to increase beyond the current estimate of  $2 \times 10^6$  kg year<sup>-1</sup>.

Safeners have not undergone the same scrutiny from regulatory bodies as their chloroacetamide co-formulates. This is in large part due to language in section 2 of the Federal Insecticide, Fungicide, and Rodenticide Act (FIFRA) that differentiates between commercial herbicide ingredients and active herbicide agents. In FIFRA, active ingredients are defined as "an ingredient which will prevent, destroy, repel, or mitigate any pest" (e.g., chloroacetamide herbicides) [17]. Because dichloroacetamides intended use is directed toward crops and not pests, and because their use is not intended to mitigate or deter growth of pests (i.e., weeds), dichloroacetamides fall under FIFRA's definition of an "inert" ingredient: "an ingredient which is not active" [17]. Inert

ingredients are not evaluated under the stricter toxicological and environmental fate and effects protocols required for active ingredients prior to distribution, sale, and use of commercial herbicide formulas [17]. Interestingly, although the EPA does not review inert ingredients with the same scrutiny as active ingredients, they acknowledge “the term ‘inert’ is not intended to imply nontoxicity; the ingredient may or may not be chemically active” [18].

The EPA is still required to review some toxicological and environmental data regarding safeners under the Federal Food, Drug, and Cosmetic Act which requires that all pesticide chemical residues be identified as “safe,” or that “there is a reasonable certainty that no harm will result from aggregate exposure to the pesticide chemical residue, including all anticipated dietary exposures and all other exposures for which there is reliable information” [19]; however, such data is submitted by chemical manufacturers and is not required to undergo a comprehensive peer-review before submission. Thus, data reported to the EPA for inert ingredients is often insufficient [1]. For example, the data submitted for safeners only briefly mentions environmental transport of the chemical (e.g., soil and aqueous mobility) that could result in direct exposure and not transformation products [19]. Environmental fate and effects data submitted for the safener benoxacor (see Table 1) is not done in the presence of co-formulates and does not take into account that benoxacor can absorb light within the solar spectrum, opening the door for potential photolysis reactions (Figure 2) [1, 19].

In contrast to the available data for dichloroacetamide safeners, we know much more about the active chloroacetamide herbicide ingredients acetochlor and metolachlor. Metolachlor is highly mobile, and in a 1988 study it was detected in 2091 of 4161 surface

water samples across the United States [20]. In a 2000 study on surface waters in Iowa, metolachlor was the most commonly detected pesticide [21]. In addition, a USGS study found metolachlor degradates (e.g., metolachlor ethane sulfonic acid and metolachlor oxanilic acid) in 99.7 % and 94.3 % (respectively) of 355 water samples from 12 stream sites in Eastern Iowa [22]. Metolachlor is suspected to be moderately toxic to aquatic life with an average acute toxicity level of  $53 \mu\text{g L}^{-1}$  (specific acute toxicity levels are:  $106 \mu\text{g L}^{-1}$  (plants);  $3,103 \mu\text{g L}^{-1}$  (benthos);  $4,334 \mu\text{g L}^{-1}$  (fish)) [23]. Likewise, the herbicide acetochlor has demonstrated equally high aqueous solubility, especially in rain run-off after herbicide application [24] and has shown toxic effects on the earth worm species *Eisenia fetida* [25]. Given the structural similarities between chloroacetamide herbicides and dichloroacetamide safeners (see Table 1) and the available data on the environmental fate and effects of chloroacetamide herbicides, there appears to be a significant gap in knowledge about the fate of the analogous dichloroacetamide safeners to their chloroacetamide herbicide counterparts.

Indeed, the classification of dichloroacetamide safeners as inert has caused the environmental fate of these widely used agrochemicals (more than  $2 \times 10^6 \text{ kg year}^{-1}$  in the US) to be largely overlooked by regulatory bodies and researchers [1]. Although the remedial effects of safeners against herbicides are well defined in the literature, little is known about safeners' environmental fate and effects. Currently, there exist only two peer reviewed studies that explore potential environmental transformation of safeners [5, 11]—one of which actually focuses on the active herbicide S-ethyl-N, N-dipropylthiocarbamate (EPTC) [11].

Interestingly, the limited work in the peer-reviewed literature suggests that safeners might not be as “inert” as they seem [1, 5, 11]. For the most part, chloroacetamides are structurally similar to their dichloroacetamide counterparts. Notably, however, chloroacetamides have only one geminal chlorine atom whereas dichloroacetamides have two geminal chlorines (see Table 1). The number of chlorine atoms has major implications for the very different biological roles of these compounds and the potential environmental fate of safeners. The difference in number of chlorine atoms also implies that safeners would not have to undergo much structural change (i.e., loss of one chlorine atom) to potentially impart comparable herbicidal and toxicological properties of their chloroacetamide counterparts [1, 5]. Thus, through naturally occurring environmental processes (e.g., photolysis or biotransformation) safeners could transform in such a way that their degradation products would exhibit a very different bioactivity than the parent compound. From a regulatory perspective, dichloroacetamide safeners could be changing from “inert” to “active.”

## 1.2. Current Literature: Environmental Fate of Safeners

### 1.2.1. Safener Adsorption and Aqueous Mobility

According to industry studies, safeners will likely be present in agricultural runoff and surface waters because they are very mobile in a variety of soils. Reports from Monsanto and Imperial Chemical Industries suggest furilazole and dichlormid (see Table 1) only weakly adsorb to soils with  $K_{ads} = 0.79 — 3.5 \text{ mL g}^{-1}$  and  $K_{ads} = 0.25 — 0.65 \text{ mL g}^{-1}$  respectively (on loamy sand, loam, silty clay loam, and clay soils), with adsorption increasing as clay content and cation exchange capacity of the soil increases [26, 27]. Because adsorption of furilazole and dichlormid to agricultural soils will be limited, these

safeners will likely move through the aqueous phase, either as runoff or through groundwater, into adjacent surface waters. No soil adsorption data exists for the benoxacor and AD-67; however, it is believed that these safeners likely will be at least as mobile as the furilazole and dichlormid [1, 2]. Comparable adsorption is expected due to the structural similarities between dichloracetamide safener compounds and because  $K_{ads}$  values reported for furilazole and dichlormid are less than those of the popular chloroacetamide herbicides acetochlor and metolachlor ( $K_{ads} = 1.82 — 10.85 \text{ mL g}^{-1}$  and  $K_{ads} = 2.5 — 11.77 \text{ mL g}^{-1}$  on sandy loam and clay loam, respectively) (see Table 1) [1, 28]. Acetochlor and metolachlor have already been reported in surface waters, thus safeners will likely be *at least* as mobile as these two herbicides [2, 28].

Indeed, a recent study of Iowa and Illinois streams detected all four safeners at concentrations ranging from 42—190 ng L<sup>-1</sup> April through June (Figure 3) [2]. Of the seven sites monitored, furilazole and benoxacor were identified at all locations with an overall detection frequency of 31% and 29%, respectively [2]. Overall, dichlormid was detected with 15 % frequency and at five of the seven sites [2]. AD-67 was only detected on three occasions, but this is likely because AD-67 is primarily used in China [1, 2, 5]. In the study, samples with the highest safeners concentrations often correlated to a storm event or near peak flow conditions, suggesting water plays a critical role in their environmental transport and mobility [2].

Acetochlor and metolachlor, the active ingredient herbicides these safeners protect against, were also detected at every site (73% and 100% overall detection, respectively) and in concentrations ranging from 10—15,000 ng L<sup>-1</sup> [2]. Increases in concentration for these herbicides were also observed during or following a storm event

or near peak flow conditions [2]. For samples with safener detections, a statistical correlation between safener concentration and co-formulate herbicide concentration was found (i.e., the higher the concentration of the safener, the higher the concentration of its corresponding chloroacetamide herbicide) (see Table 1, Figure 3) [2].

This study illuminates a link between chloroacetamide herbicide use and dichloroacetamide safener use, and suggests safeners are indeed highly mobile in aqueous environments. The active herbicides were detected more frequently and at higher concentrations, but this likely reflects the mass used in herbicide formulations (i.e., safeners typically constitute ~10-15% of the active herbicides mass in commercial formulas). Because acetochlor and metolachlor are assumed to not transform to any appreciable amount during hydrolysis, adsorption, and direct photolysis [1, 29], and the work of Woodward et al. suggests safeners are highly mobile [2], the environmental transformation of safeners could be a major fate pathway in the net environmental transformation of herbicide formulations as they make up a significant mass percent of the formulation relative to other added ingredients [1, 10].

### 1.2.2. Safener Reduction on Iron Minerals

One peer-reviewed study on abiotic reactions of benoxacor found that it had the potential to undergo hydrogenolysis, a type of reductive dechlorination reaction, to produce a chloroacetamide analogue [5]. Benoxacor was found to undergo such reductive hydrogenolysis in a system of iron hydroxide mineral (e.g., goethite and hematite) amended in solution with Fe (II) [5]. The Fe (II) in the amended hydroxide slurry served as the reductant, where Fe (II) associated with iron mineral phases have long been recognized as potential reductants for pollutants in aquifers and sediments [5]. Benoxacor

reduction by Fe (II) in the presence of goethite produced a monochlorinated analogue (Figure 4) where the reduced chloroacetamide is denoted as MB in Figure 4 [5]. The compound MB (see Figure 4) has a structure analogous to that of acetochlor (see Table 1); acetochlor is an herbicide commonly co-formulated with benoxacor and is a suspected human carcinogen [4]. Although no toxicology data exists on the compound MB, it is speculated that this monochloric species would have similar herbicidal effects as the chloroacetamide acetochlor. Not only would MB likely be more toxic to plant life, but transformation of benoxacor to MB would likely result in a more toxic and carcinogenic compound to humans as chloroacetamides are better alkylating agents than dichloroacetamides (due to the one geminal chlorine instead of two) and thus better mutagens [5]. Significantly, if the compound MB expressed some of acetochlor's herbicidal properties, then the reaction would have produced an "active" ingredient from an "inert" compound [5, 17].

Indeed, like benoxacor, chloroacetamide analogues of these other safeners can be formed and are stable. In the same study of benoxacor hydrogenolysis, AD-67 and dichlormid underwent the same reduction to chloroacetamide compounds (see Figure 4) [5]. One of the three chloroacetamide analogues produced during dichlormid reduction was CDAA (see Figure 4) [5]. CDAA—sometimes referred to as allidochlor—was previously used as an active ingredient in herbicides but was subsequently banned due to toxicity concerns [1, 5, 30].

### 1.2.3. Safener Direct Photolysis

As safeners will likely mobilize to surface waters, an important but largely unanswered research question relates to how safeners react in natural aquatic systems.



Although safeners can be reduced in the presence of iron minerals in amended Fe (II) hydroxide slurries, there remain many other unexplored pathways for safener transformation in aqueous environments. Work by Sivey and Roberts (2012) supported the claim by chemical manufacturers that dichloroacetamide safeners are recalcitrant to hydrolysis [5]. Thus, hydrolysis is not likely to contribute to their environmental transformation. Because safeners are generally applied to crops during spring and summer months (April through June) [2], photolysis (i.e., a reaction with sunlight) in aqueous media is a potential pathway for safener transformation in the environment [1].

Significantly, the safener benoxacor absorbs light within the solar spectrum (see Figure 2). Absorption of light within the solar spectrum by benoxacor suggests that this safener has the potential to undergo direct photolysis (i.e., photolysis not mediated by a photosensitive intermediate) under natural sunlight [31]. Preliminary studies by the Cwiertny group have shown that direct photolysis of benoxacor might be a major transformation route in environmental and aquatic systems. Currently, no study exists on the direct photolysis of benoxacor, and the EPA does not mention photolysis as a potential environmental fate in its final rule of benoxacor [19].

Although AD-67, dichlormid, and furilazole can't absorb sunlight within the solar spectrum (see Figure 2), one study showed dichlormid can directly absorb light at lower wavelengths (i.e., higher energy light) such as  $\lambda \geq 250$  nm. Photolysis of dichlormid under UV light produced one of the same chloroacetamide analogue observed by Sivey et al, CDAA [11]. As Woodward et al revealed, safeners are mobile and are likely to be found in surface waters [2]. Thus, because rural and agricultural communities often use surface water systems to treat for drinking water, and UV disinfection is becoming a

more popular method for treating drinking water due to health concerns of chlorination byproducts, these safeners could be exposed to  $\lambda \geq 250$  nm during these disinfection processes [32].

#### 1.2.4. Safener Indirect Photolysis

For AD-67, dichlormid, and furilazole, the three commonly used dichloroacetamides that do not absorb light within the solar spectrum (see Figure 2), their environmental transformation could be mediated by a photosensitive intermediate (i.e., indirect photolysis) [1, 31, 33]. Indirect photolysis is a common environmental transformation pathway for compounds otherwise photo-stable under natural sunlight [31]. Photosensitizers (e.g., humic substances) absorb light to produce reactive intermediates like singlet oxygen ( $^1\text{O}_2$ ), hydroxyl radical ( $\bullet\text{OH}$ ), and triplet state organic matter ( $^3\text{DOM}$ ), all of which are highly reactive and could induce environmental dechlorination in compounds like safeners, which contain electron rich functionalities likely reactive toward photooxidants (see Table 1) [1, 31]. Humic substances would likely be present in agricultural run-off and surface waters that are susceptible to sunlight exposure [1, 31]. Not only could humic substances promote environmental transformation, but nitrate ( $\text{NO}_3^-$ ) and nitrite ( $\text{NO}_2^-$ ) could also be involved in indirect photolysis [31, 33]. These species are commonly found in surface waters of agricultural lands (like Iowa, where safener containing herbicides are commonly used) with typical summertime concentrations as high as  $10 \text{ mg L}^{-1}$  (as N) [31, 33, 34]. Nitrate and nitrite can absorb light to produce  $\bullet\text{OH}$ , nitric oxide ( $\text{NO}\bullet$ ), and a host of other short-lived and reactive species capable of inducing safener transformation [31, 33].

### 1.3. Research Goals and Hypothesis

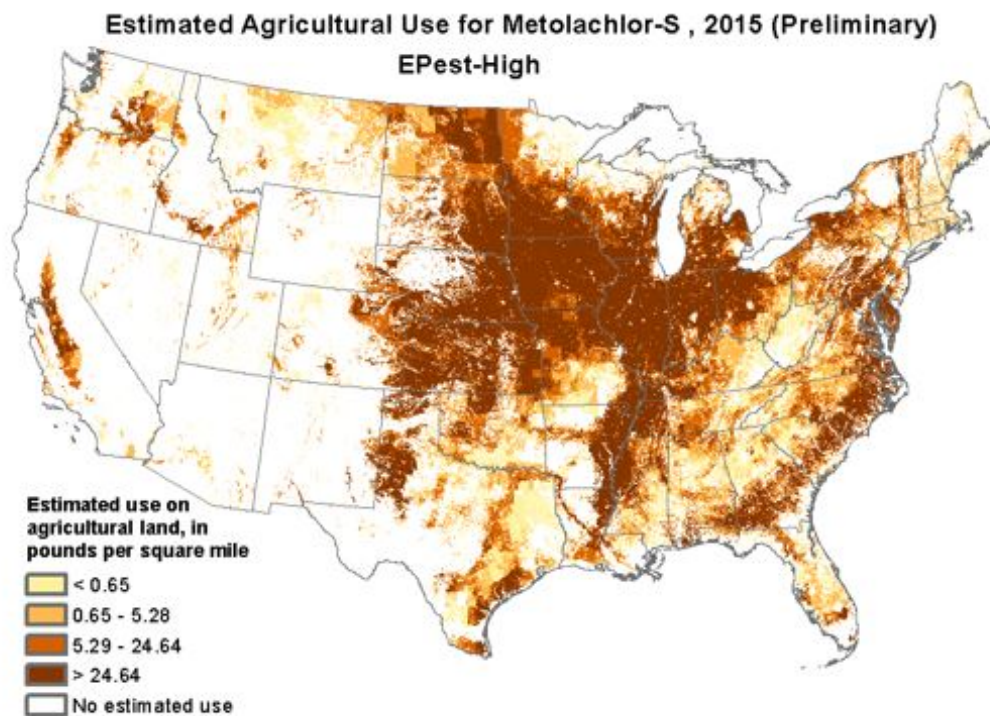
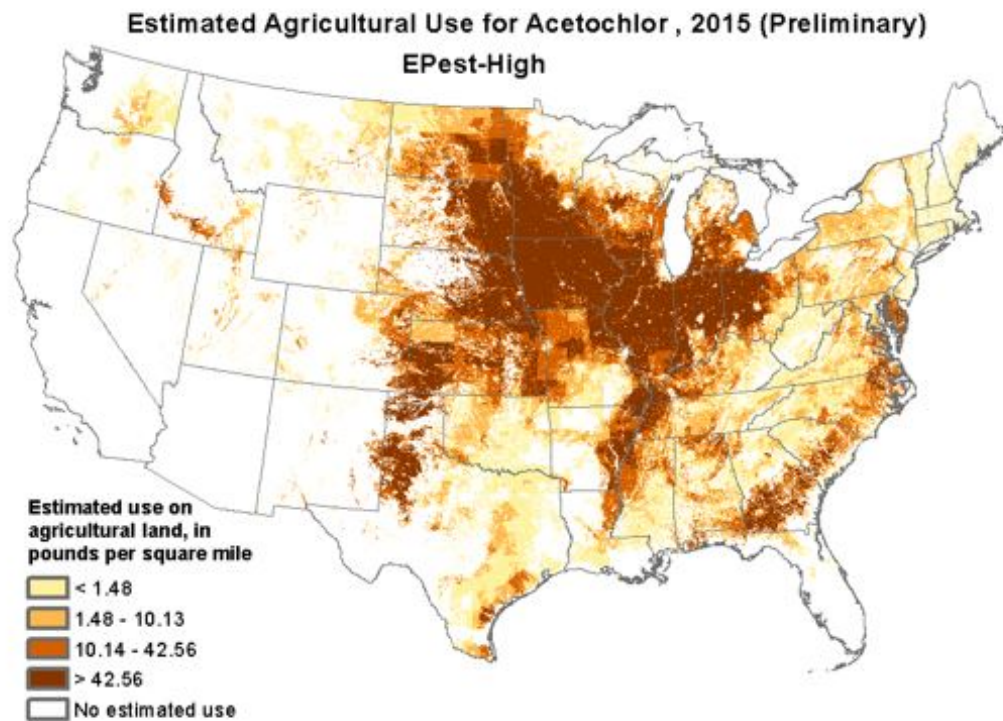
As of yet, there exists little data regarding the widely used dichloroacetamide safeners even though available research shows their biotoxicity can be altered in the environment. Because safeners will likely be present in surface waters during summer months, aquatic photolysis could be a major environmental transformation route for this class of compounds. If any four of the dichloroacetamide safeners (see Table 1) could form an analogous chloroacetamide compound during photolysis, it could represent a major pathway for safener transformation in the environment, and one which would change safeners' toxicity [1, 5].

This project aims to be the first comprehensive study of safener photolysis. Herein, we will study the nature of safener photolysis (i.e., direct photolysis, indirect photolysis, photolysis rates, natural and simulated aquatic matrices) as well as identify major photo-transformation products of safener photolysis. We believe safener photolysis will be a likely route for environmental transformation in natural aquatic systems. The overarching goal of this project is to quantify and describe that transformation.

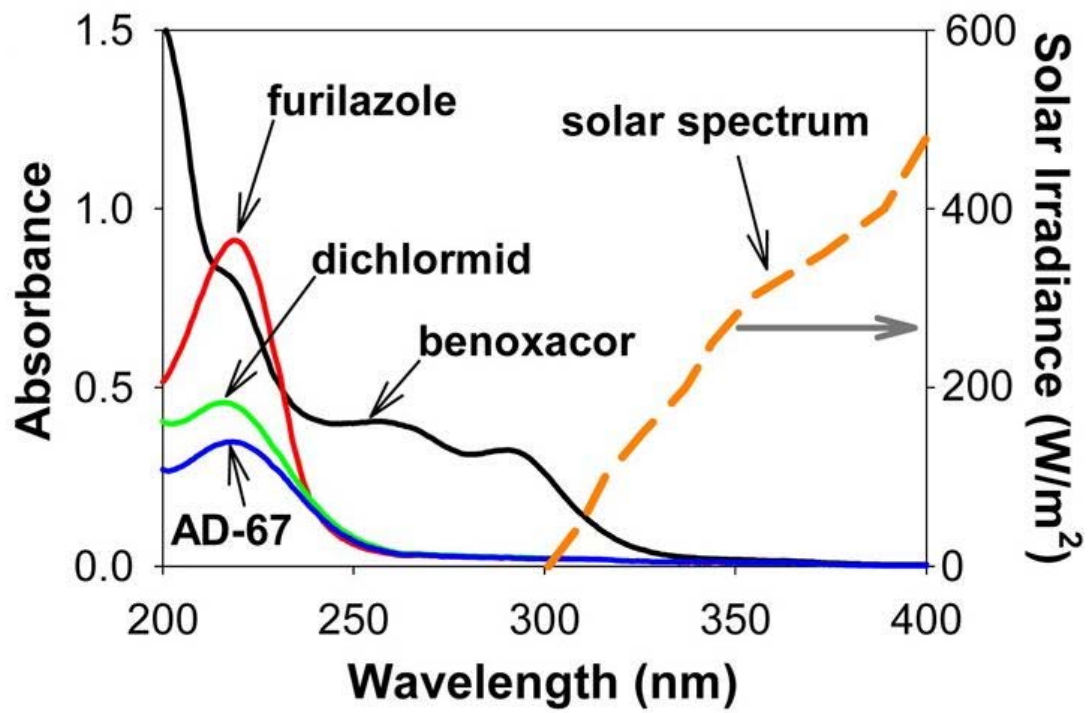
We hypothesize that:

- Based on overlap with the solar spectrum, benoxacor will rapidly photolyze by absorbing light within the solar spectrum to form new photoproducts.
- AD-67, dichlormid, and furilazole will react through indirect photolysis because they contain electron rich functionalities likely reactive toward photooxidants like ROS generated from humic substance and nitrate/nitrite photolysis, which will likely be found alongside safeners in agricultural runoff.

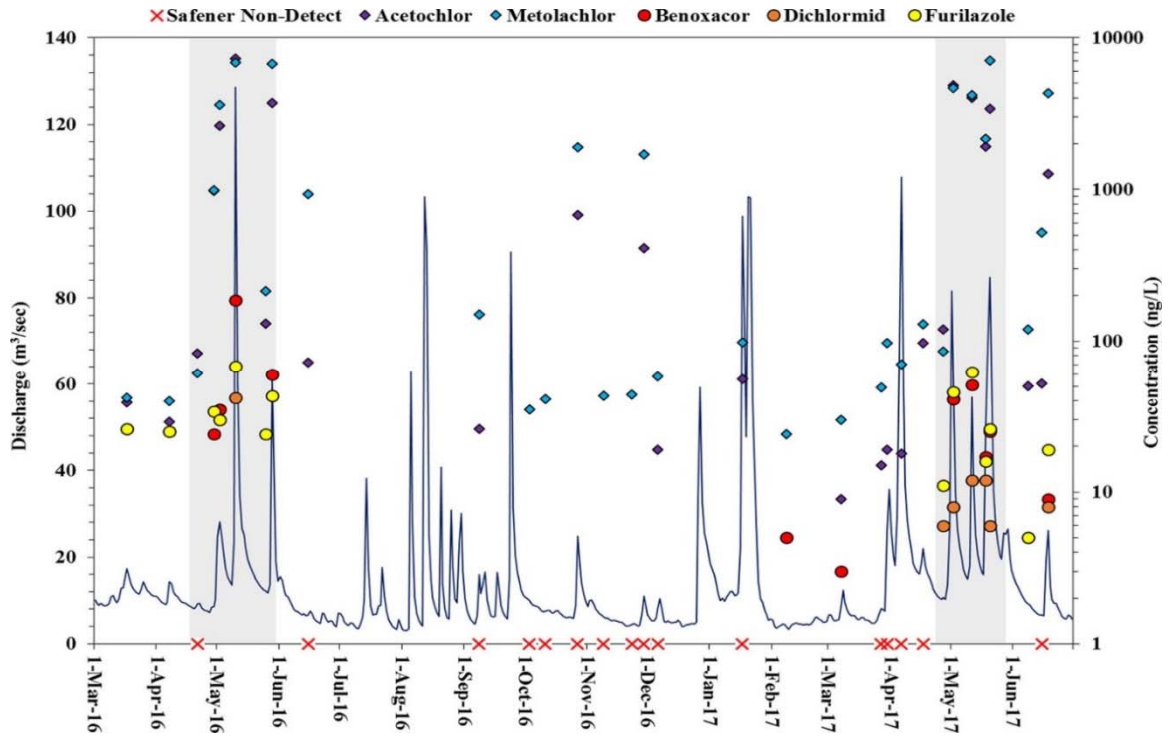
- AD-67, dichlormid, and furilazole will react through and direct photolysis at  $\lambda \geq 250$  nm to yield new photoproducts because they can weakly absorb light in this range.
- Safener photoproducts will exhibit different toxicological properties than their parent compounds based on their level of chlorination (i.e., partially dechlorinated dichloroacetamides will form the more herbicide like chloroacetamides) and physical properties (i.e., fully dechlorinated compounds could be less mobile in aqueous systems and more likely to bioaccumulate).



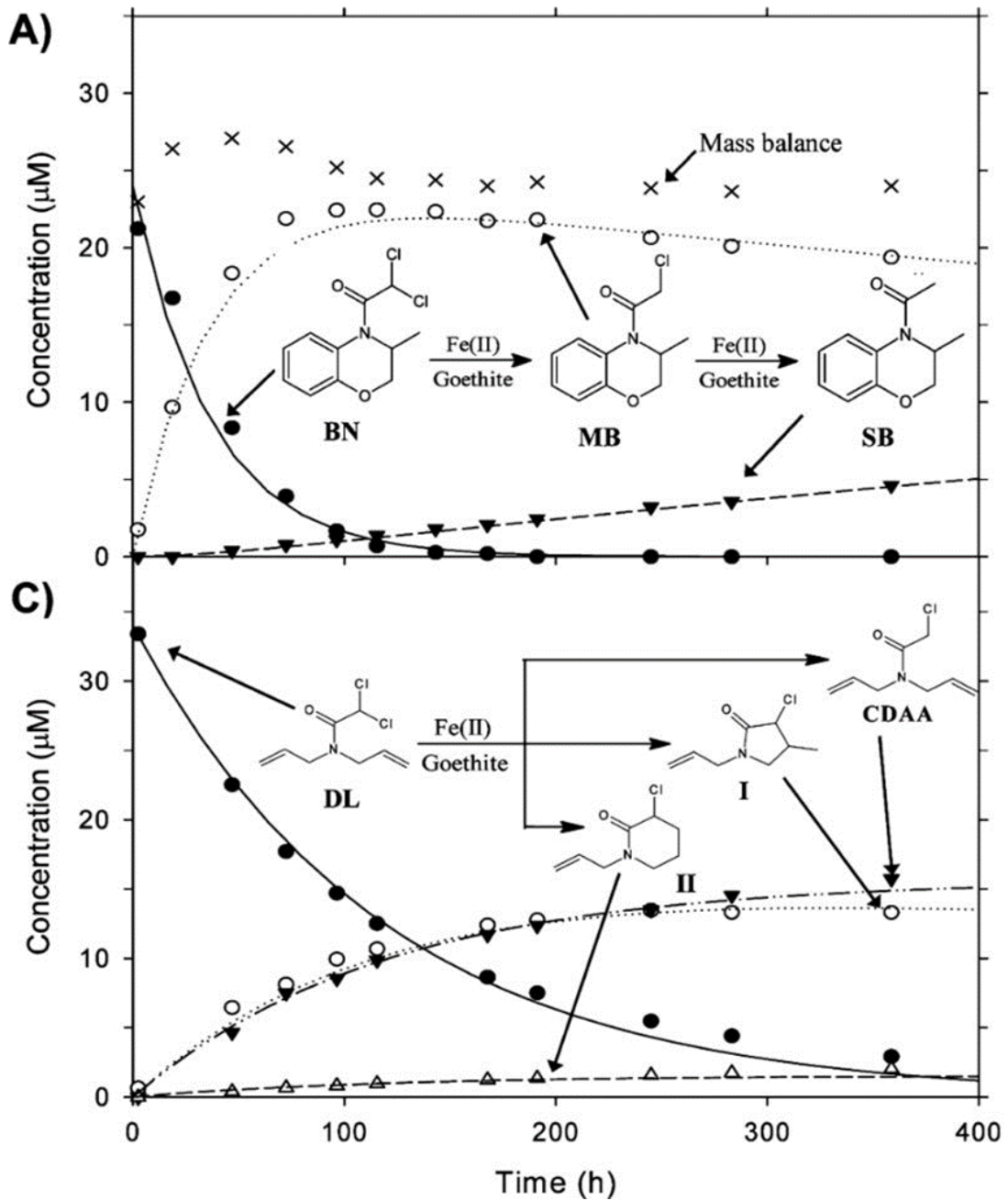
**Figure 1** Preliminary usage (lbs mile<sup>-2</sup>) of the herbicides acetochlor and metolachlor in 2015.



**Figure 2** UV-Vis absorbance of four dichloracetamide safeners plotted against solar irradiance.

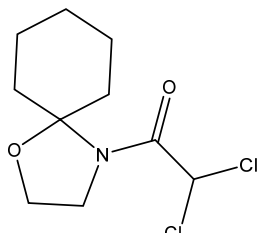
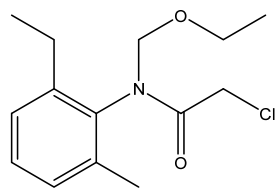
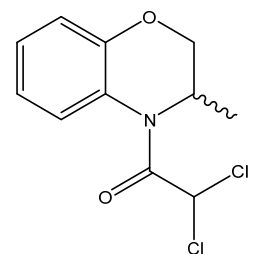
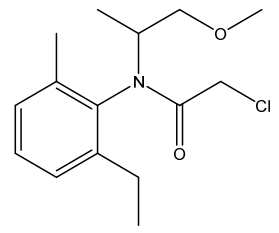
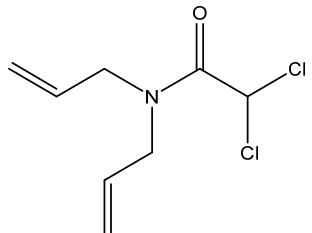
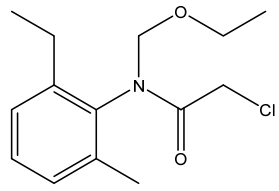
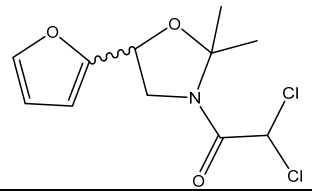
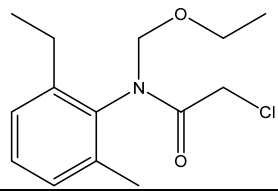


**Figure 3** Occurrence of the commonly used dichloroacetamide safeners in select Iowa and Illinois creeks from Woodward et al.



**Figure 4** Reactions of benoxacor and dichlormid in Fe (II) amended goethite slurries. MB represents the chloroacetamide analogue of benoxacor reduction; CDAA, I, and II represent the chloroacetamide analogues of dichlormid reduction.



Dichloroacetamide Safener	Chloroacetamide Herbicide	Crop
<p><b>AD-67</b></p> 	<p><b>Acetochlor</b></p> 	Corn
<p><b>Benoxacor</b></p> 	<p><b>Metolachlor</b></p> 	Corn
<p><b>Dichlormid</b></p> 	<p><b>Acetochlor</b></p> 	Corn
<p><b>Furilazole</b></p> 	<p><b>Acetochlor</b></p> 	Cereals

**Table 1** Dichloroacetamide safeners adjacent to the chloroacetamide herbicides and crops with which they are commercially mixed and applied.

## Chapter 2 Materials and Methods

### 2.1. Chemicals

All chemicals were used as received. As described, the four dichloroacetamides analyzed in photolysis experiments were AD-67 (CAS 71526-07-3), benoxacor (Fluka, 99.4%, CAS 98730-04-2), dichlormid (CAS 37764-25-3), and furilazole (Fluka, 99.6%, CAS 121776-33-8). All experiments were conducted in buffered solutions of deionized water (Millipore, Q-Grad 2, CAS 7732-18-5) and potassium phosphate buffer (RPI, CAS 7778-77-0). The pH was adjusted using hydrochloric acid (Fisher Scientific, ACS grade, CAS 7647-01-0) and sodium hydroxide (Fisher Scientific, ACS grade, 1310-73-2). Acetonitrile (Fisher Scientific, Optima grade, CAS 75-05-8) was used as a solvent for stock solution preparation and as a liquid phase during HPLC analysis. Deionized water (Millipore, Q-Grad 2, CAS 7732-18-5) was used to prepare buffered solutions and also used as an HPLC mobile phase. Chloroform (Fisher Scientific, ACS grade, CAS 67-66-3) was used as the non-polar phase during liquid-liquid extraction to isolate benoxacor photoproducts. An actinometer system of 4-nitroanisole (Sigma, CAS 100-17-4) and pyridine (Fischer Scientific, CAS 110-86-1) was used to calculate benoxacor quantum yield ( $\Phi$ ). During indirect photolysis experiments, Elliot soil humic acid (International Humic Substances Society-IHSS), Pahokee Peat humic acid (IHSS), Sewanne River fulvic acid (IHSS), Sewanee River humic acid (IHSS), potassium phosphate (RPI, CAS 7778-77-0), sodium nitrate (RPI, CAS 7631-99-4), and sodium nitrite (RPI, CAS 7632-00-0) were used to generate reactive oxygen species (ROS) and other radical intermediates.

## 2.2. Photolysis Experiments

### 2.2.1. Direct Photolysis Experiments

Most direct photolysis experiments were conducted under a commercially available 1000W Newport Xe arc lamp. In order to generate a spectrum similar to sunlight, the beam was passed through an AM 1.5 filter, a recirculated water filter to remove IR radiation, and a 305 nm long pass filter. Lamp irradiance was monitored periodically using an ILT 950 spectroradiometer (International Light Technologies, Peabody, MA) (Figure 5a).

To conduct reactions in idealized natural aquatic environments, we used matrices of 5 mM potassium phosphate buffer (pH 2, 5, 7, or 9). Select experiments were conducted in natural aquatic systems and used water from the Iowa River passed through a 25 micron filter. Concentrated safener stock solutions were freshly prepared in acetonitrile and stored in a freezer (10 mM,  $\sim -18^{\circ}\text{C}$ ) until use. Initial aqueous safener concentrations in direct photolysis experiments were 10  $\mu\text{M}$  (AD-67 = 2.52 mg/L, furilazole = 2.78 mg/L, benoxacor = 2.60 mg/L, dichlormid = 2.08 mg/L). Although these concentrations are higher than those expected in natural surface waters, they were necessary to accurately monitor reaction progress and identify photoproducts during HPLC-DAD analysis. In a set of experiments conducted by Monica McFadden, low concentrations of safeners were photolyzed (e.g., 500  $\mu\text{g L}^{-1}$  or 1.92  $\mu\text{M}$ ) and were still accurately detected via HPLC-DAD. Photolyzed safener solutions were contained in a water-jacketed borosilicate reaction vessel (37 mm inner diameter x 67 mm depth, total volume  $\sim 50$  mL; Chemglass). A constant temperature of  $\sim 20^{\circ}\text{C}$  was maintained with a water recirculating bath to avoid evaporation (Fisher Scientific Isotemp 3016S).

Solutions were continuously mixed by a magnetic stir bar and stir plate. Aliquots of reaction mixtures (500  $\mu\text{L}$ ) were periodically drawn and monitored via HPLC-DAD analysis to track reaction progress and photoproduct production.

During a small set of experiments in which safeners were photolyzed with  $\lambda \geq 250$  nm to simulate drinking water UV disinfection systems, a 200 W Newport Mg(Xe) arc lamp equipped with a 250 nm cut on filter was used as a light source. Experimental procedures remained the same for this set of lower wavelength photolysis except for the change in light source.

In addition to experiments conducted in buffered aqueous solutions, some experiments were conducted in acetonitrile to determine the role of water in photoproduct formation. These experiments were photolyzed under the 1000 W Xe lamp in water jacketed reaction vessels, where 100 or 500  $\mu\text{M}$  safener was prepared in 20 mL acetonitrile and photolyzed. Upon one hour of photolysis, an aliquot of this reaction was spiked into 5 mM pH 7 phosphate buffer (10  $\mu\text{M}$  initial safener concentration) and either kept in the dark or placed back under the lamp for continued photolysis. Both dark and light stability of the spiked photoproducts was monitored periodically via HPLC.

### 2.2.2. Quantum Yield

To calculate the quantum yield ( $\Phi$ ) of benoxacor, we used a chemical PNA-pyridine actinometer system to relate a well-defined quantum yield (i.e., the quantum yield of the PNA-pyridine system) to the quantum yield of our compound of interest (2-1):

$$\Phi_c = (\Phi_{PNA-pyr}) \left( \frac{k_c \sum_{300nm}^{400nm} (\epsilon_{\lambda, c} \times L_{\lambda})}{k_{PNA-pyr} \sum_{300nm}^{400nm} (\epsilon_{\lambda, PNA-pyr} \times L_{\lambda})} \right) \quad (2-1)$$

where  $\Phi$  is the quantum yield;  $k$  is the first-order rate constant ( $\text{min}^{-1}$ );  $\epsilon$  is the molar absorptivity ( $\text{M}^{-1} \text{cm}^{-1}$ ); and  $L$  is the irradiance ( $\text{W m}^{-2} \text{nm}^{-1}$ ) of the 1000 W Xe lamp at a given wavelength (note: subscripts  $c$  and PNA-pyr denote the compound of interest and the actinometer system, respectively). This approach is commonly used in experimental photochemistry and the procedure is well described in the literature [31, 37, 38]. First order rate constants were calculated for benoxacor in pH 7 potassium phosphate buffer and the PNA/pyridine solution (10  $\mu\text{M}$  PNA, 20 mM pyridine) in deionized millipore water (0.074  $\text{min}^{-1}$  and 0.070  $\text{min}^{-1}$ , respectively) using an integrated first order rate law (Figure 6). Lamp irradiances ( $L_\lambda$ ) were measured immediately after each experiment, and in order to minimize and accurately quantify differences in irradiance between trials, solutions were photolyzed shortly after one another. Molar absorptivity ( $\epsilon$ ) found using Beer's Law (2-2):

$$A = \epsilon bc \quad (2-2)$$

where  $A$  is absorbance (measured with Thermo Scientific Genesys 10uv),  $b$  is the path length of the quartz cuvette (1 cm), and  $c$  is the concentration of benoxacor (10  $\mu\text{M}$ ). A molar absorptivity was calculated for each wavelength ( $\lambda$ ) across the range range 300 nm – 400 nm. A molar absorptivity for PNA/pyridine at each wavelength in this range was provided by Laszakovits et al. [38]. The quantum yield of the PNA/pyridine system was found using the concentration of pyridine (20 mM) and the equation provided by Laszakovits et al. [38]:

$$\Phi_{PNA-pyr} = 0.29[\text{pyr}] + 0.00029 \quad (2-3)$$

### 2.2.3. Indirect Photolysis Experiments

Because indirect photolysis is often a slow process, experiments were conducted in a SunTest CPS+ solar simulator (Atlas Material Testing Technology, Mount Prospect, IL) (Figure 5b). Although this irradiance is approximately three times the irradiance of the sun at Earth's surface, this intensity setting allowed us to speed the rate of indirect photolysis to convert more safener over 5 hour time scales. Solutions were photolyzed in quartz tubes held at a 30° angle. Cork stoppers were used to combat evaporation; however, the average solution temperature was ~ 30 °C, thus with cork stoppers evaporation at this temperature appeared to be negligible.

Experimental procedures for creating reaction matrices during indirect photolysis experiments were the same as those for direct photolysis experiments except for the addition of photosensitizers to reaction solutions. Photosensitizers were added to generate reactive species including 10 mg L<sup>-1</sup> sodium nitrate ( $\bullet\text{OH}$ ), 10 mg L<sup>-1</sup> sodium nitrite ( $\bullet\text{OH}$ ,  $\text{NO}\bullet$ ), and 10 mg L<sup>-1</sup> humic acid ( $\bullet\text{OH}$ ,  $^1\text{O}_2$ , and  $^3\text{DOM}^*$ ). Stock solutions of sodium nitrate and sodium nitrite were prepared in deionized water. Stock solutions of humic acids were prepared in deionized water adjusted to pH 12 to ensure complete solubility; after dissolution, the pH was readjusted to pH 7.

### 2.3.4. Photoproduct Identification

To identify benoxacor direct photolysis transformation products, reaction matrices were significantly scaled-up in both mass of safener and overall volume (~20 - 50 mg/L safener, ~500 - 1000 mL reaction volume). Solutions were irradiated in a 1 L borosilicate glass beaker by either an Atlas Suntest CPS+ solar simulator with an irradiance setting of 750 W m<sup>-2</sup> or a 200 W Newport Mg(Xe) arc lamp equipped with a 250 nm cut on filter.

Photolysis at lower wavelengths did not change the product distributions observed under simulated sunlight but instead increased the rate of reaction which proved helpful in photolyzing a larger mass of safener. Reaction progress was monitored through HPLC analysis and allowed to proceed until products appeared to stop accumulating (~1.5 – 12 h). Upon reaction completion, samples were extracted into chloroform and concentrated to an oil/residue with compressed air (~ 78% N<sub>2</sub>, ~20% O<sub>2</sub>). The crude reaction residues were reconstituted as highly concentrated solutions in acetonitrile (~10-20 mg crude residue in 5-7 mL) and were immediately separated via HPLC-DAD analysis and a semi-preparative column (described in Analytical Methods).

### 2.3. Analytical Methods

Analytical methods follow those developed by Pflug et al. 2017 [39]. Photolysis reactions were monitored and analyzed with an Agilent 1260 high performance liquid chromatography system equipped with a diode array detector (HPLC-DAD). HPLC methods used an Agilent Zorbax Eclipse XDB-C<sub>18</sub> column (4.6 x 150 mm, 3.5 μm), acetonitrile and water graded eluent (1 mL min<sup>-1</sup>, Table 2), and 20 μL injection volume. Reaction progress was monitored at 220 nm for parent compounds. All photoproducts had absorbance maximums near 220 nm, thus their formation was monitored at 220 nm also.

In experiments used to generate larger masses of benoxacor photoproducts for identification and characterization, HPLC separation was used. Products were separated on a Beckman System Gold instrument, a 166P VWD connected to a 128P solvent module. The method used an acetonitrile and water graded eluent (2 mL min<sup>-1</sup>), 220 or

240 nm wavelength detection, and a Restek Ultra C<sub>8</sub> semi-preparative column (10 x 250 mm, 5 μm).

High resolution electrospray ionization time-of-flight mass spectrometry (HR-ESI-TOFMS) data was gathered on benoxacor photolysis reaction mixtures by a Waters Premier Q-TOF instrument using the same Agilent Zorbax Eclipse XDB-C<sub>18</sub> column from HPLC-DAD analysis. The same acetonitrile and water gradated eluent was used (Table 2) with the addition of 0.1% formic acid solution and collected using a reference standard of leu-enkephalin and positive electrospray ionization. High resolution electron ionization time-of-flight mass spectrometry (HR-EI-TOFMS) data was gathered on the same instrument via direct injection using a leu-enkephalin reference standard and electron ionization over a range of 120-1000 Da.

To analyze and identify products using nuclear magnetic resonance spectroscopy (NMR), <sup>1</sup>H NMR, Heteronuclear Single Quantum Coherence (HSQC), and Heteronuclear Multiple Bond Correlation (HMBC) spectra were recorded using a Bruker AVANCE-600 spectrometer using CDCl<sub>3</sub> as the solvent. Chemical shift values were referenced to the residual solvent signals ( $\delta_H/\delta_C$ , 7.26/77.2). All NMR data were processed using Bruker Topspin 3.5 software.



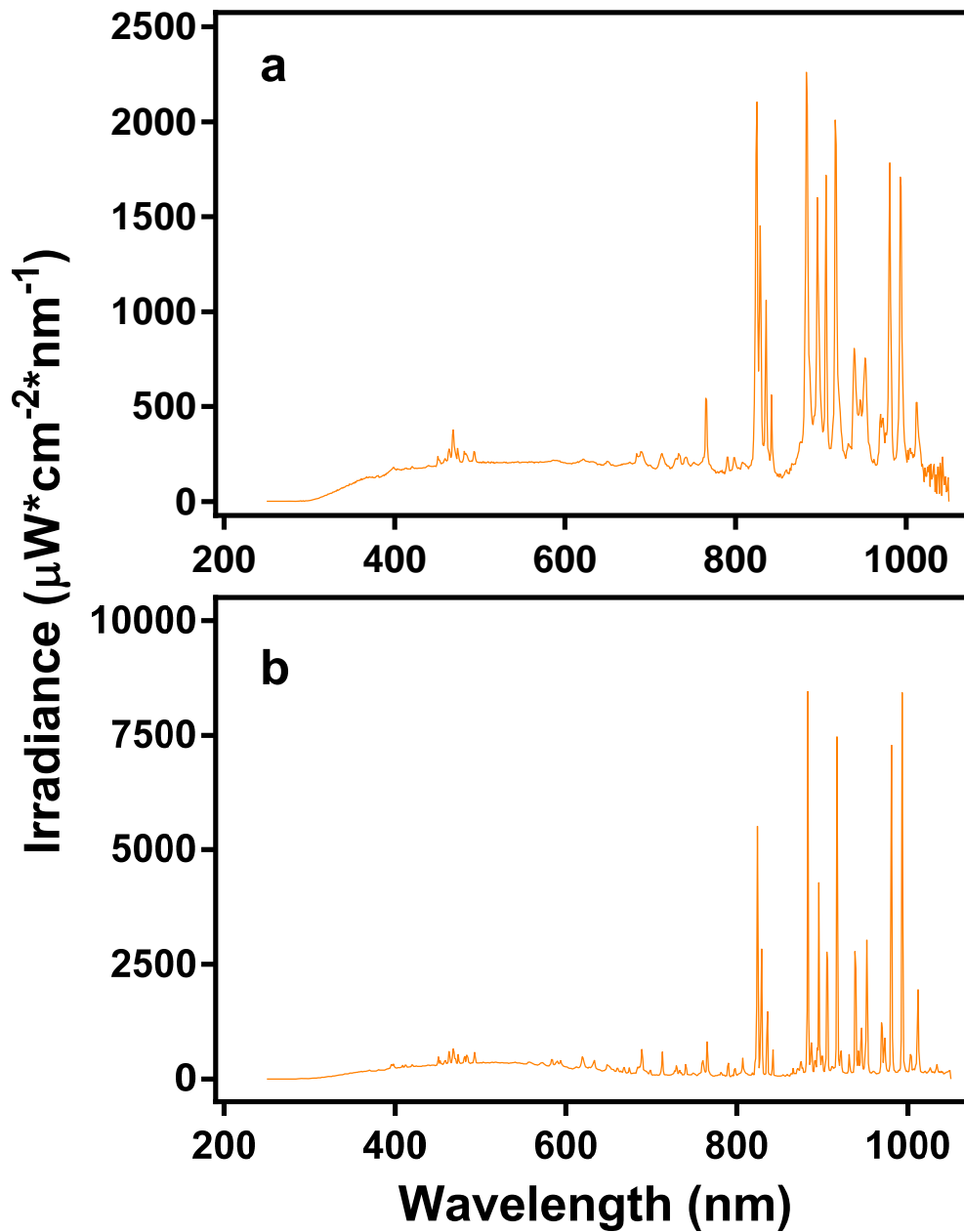


**Figure 5** Irradiance spectrum of 1000 W Newport Xe lamp equipped with 305 nm cut-on filter (a) and a SunTest CPS+ solar simulator at  $750 \text{ W m}^{-2}$  output (b). Output over 300-400 nm is  $8.81 \times 10^{-3} \text{ W cm}^{-2}$  (a) and  $1.26 \times 10^{-2} \text{ W cm}^{-2}$  (b).

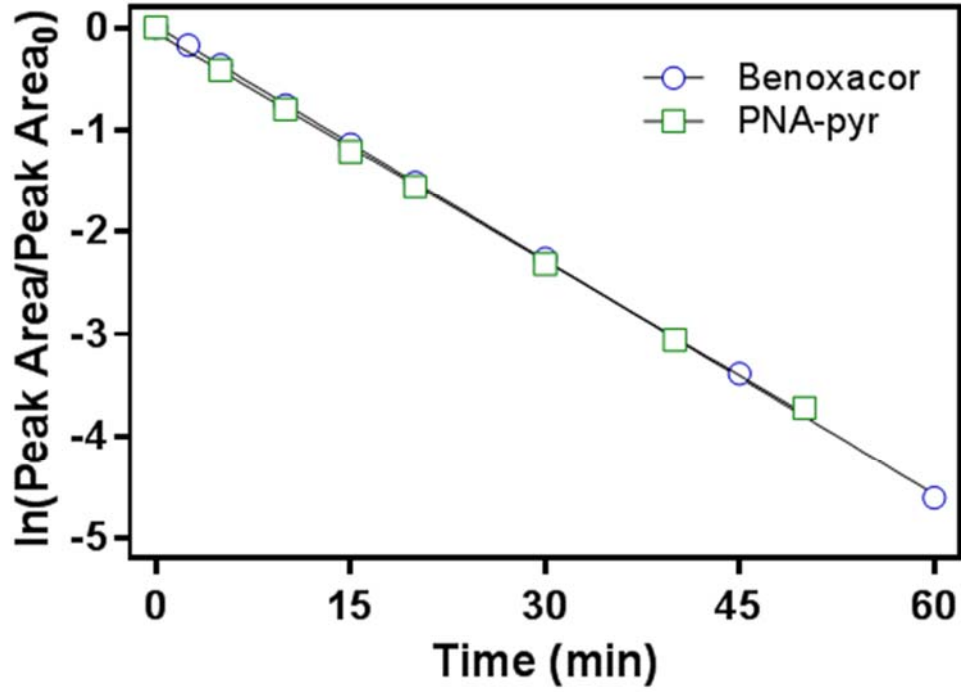


**Figure 6** First order integrated rate laws for PNA-pyr actionmeter ( $R^2 = 0.999$ ) and benoxacor in 5 mM pH 7 potassium phosphate buffer ( $R^2 = 0.999$ ).

Time (min)	% Composition ACN	% Composition DI H <sub>2</sub> O
0	25	75
11	80	20
12	25	75
15	25	75

**Table 2** HPLC solvent gradient.

## Chapter 3 Direct Photolysis of Benoxacor and Identification of Transformation Products

### 3.1. Introduction

Benoxacor is a dichloroacetamide safener commonly sold pre-mixed in the herbicide formulation Dual II Magnum, which contains metolachlor as the active ingredient. Benoxacor is present in Dual II Magnum and other formulations to protect the crop, primarily corn, from incidental damage from the herbicidal activity of metolachlor. Benoxacor limits metolachlor toxicity by stimulating production of glutathione-s-transferase isozymes capable of breaking down metolachlor [40]. Because benoxacor is not active toward pests (e.g., weeds), it is classified as “inert” for regulatory purposes [17, 19]. Consequently, there are very few peer reviewed studies on the environmental fate of benoxacor and no official domestic or global use data. Based on preliminary estimates for metolachlor use in the United States during 2015, benoxacor use is expected to surpass  $3 \times 10^6$  kg year<sup>-1</sup> [36].

Previous work by the Cwiertny group indicates benoxacor may undergo direct photolysis because its absorbance spectrum overlaps with wavelengths of light available at the earth’s surface [1]. Direct photolysis is a photochemical reaction involving only light and the compound of interest (i.e., benoxacor). During direct photolysis, ground-state electrons occupying bonding orbitals (i.e.,  $\sigma$  or  $\pi$ -orbitals) or non-bonding orbitals (i.e.,  $n$ -orbitals) are promoted to higher energy anti-bonding orbitals (i.e.,  $\sigma^*$  or  $\pi^*$ -orbitals) through interactions between only the electromagnetic fields of the compound and a photon of radiation [31]. After an electron is transitioned into a higher energy orbital (i.e.,  $\pi \rightarrow \pi^*$  or  $n \rightarrow \pi^*$ ), the compound is in an *excited state* and can undergo any of

several chemical reactions including fragmentation, intramolecular rearrangement, isomerization, hydrogen abstraction, dimerization, or electron transfer [31].

The absorbance spectrum of benoxacor across the UV and visible light range reveals local maxima at 216, 258, and 290 nm, with a broad absorbance band that extends well above 300 nm (Figure 7). Although most compounds can absorb light at extremely low wavelengths (i.e., high energy wavelengths), especially in the UVC region of ultraviolet light ( $100 \text{ nm} \leq \lambda \leq 280 \text{ nm}$ )—where wavelength is inversely proportional to energy—compounds that can absorb light at wavelengths overlapping with the energy of light at the Earth's surface (i.e.,  $\lambda \geq 305 \text{ nm}$ ) may undergo chemical reactions, assuming a sufficient photo-efficiency, or quantum yield [31]. Quantum yield ( $\Phi$ ) is defined as the numbers of molecules transformed per number of photons absorbed at a given wavelength or over a range of wavelengths (3-1).

$$\Phi(\lambda) = \frac{\text{\# of molecules decayed (or transformed)}}{\text{\# of photons absorbed}} \quad (3-1)$$

In many cases, after electron promotion to an excited state, a compound might release the absorbed energy in ways that do not result in chemical changes, such as thermal energy, rotational and vibrational motion, electromagnetic radiation (i.e., fluorescence and phosphorescence), or photosensitization (i.e., transferring energy to a different molecule) [31]. In these scenarios, the compound of interest remains unchanged over the process of excitation to de-excitation. Accordingly, the quantum yield ( $\Phi$ ) represents a measure of how efficiently a molecule transforms (i.e., undergoes a chemical change) when it interacts with a photon and absorbs energy. Some typical values of  $\Phi$  for organic chemicals that are or may represent common pollutants range from  $1.0 \times 10^{-2}$  for anthracene to  $2.9 \times 10^{-5}$  for nitrobenzene ( $\lambda_{\text{measured}} = 313 \text{ nm}$ ) [31].

Despite the potential for benoxacor to directly photolyze in surface waters based on its ability to absorb available light energy in the solar spectrum (see Figure 7), there has been little to no investigation of its photodegradation. This dearth of literature is evident not only in the peer-reviewed literature but also the non-peer-reviewed grey literature that consists of fate assessments conducted by industry as part of the chemical review process.

In this work, we aim to provide a comprehensive study of the phototransformation of benoxacor. Our objectives were to (1) measure rates of benoxacor direct photolysis in a variety of aquatic matrices, (2) quantify the quantum yield for this process, and (3) identify the formation pathway and structures of major benoxacor phototransformation products. To accomplish these objectives, we conducted photolysis experiments under a 1000 W Xe lamp with a 305 nm cut-on filter to produce simulated sunlight. Experiments were conducted in both idealized (i.e., buffered and free of possible photosensitizers) and real aquatic matrices, and reaction progress was monitored via HPLC-DAD. Through our HPLC-DAD analysis, we were able to quantify reaction rates and monitor the growth of benoxacor photoproducts. Select photoproducts, based on relative abundance and potential to bio-accumulate (i.e., less polar), were later isolated and subsequently characterized via high resolution mass spectrometry and nuclear magnetic resonance spectroscopy to elucidate their structure.

### 3.2. Timescale for Benoxacor Direct Photolysis

Benoxacor rapidly photolyzed when irradiated under environmentally relevant conditions ( $\lambda > 305$  nm) (Figure 8). Because there were no other photosensitizing agents

(e.g., dissolved organic matter) present in our idealized experimental systems, we attribute benoxacor decay to reaction with the simulated sunlight, or direct photolysis.

Benoxacor direct photolysis followed first-order (i.e., exponential) decay (see Figure 8) as described by Equation 3-2, where  $[Benoxacor]_t$  (in mol L<sup>-1</sup>) is the concentration of benoxacor at a given time along the reaction coordinate,  $[Benoxacor]_0$  (also in mol L<sup>-1</sup>) is the initial concentration of benoxacor in solution,  $k$  is the first-order rate constant (min<sup>-1</sup>) for direct photolysis, and  $t$  is the irradiation time (min):

$$[Benoxacor]_t = [Benoxacor]_0 e^{-kt} \quad (3-2)$$

The first-order rate constant,  $k$  (min<sup>-1</sup>) was calculated by integrating and linearizing Equation 3-2, after which its value can be determined from the slope via linear regression (see Equation 3-3):

$$\ln[Benoxacor]_t = \ln[Benoxacor]_0 - kt \quad (3-3)$$

The half-life of benoxacor, or the timescale necessary for the concentration of benoxacor to decrease by half, was then calculated from Equation 3-4. Consistent with its rapid photolysis, we determined the half-life of benoxacor at pH 7 to be just under 8 minutes (Table 3).

$$t_{1/2} = \frac{\ln 2}{k} \quad (3-4)$$

To quantify the quantum yield ( $\Phi$ ) of benoxacor, we used the PNA/pyridine actinometer system outlined in Chapter 2. Quantum yield was calculated over the range of 300-400 nm. In this range, the actinometer and benoxacor exhibited comparable molar absorptivities (Figure 19). We calculated an average quantum yield of benoxacor of  $\Phi_{benoxacor,avg} = 1.4 \times 10^{-1}$ —a relatively large quantum yield [31]—suggesting

benoxacor is a highly photoefficient organic micropollutant compared to other photoactive compounds like anthracene and nitrobenzene (see Table 3) [31].

At pH 7, direct photolysis of benoxacor resulted in the formation of four major photoproducts, which we identified as product A [PA], product B [PB], product C [PC], and product E [PE], as well as several minor photoproducts. Relative product abundance was based on integrated peak areas with their absorbance monitored at 220 nm, a wavelength at which all products absorbed light. Thus, in our assignment of relative product abundance, we assumed that all species exhibited comparable extinction coefficients for light absorbance at 220 nm, such that relative absorbance correlates directly to their relative mass concentration.

Photoproducts were detected almost immediately. [PA], [PB], and [PC] were relatively stable over the timescales of benoxacor decay ( $\sim 1$  h in our experimental systems). After an initial steady increase in their abundance, their concentration plateaued after  $\sim 40$  min of irradiation, at which point nearly all of the benoxacor had been degraded (see Figure 8). In contrast, [PE] exhibited the concentration profile of a reactive intermediate—it formed rapidly but reached a maximum concentration after  $\sim 5$  min of irradiation and subsequently decayed away relatively rapidly over the next 15 min ( $t_{1/2} \sim 12$  min) (see Figure 8). Notably, [PE] absorbs light within the solar spectrum, with local absorbance maximums at 225 and 320 nm (Figure 9). Thus, its decay over time is likely driven by photochemistry. We note that a handful of other minor photoproducts were observed but they were not extensively characterized because of their limited extent of formation.



Notably, all major products eluted earlier than benoxacor on a C-18 HPLC column (e.g., [PA] eluted at 4.1 min whereas benoxacor eluted at 10.7 min), suggesting that photoproducts possess greater polarity (Table 4). Another notable observation was the similar elution times shared by [PA], [PB], and [PC] (see Table 4), all of which were within a 1 minute window using our analytical method (see Table 4). Further, these three products exhibited similar—if not identical—UV-vis absorbance spectra (Figure 9; Table 4). [PA] and [PB] had absorbance maxima at 220, 250, and 305 nm while [PC] had maxima of 218, 250, 290 nm (Figure 9). Although these products are less photoactive than benoxacor (i.e., they form and are relatively stable under the same photolysis timescale over which benoxacor rapidly decays), [PA] and [PB] both have absorbance patterns that overlap with the solar spectrum (see Figure 7; Figure 9). Likewise, [PC] has a local absorbance maximum at 290 nm which causes it to weakly absorb around 300 nm (Figure 9).

Based on their similar absorbance spectra (see Figure 9), elution time (see Table 4), and relative abundance (Figure 8), it is likely that [PA], [PB], and [PC] are formed through similar photochemical pathways and are structurally similar compounds. Further, based on their absorbance patterns, [PA], [PB], and [PC] might be reactive over longer periods of irradiation (i.e., a day or multiple day/night photolysis cycles). The photoactivity of these products is explored further in Section 3.5.

### 3.3. Influence of Aquatic Matrix on Benoxacor Photolysis

To explore environmental factors that might influence the rate of benoxacor photolysis and product formation, additional photolysis experiments were conducted in a variety of aquatic matrices. First, we conducted direct photolysis experiments at pH 5, 7,

and 9 in pH-adjusted phosphate buffer (5 mM). The rate of benoxacor photolysis showed little dependence on solution pH (Figure 10), with half-lives in all systems once again on the order of 8 min (see Table 3). The independence of benoxacor photolysis on pH is not surprising as there are no ionizable acid-base groups in its structure that could contribute to pH-dependent photoactivity (see Table 1).

Photoproduct formation was also largely independent of pH, with the exception of pH 9 systems (see Figure 10). At pH 9, the relative yields of photoproducts were altered, with increased production of a photoproduct that was more hydrophobic (i.e., later eluting on a C-18 column) than the other major photoproducts that were detected (Figure 11 and Figure 12). While trace amounts of this product, Product D ([PD]), were detected at pH 7 (see Figure 11), it accumulated considerably at pH 9 and exhibited stability comparable to [PA], [PB] and [PC] (see Figure 10, Figure 12). It appears, therefore, that some processes influencing photoproduct formation and/or stability are base catalyzed. More practically, it suggests that photoproduct distributions may be more complex in slightly alkaline surface waters.

Additional experiments were conducted in filtered (0.2  $\mu\text{m}$ ) Iowa River water, which was chosen as a more complex, environmentally relevant matrix containing dissolved organic matter, hardness, and alkalinity. Notably, Iowa Rivers water has a pH value around 8.5 because of limestone Silurian-Devonian aquifers underlying much of Johnson County [41]. The rate and product yield of benoxacor photolysis in Iowa River water matched those measured in model systems at pH 9 (Figure 13), including significant production of [PD]. Thus, co-solutes present in the natural water sample exerted a negligible effect on benoxacor photolysis. Consistent with this scenario, we

calculated wavelength dependent screening factors ( $S_\lambda$ ) for direct photolysis of 10  $\mu\text{M}$  Benoxacor in filtered Iowa River water according to the method of Leifer [31, 37]. These screening factors varied between 0.92-0.97 over 300 nm to 400 nm, suggesting light screening in 0.2  $\mu\text{m}$ -filtered Iowa River water was indeed negligible.

We also explored the influence of metolachlor—an herbicide active ingredient often used with benoxacor—on benoxacor photolysis. As previously reported in both peer-reviewed and industry literature, metolachlor is generally considered stable under natural sunlight [29]. When benoxacor is photolyzed at pH 7 (5 mM phosphate buffer) in the presence of metolachlor (from 0  $\mu\text{M}$  – 100  $\mu\text{M}$ ), we observed no appreciable change in its first-order decay constant (Figure 14) nor any change in benoxacor product distributions (Figure 15). Thus, while these two compounds are co-formulants and their surface water concentrations appear correlated [2], the presence of metolachlor does not affect benoxacor photodegradation in environmental systems.

### 3.4. The Role of Water in Photoproduct Formation

A small subset of experiments was conducted in a non-aqueous solvent, acetonitrile, to explore the dependency of benoxacor photolysis on water. Building off the pH-dependent trends in photoproduct formation observed at pH 9, a role for water in photoproduct formation would be expected to produce different types and yields of photoproducts relative to those products observed in an organic solvent. Indeed, photolysis of benoxacor (500  $\mu\text{M}$ ) in acetonitrile (Figure 16) yielded a different distribution of photoproducts compared to the distribution observed in water. [PA] and [PB]—two of the three major photoproducts generated in water—were not produced at appreciable quantities in acetonitrile. Also, [PE], the reactive intermediate observed water

(see Figure 8), was more stable in acetonitrile (see Figure 16). Formation of [PD] was also observed to a greater extent in acetonitrile, whereas it was only observed at significant levels in alkaline aqueous systems ( $\text{pH} > 7$ ).

To explore possible relationships between photoproducts generated in acetonitrile and water, an aliquot of the photoproduct mixture generated in acetonitrile was diluted into 5 mM phosphate buffer at pH 7 and subsequently photolyzed (see Figure 16). Upon photolysis in aqueous solution, [PE] quickly decayed away while formation of [PA] and [PB] was observed. Notably, [PE] was stable in water in dark control experiments (Figure 17). Thus, the degradation of [PE] appears driven by light, which is consistent with its broad absorbance band from 300 to 340 nm (Figure 9). It appears that in aqueous environments [PE] acts as a source for the formation of [PA] and [PB], and potentially also [PC].

We note that several products observed during photolysis in acetonitrile were not detected during photolysis in water. These additional products were stable in water, both in the presence and absence of light. Thus, we assume the production of these additional products is an artifact of photolysis in acetonitrile, and they are not relevant to benoxacor photolysis in aqueous or environmental systems.

A second experiment was conducted to explore the stability of acetonitrile photolysis products in dark solutions of water. Notably, this second experiment was conducted at an initial benoxacor concentration of 100  $\mu\text{M}$ . Because the initial concentration was five times less than the previous acetonitrile experiment discussed above, nearly complete benoxacor conversion occurred (Figure 17). During this sixty minute photolysis period, [PE] accumulated and began to decay (see Figure 17) as was

observed in aqueous solution (see Figure 8). An absorption spectrum of product [PE] shows it readily absorbs light past 305 nm, having a local absorbance maximum at 320 nm (see Figure 9). Thus, in both aqueous and non-aqueous systems, [PE] decays away after sufficient photolysis time based on the starting benoxacor concentration. Greater stability of [PE] in acetonitrile is also evidence in the role of water in the formation of [PA] and [PB], as without water present [PE] is able to accumulate to a greater extent and not react to [PA] and [PB] (see Figure 12).

Finally, another set of photolysis experiments in acetonitrile was conducted, but aliquots of the reaction mixture were then spiked into either pH 5 or 9 buffer where photolysis was continued (Figure 18). [PD] did not continue to accumulate during photolysis at pH 5 and remained stable; however, [PD] accumulated during photolysis at pH 9 (Figure 18) as observed in previous aqueous experiments conducted at pH 9 (Figure 10). Thus, its continued formation is still dependent on pH in aqueous systems.

### 3.5. Long-Term Photolysis Experiments

[PA] and [PB] absorb light well within the solar spectrum, or  $\lambda \geq 305$  nm (see Figure 9), which means they also could be susceptible to direct photolysis under environmentally relevant conditions. [PC] absorbs light within the solar spectrum to a lesser extent (see Figure 9), but nevertheless could also be susceptible to direct photolysis over long enough time scales. To investigate whether [PA], [PB], and [PC] degrade when exposed to simulated sunlight, we conducted long-term, multi-day photolysis experiments. During these experiments, 10  $\mu$ M solutions of benoxacor were photolyzed over two complete cycles of 12 h of light (i.e., irradiation from the Xe arc lamp) followed by 12 h in the dark. This was intended to mimic how benoxacor and its photoproducts

might behave during diurnal light-dark cycling over multiple days in natural aquatic systems. We note that all products were stable in the dark, such that the results of these long-term photolysis experiments shown in Figure 13 simply present data as a function of total irradiation time (total 24 h).

Across 24 h of irradiation, we discovered that [PA], [PB], and [PC] all decay while a sixth product—product F [PF]—began to accumulate over time, as well as several more polar and less abundant products (Figure 20). Notably, [PF] was significantly less polar than [PA] and [PB], eluting approximately one minute before benoxacor (see Table 4). While [PF] appeared to be stable over these longer irradiation timescales, [PF] also absorbs light within the solar spectrum (see Figure 9).

Other minor products were present during long-term photolysis similar to the initial 1 h photolysis of benoxacor. As in the initial 1 h photolysis, we assumed all products exhibited comparable extinction coefficients for light absorbance at 220 nm, such that relative absorbance correlated directly to relative mass concentrations. [PF] was more abundant than other products under these considerations. In addition, the minor products eluted earlier than [PF] on a C-18 column during HPLC analysis, suggesting they are more polar. In favor of identifying a compound that appeared more abundant and showed a greater potential to bioaccumulate, we focused on isolating [PF] over the more minor, long-term photolysis products during our product identification.

### 3.6. Identifying Photoproducts

#### 3.6.1. Identifying [PE]

Before scaling up reactions, the identity of benoxacor photoproducts was explored using high-resolution mass spectrometry analysis of photoproduct mixtures generated

from 10  $\mu\text{M}$  initial benoxacor after one hour of irradiation in pH 7 phosphate buffer, similar to Figure 8. These analysis were conducted at the University of Iowa's High Resolution Mass Spectrometry Facility (HRMSF) using methods developed in the Cwiertny lab as described in Chapter 2. These mass spectrometry data were the basis for our initial structural assignments of benoxacor photoproducts.

To isolate the intermediate [PE], we first conducted LC high-resolution mass spectrometry (LC-HRMS) analysis on benoxacor photoproduct reaction mixtures after 5 minutes of photolysis, where we suspected the concentration of [PE] reached a relative maximum (see Figure 10, Figure 12). Unfortunately, LC-HRMS analysis of these mixtures yielded no observable products. We suspect [PE] ionized poorly during LC-HRMS analysis as 10  $\mu\text{M}$  benoxacor standards also ionized poorly using the same LC-HRMS methods. Given [PE]'s propensity to accumulate to greater concentrations in acetonitrile (see Figure 12, Figure 16), we conducted complementary analysis of samples generated in acetonitrile and 500  $\mu\text{M}$  benoxacor via HRMS and GC-MS. Once again, LC-HRMS yielded no observable products; however, GC-MS showed benoxacor and acetonitrile-generated photoproducts ionized well during analysis. Although difficult to directly correlate products observed on HPLC to those on GC-MS, we observed a peak with a significant relative abundance compared to other products with an  $m/z$  for  $\text{M}^{++}$  at 223 (Figure 21). We believe this compound is [PE]. Based on mechanistic data in the literature [42], a monchlorinated compound with  $\text{M}^{++}$  at  $m/z$  223 fits our proposed pathway for the formation of [PE] (Figure 22). Because of the natural abundance of the chlorine-37 isotope, a chlorinated photoproduct would result in a peak approximately two mass units larger ( $m/z \sim 225$ ) than the parent ion. If two chlorines were present, this

isotope peak would be approximately 2/3 the percent abundance of  $M^{+}$ ; if one chlorine is present, the isotope peak would be 1/3 the percent abundance of  $M^{+}$ . In our GC spectrum, [PE] appears to be a monochlorinated compound based on the characteristic isotope peak at  $m/z$  225 (Figure 21). This is notable, as some transformations of dichloroacetamide safeners have produced monochlorinated byproducts with structures—and potentially also bioactivities—comparable to “active” herbicide ingredients [5, 11]. Although [PE] appears to be a relative short lived intermediate in simulated sunlight (see Figure 10, Figure 12), if [PE] was formed and transported out of the photic zone before subsequent photolysis it might impose a new toxicity to aquatic life.

Based on the observed concentration profiles, trends in photoproduct formation in water versus acetonitrile, and the monochlorination of [PE], we propose that [PE] is the first primary photoproduct and that other products (e.g., [PA], [PB] and [PC]) are likely generated from its subsequent photochemical reaction, where some products' formation (e.g., [PA] and [PB]) likely depend on the presence of water (see Figure 12).

Our assignment of [PE]'s structure (see Figure 22) is based on GC-MS data (see Figure 21) and proposed mechanisms for the direct photolysis chloroacetamide herbicides [6, 9]. For example, the direct photolysis of metolachlor under UV light (Figure 23) and acetochlor (Figure 24) occurs via radical elimination reactions of chlorine and the subsequent addition of an oxygen atom via water [6, 9]. Both studies proposed various ring closure steps alongside the addition of oxygen via water. Based on these earlier reports and the similarities between chloroacetamide and dichloroacetamide structures,



we hypothesize that comparable phototransformation pathways take place during benoxacor photolysis.

### 3.6.2. Identifying [PA], [PB], and [PC]

To identify [PA], [PB], and [PC], we photolyzed 10  $\mu$ M benoxacor in 5 mM pH 7 phosphate buffer for one hour and analyzed the reaction mixture through LC-HRMS. Although benoxacor and [PE] were difficult to observe through LC-HRMS, [PA-C] were able to ionize to a measureable amount. [PA] had a parent ion mass  $(M + H)^+$  at  $m/z$  206.1 (Figure 25) with an  $(M+Na)^+$  adduct at  $m/z$  228.1 and a  $(M+K)^+$  adduct at  $m/z$  244.0. The  $(M+K)^+$  was likely so abundant because the reaction was conducted in 5 mM potassium phosphate buffer. Notably, there was no evidence of a chlorine substituent in the [PA] structure (i.e., no chlorine-37 isotope peak at  $m/z$   $\sim$ 208). Likewise, analysis of [PB] (Figure 26) and [PC] (Figure 27) revealed parent ion masses  $(M + H)^+$  at  $m/z$  206.1 and 206.1, respectively, with the same sodium and potassium adducts observed for [PA]. Additionally, the characteristic signatures of chlorine substitution were also absent in their mass spectra. Thus, the three most abundant benoxacor photoproducts after one hour of photolysis appeared to be fully dechlorinated and isotopes of one another.

Evidence of complete dechlorination is also an important clue in determining the potential structures for [PA], [PB], and [PC]. Benoxacor's mass is 259.02 amu, such that the loss of two chlorine-35 atoms would be expected to result in a product with a mass of 189.1 amu. Because all three photoproducts have a parent ion at  $m/z$   $\sim$ 206.1, some sort of addition reaction must also be taking place during product formation. Based on the difference in mass between the photoproducts and a fully dechlorinated benoxacor

derivative, it appears the addition of oxygen atoms via water was a likely source for this mass.

To analyze [PA-C] via direct injection HRMS for product identification, we conducted a smaller subset of “scaled-up” experiments. In these experiments, the mass of benoxacor was greatly increased to facilitate generation of enough photoproduct for isolation via liquid-liquid extraction and semi-preparative column fractionation—approximately 1-2 mg of [PA-C] each were isolated. Using direct injection HRMS data, we propose structures for [PA], [PB], and [PC] in Figure 28. To propose the mechanism for formation of [PA], [PB], and [PC], we examined the same studies of metolachlor and acetochlor photolysis used to propose [PE]’s structure and mechanism [6, 9]. As [PE] appears to be the intermediate that leads to formation of [PA], [PB], and [PC], we believed that the formation of [PA-C] proceeds through [PE] and results in elimination of –Cl, evidenced by HRMS data (see Figure 25-27).

Interestingly, [PC] still forms in acetonitrile, whereas [PA] and [PB] do not, although [PA-C] appear to be isomers of one another. [PE] is less stable in aqueous environments and the potential for oxidation by water could push the reaction pathway from [PE] in the direction of [PA-C]—where [PA] and [PB] are observed in greater abundance—rather than the observed [PE] to [PC] (and several other products) observed in acetonitrile.

A search through chemical databases reveals structures [PA-C] are not yet reported in the literature. As such, no toxicological data exists on these products yet. Because these compounds lose both chlorine atoms and do not form a chloroacetemide

structure, it is likely their chemical properties likely differ from chloroacetamide herbicides, and that they don't have the same herbicidal activity [1].

### 3.6.3. Identifying [PD]

Unfortunately, we have not been able to identify [PD] as of yet. As in the case of [PE], [PD] seems to ionize poorly during LC-HRMS analysis. However, based on product yield plots (see Figure 12), high pH experiments (see Figure 10, Figure 13), and the proposed mechanism for the formation of [PA-C] from [PE] (see Figure 28), we believe [PD] is likely formed through base catalyzed elimination of HCl from [PE] (see Figure 22), a well described E-2 elimination reaction [31]. Thus, like [PA-C], we believe [PD] is a fully dechlorinated compound formed through the monochlorinated [PE]. Unlike [PA-C], we believe [PD] is only formed in alkaline conditions (see Figure 12, Figure 13).

### 3.6.4. Identifying [PF]

Interestingly, although we first believed that [PA], [PB], and [PC] were the major products formed during benoxacor photolysis, analysis of their individual absorbance spectra revealed that [PA] and [PB] could absorb light within the solar spectrum (i.e.,  $\lambda \geq 300$  nm) (see Figure 9). Under environmentally relevant conditions, benoxacor and its photoproducts would likely be exposed to sunlight and photolyzed over the course of several day/night cycles, not just one hour intervals. Thus, we anticipated that [PA] and [PB] would be exposed to sunlight significant amounts of sunlight as well.

Long-term photolysis of benoxacor revealed the formation of a potential “sink” product less polar than benoxacor but more polar than the other major products based on retention times on a C-18 column during HPLC analysis (see Figure 20, Table 4). To

isolate and identify this late forming photoproduct, a scaled up reaction was conducted similar to the experiment conducted to isolate [PA], [PB], and [PC] for NMR described above and in materials and methods. After completion of this experiment, only 9 mg of crude reaction residue was extracted from an initial 20 mg benoxacor in 1 L water after over 30 hours of photolysis under a 1000W Xe lamp. Following HPLC separation to isolate [PF] via a semi-preparative column, not enough [PF] was extracted to register on an analytical balance.

To generate a measurable, milligram quantity of [PF], 50 mg of benoxacor was dissolved into 20 mL of acetonitrile (to ensure solubility), which was spiked into approximately 500 mL deionized water. This solution was photolyzed under a 200 W Mg(Xe) lamp with a 250 nm cut-on filter. While benoxacor and its photoproducts would not be exposed to wavelengths of light this low in natural systems, HPLC analysis revealed [PF] still formed and [PA], [PB], and [PC] decayed under these conditions in a way similar to the decay observed in Figure 20. Significantly, the rate of reaction was greatly increased and [PF] formed noticeably faster exposed to low wavelength UV light compared to photolysis with the 1000 W Xe lamp ( $\lambda > 305$  nm). This solution was photolyzed for a total of 12 hours over two days and extracted into chloroform, resulting in 29 mg of crude reaction residue. HPLC isolation of [PF] via a semi preparative column gave approximately 1 mg of [PF] residue.

Subsequent direct injection HRMS analysis of the isolated fraction of Product F gave a parent ion (M+H)<sup>+</sup> at  $m/z$  178.0860 (Figure 30). Based on HRMS data, chloroacetamide photolysis mechanisms (see Figure 23, Figure 24), and proposed mechanisms of benoxacor metabolism in *Zea mays* cells[42], we were able to propose the

structure in Figure 29 for [PF]. Initially, we were surprised to find that a compound with the structure of [PF] would be significantly less polar than [PA], [PB], and [PC], and that [PF] would have a more comparable polarity to benoxacor. Largely, we were surprised because of perceived structural similarities of [PF] to [PA], [PB], and [PC]. Except for the number of oxygen molecules, which only differ by one, the early eluting products [PA], [PB], and [PC] are comparable to [PF], and we believed close enough in structure to have similar polarities. To confirm that retention times were as expected for these four compounds, we compared experimental and predicted octanol-water partitioning coefficients. Experimentally, benoxacor was shown to have a LogP: octanol-water value of 2.70, a moderately non-polar compound. For comparison, using the software ChemDraw and its predictive LogP: octanol-water calculator benoxacor has a LogP value of 2.3. Likewise, using ChemDraw the LogP values for [PA], [PB], and [PC] range from 0.52 to 1.02. Using the same experimental LogP calculator, we found a value of 1.23 for [PF]. While these values are not exact, they provide a basis for explaining the observed relative elution times on a C-18 column using our HPLC method.

A search through several chemical databases reveals [PF] is also a newly reported structure. As such, there is no toxicological data for [PF]. Future studies might include scaled up isolation or synthesis of [PF] to explore toxicological effects, both from the isolated compound and in herbicide product mixtures. Significantly, [PF]—like [PA], [PB], and [PC]—does not have a chloroacetamide functional group. Thus, it is not anticipated that product F has the same herbicidal or toxicological characteristics as chloroacetamide herbicides such as metolachlor and acetochlor.

### 3.7. Conclusions

Benoxacor rapidly photolyzed under environmentally relevant conditions to yield new and previously unreported transformation products. Because of benoxacor's short half-life under simulated natural sunlight, it is likely direct photolysis will be an important environmental fate pathway for this widely used dichloroacetamide safener, a pathway which has not been acknowledged by its current legal registration [19]. Most photoproducts benoxacor generated were fully dechlorinated suggesting they will have different toxicological and biochemical characteristics than both benoxacor and chloroacetamide herbicides; however, the intermediate [PE] is monochlorinated which leaves open the possibility this compound has more herbicide-like toxicity and bioactivity. Because these products are all more polar than benoxacor, and because benoxacor is highly mobile in the environment [2], it is likely these transformation products will remain mobile in surface waters as well.

Although we are confident in the chlorination of benoxacor photoproducts based on HRMS data (i.e, [PE] is monochlorinated and [PA], [PB], [PC], and [PF] are dechlorinated), the structures proposed are based on hypothetical pathways derived from benoxacor and chloroacetamide herbicide studies [6, 9, 42]. As of yet, we have not been able to confirm benoxacor products via synthetic reference compounds and convincing NMR data. Such confirmation would be valuable in future studies; however, this study exists as an overview of benoxacor photolysis to demonstrate its relevance in benoxacor environmental transformations. Because of the complex systems created during photolysis, preliminary product identification is often done on the basis of HRMS data [6, 9], as we reported here.

Benoxacor photolysis illustrated how photochemical transformations can yield markedly different compounds from both the initial parent compound and among the photoproducts generated. Further, it illustrates and what an important, complex, and ultimately unpredictable fate pathway photolysis can be.

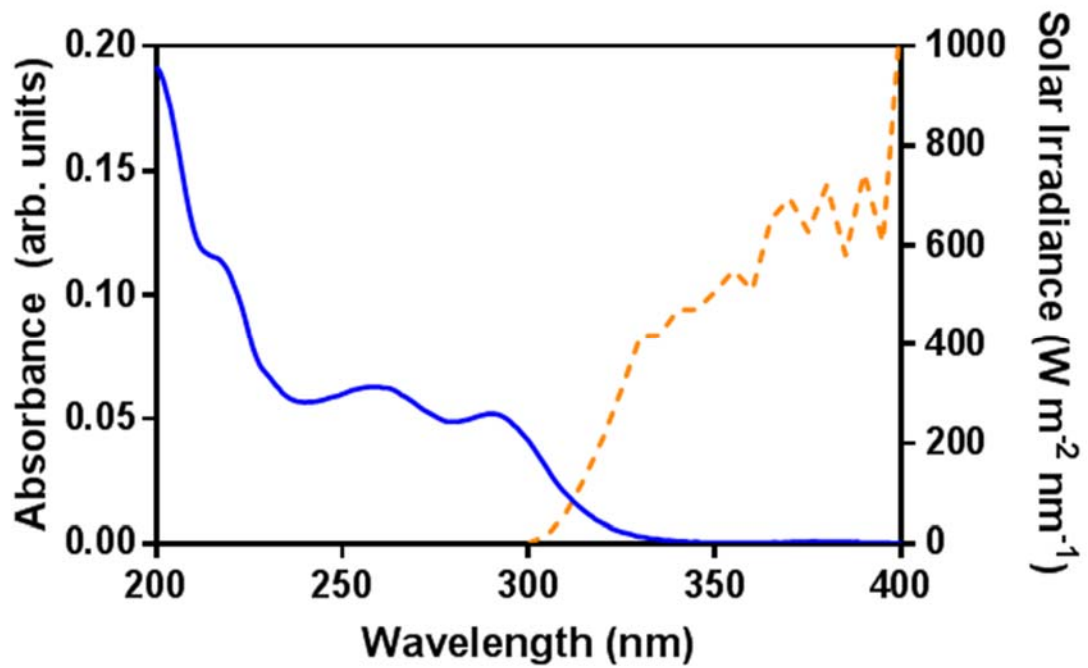


**Figure 7** Solid blue line shows UV-vis absorbance spectrum of benoxacor. Dashed line represents typical solar irradiance near sea-level. Maximum absorbance peaks were found at 216, 258, and 290 nm.



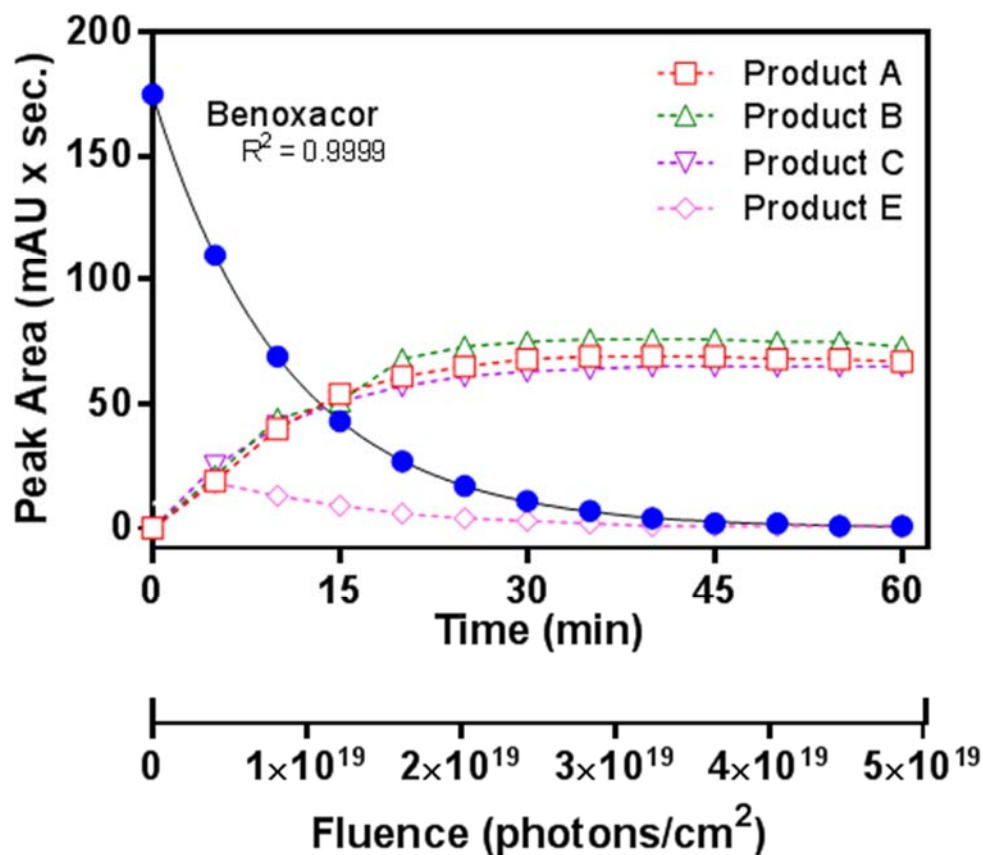


**Figure 8** Benoxacor photolysis at pH 7 using simulated sunlight from a 1000 W Xe lamp ( $\lambda \geq 305$  nm; AM 1.5 filter; Irradiance:  $8.81 \times 10^{-3} \text{ W cm}^{-2}$ ). Benoxacor decay was modeled as a first order process, with exponential decay model fit shown (solid black line;  $k_{\text{obs}}=0.093$ ,  $R^2 = 0.9999$ ). At a detection wavelength of 220 nm, three major photoproducts (defined as Products A, B, and C) and one minor product (Product E) were observed (where dashed lines are not model fits but simply shown to help illustrate the concentration profile of products over time).

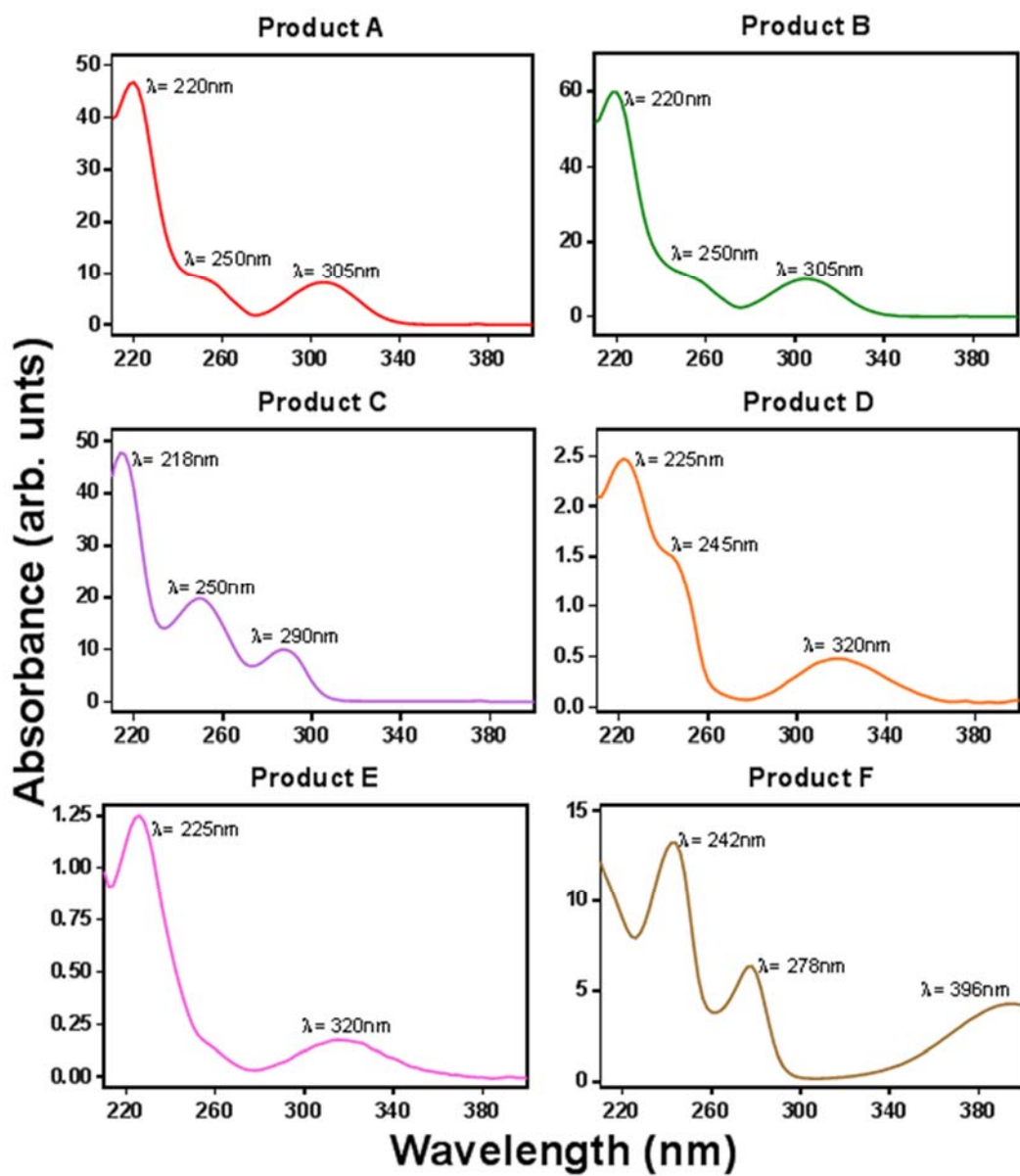
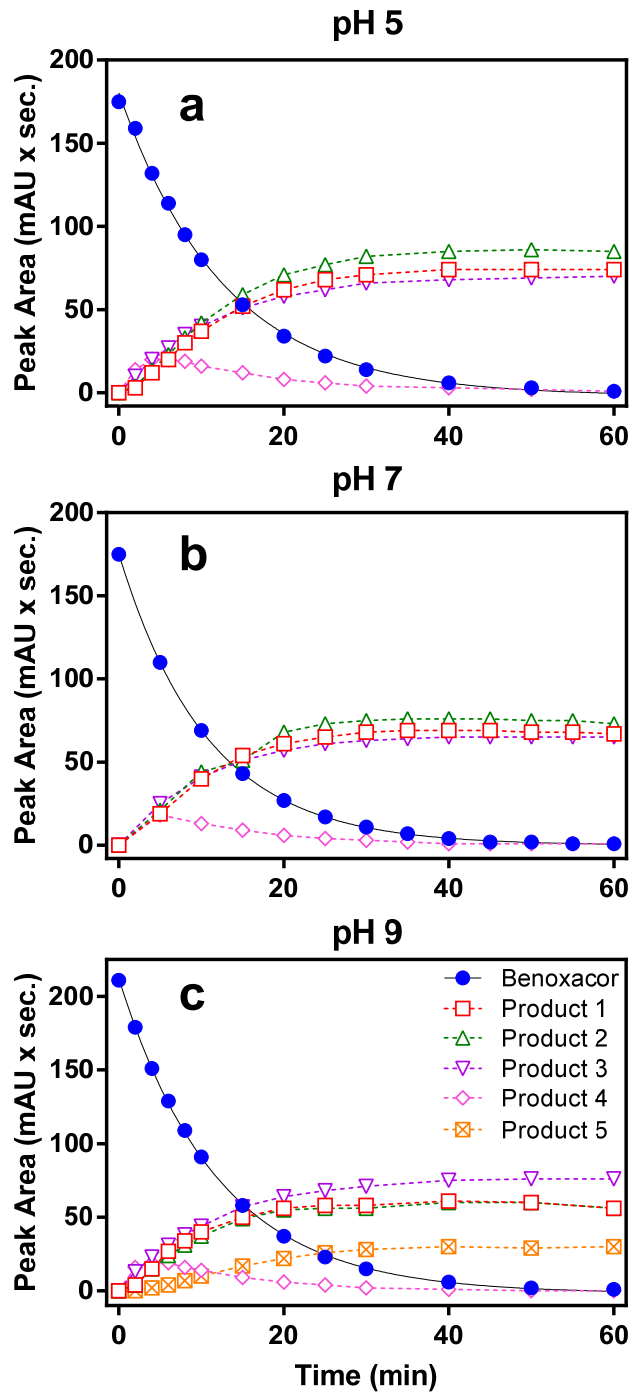
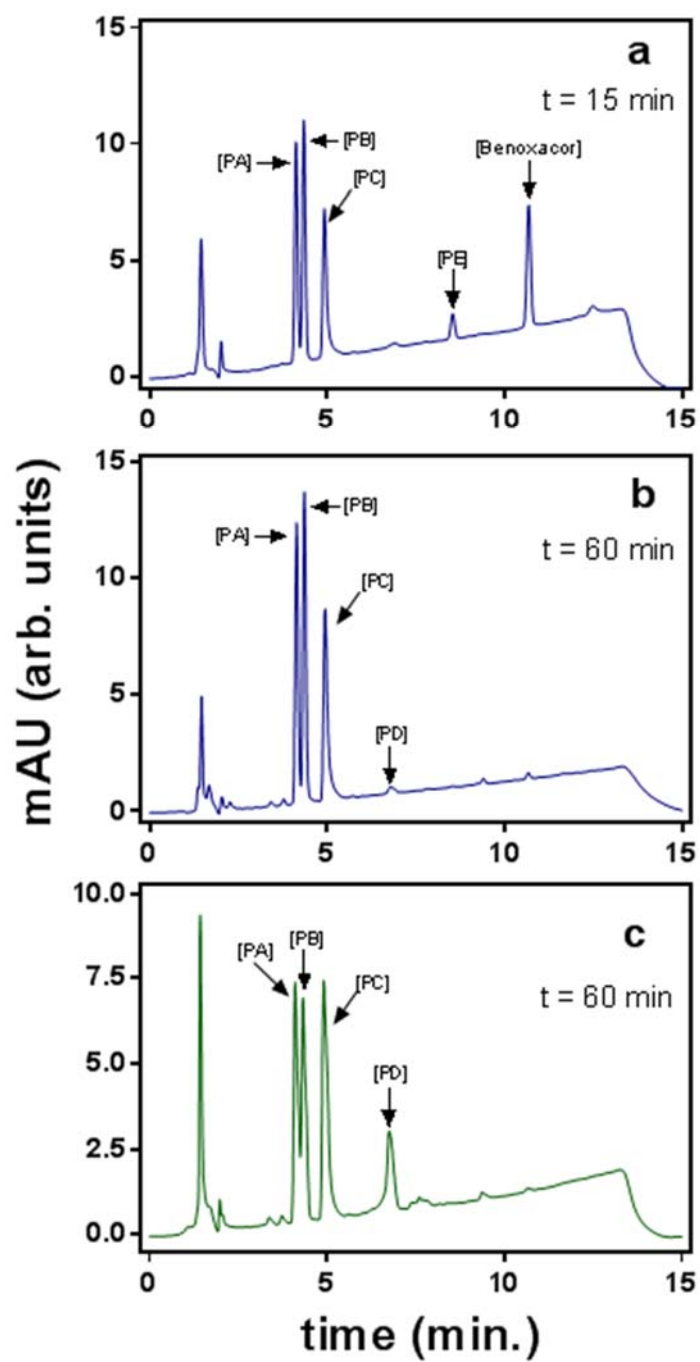


Figure 9 Absorbance spectra of benoxacor photoproducts.



**Figure 10** Benoxacor rate of decay shows little variance across pH 5 (10a), 7 (10b), and 9 (10c). However, at pH 9, product D (denoted by orange squares) has a significant peak area.



**Figure 11** HPLC traces of benoxacor reactions mixtures after 15 min of photolysis at pH 7 (5a), 60 min of photolysis at pH 7 (5b), and 60 min of photolysis at pH 9 (5c) (monitored at 220 nm).

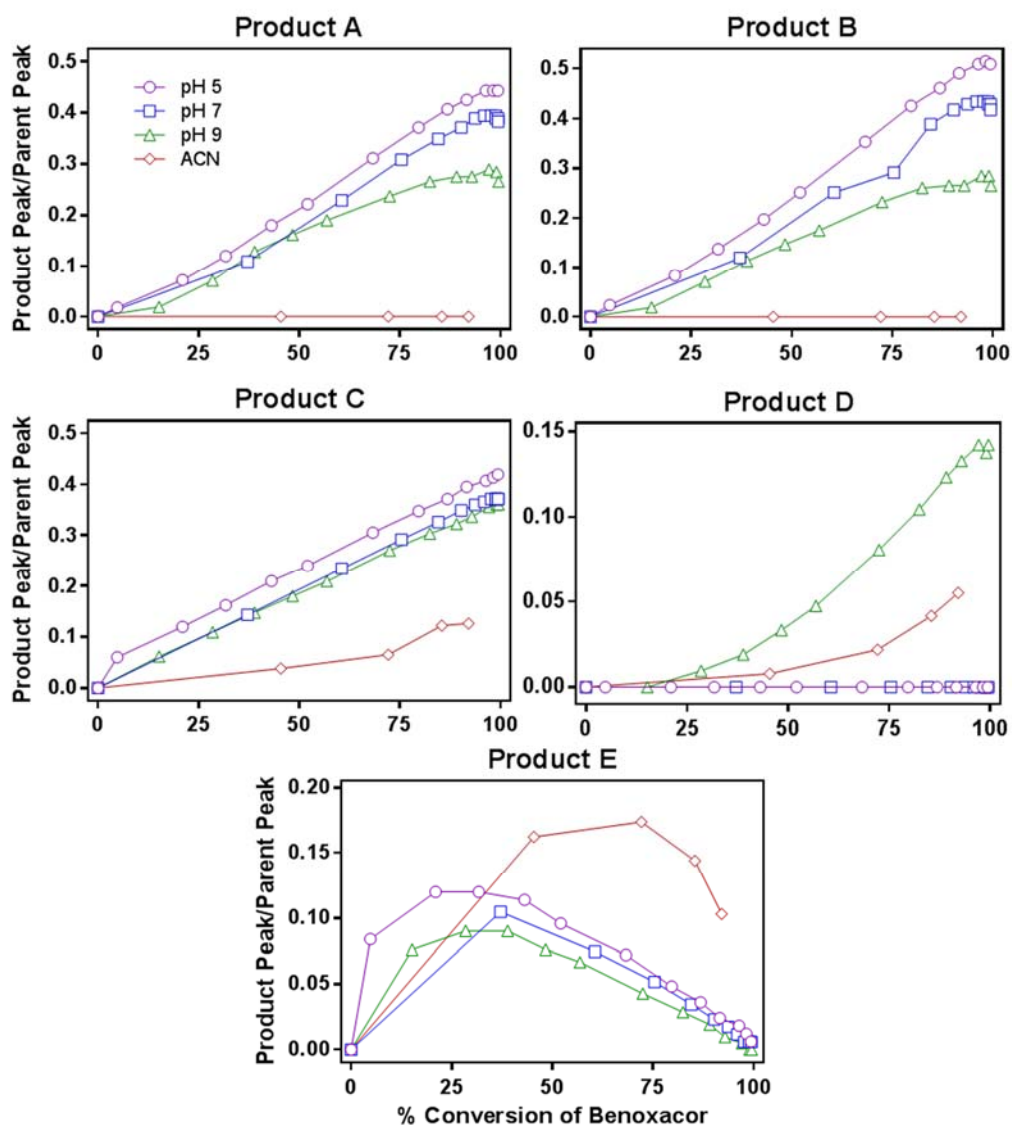


**Figure 12** Conversion of benoxacor photoproducts at pH 5, 7, 9 and in acetonitrile. Product peaks at a given percent conversion are normalized to the initial benoxacor starting peak area.

## Iowa City River Water

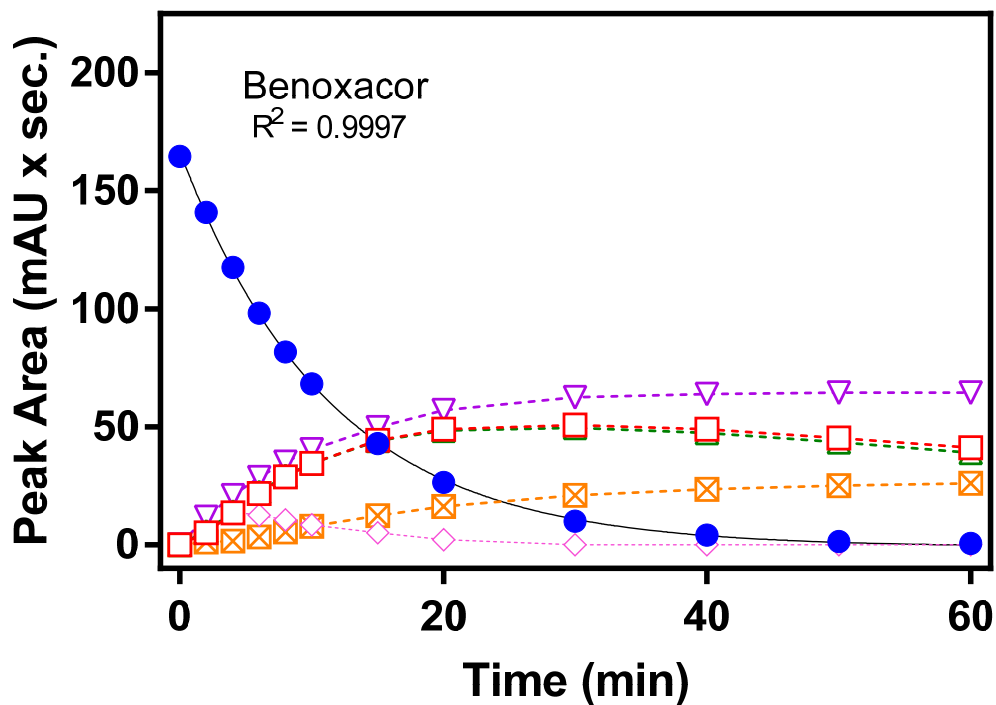


**Figure 13** Benoxacor photolyzed in Iowa City river water (pH = 8.5). Similar to benoxacor photolysis at pH 9, product D is a major product at pH 8.5. This figure shows benoxacor photolyzes the same way in environmentally as it does in simulated natural aquatic systems.

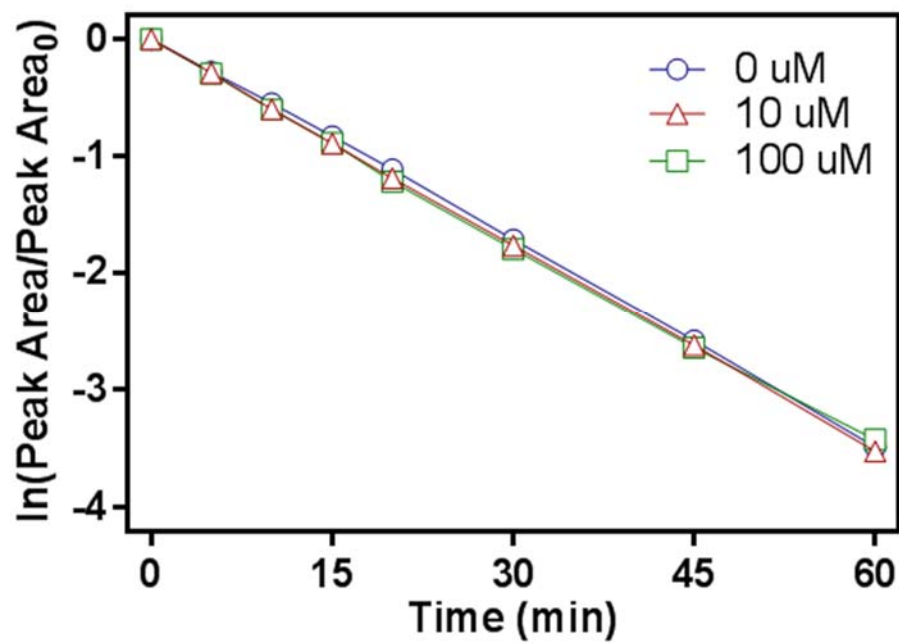


**Figure 14** Integrated first-order rate of benoxacor photolysis in pH 7 buffer in 0, 10, and 100 uM metolachlor.

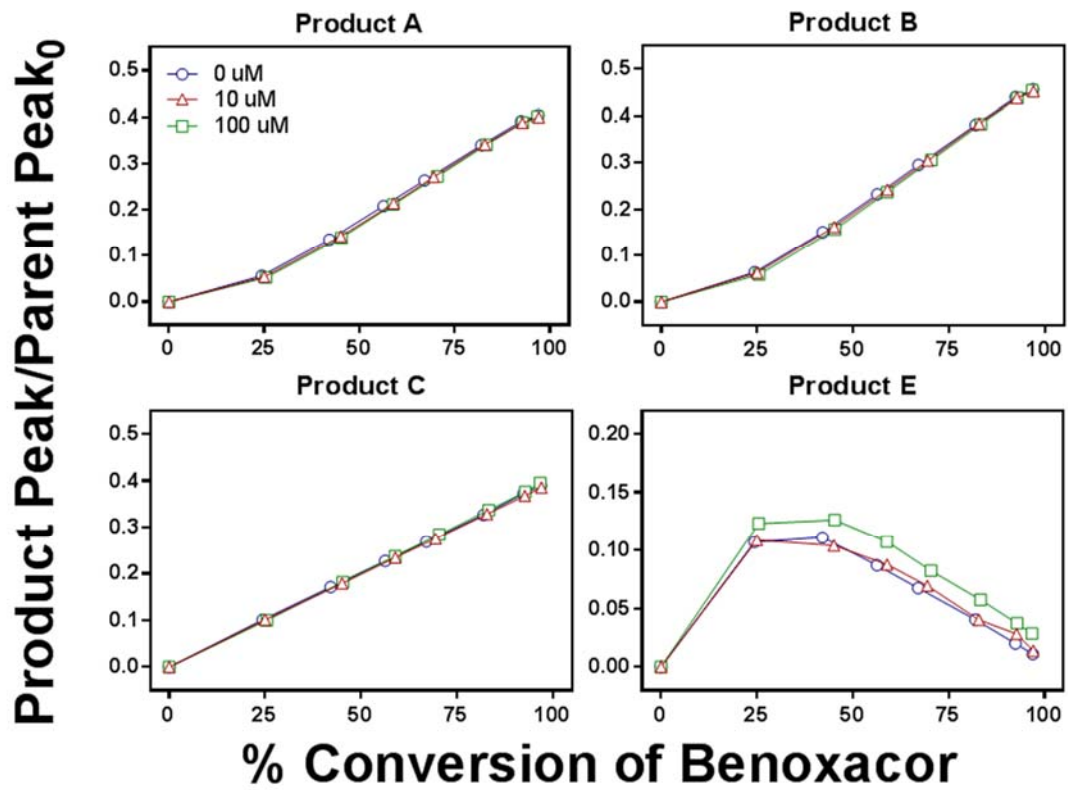
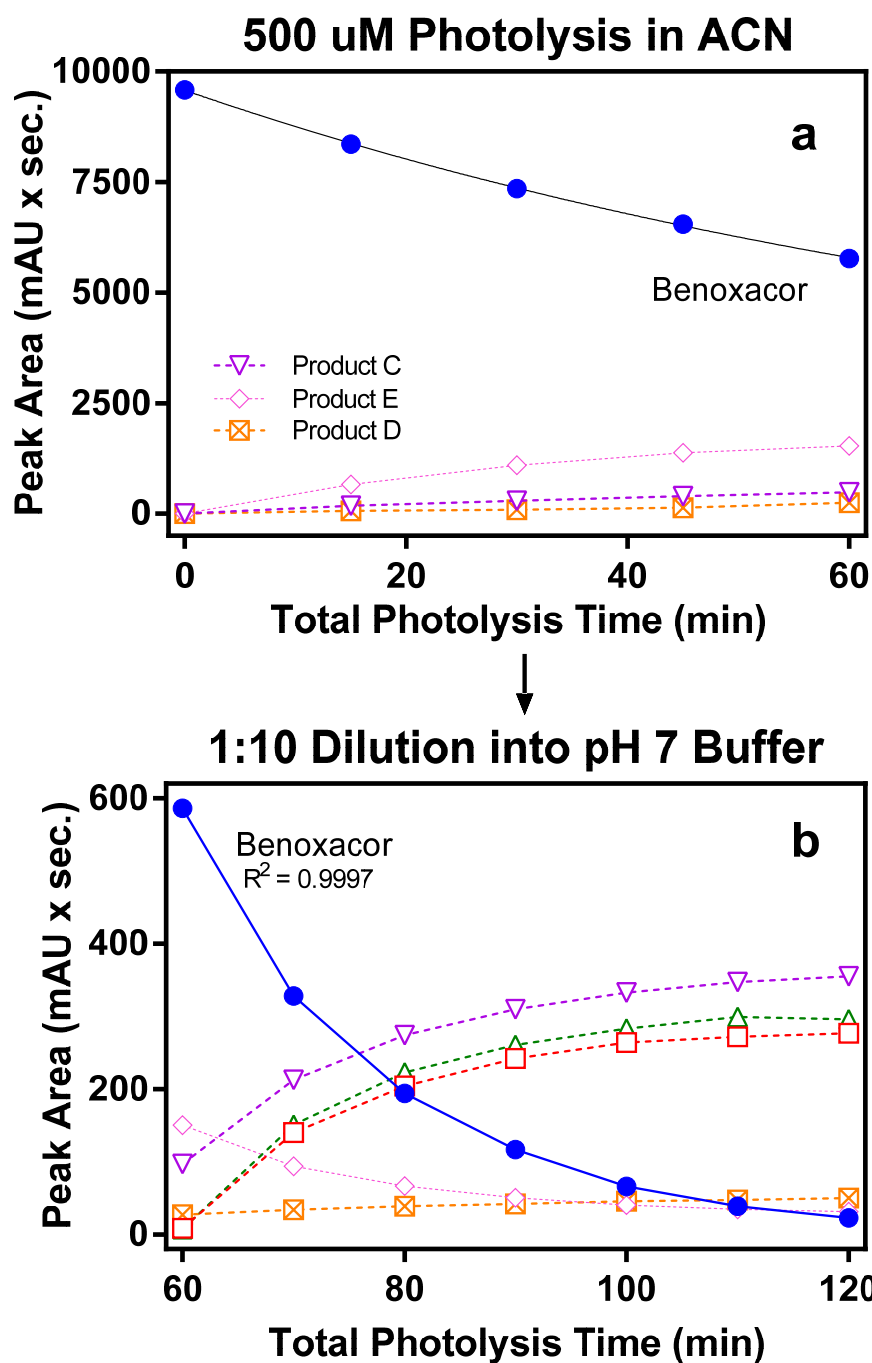
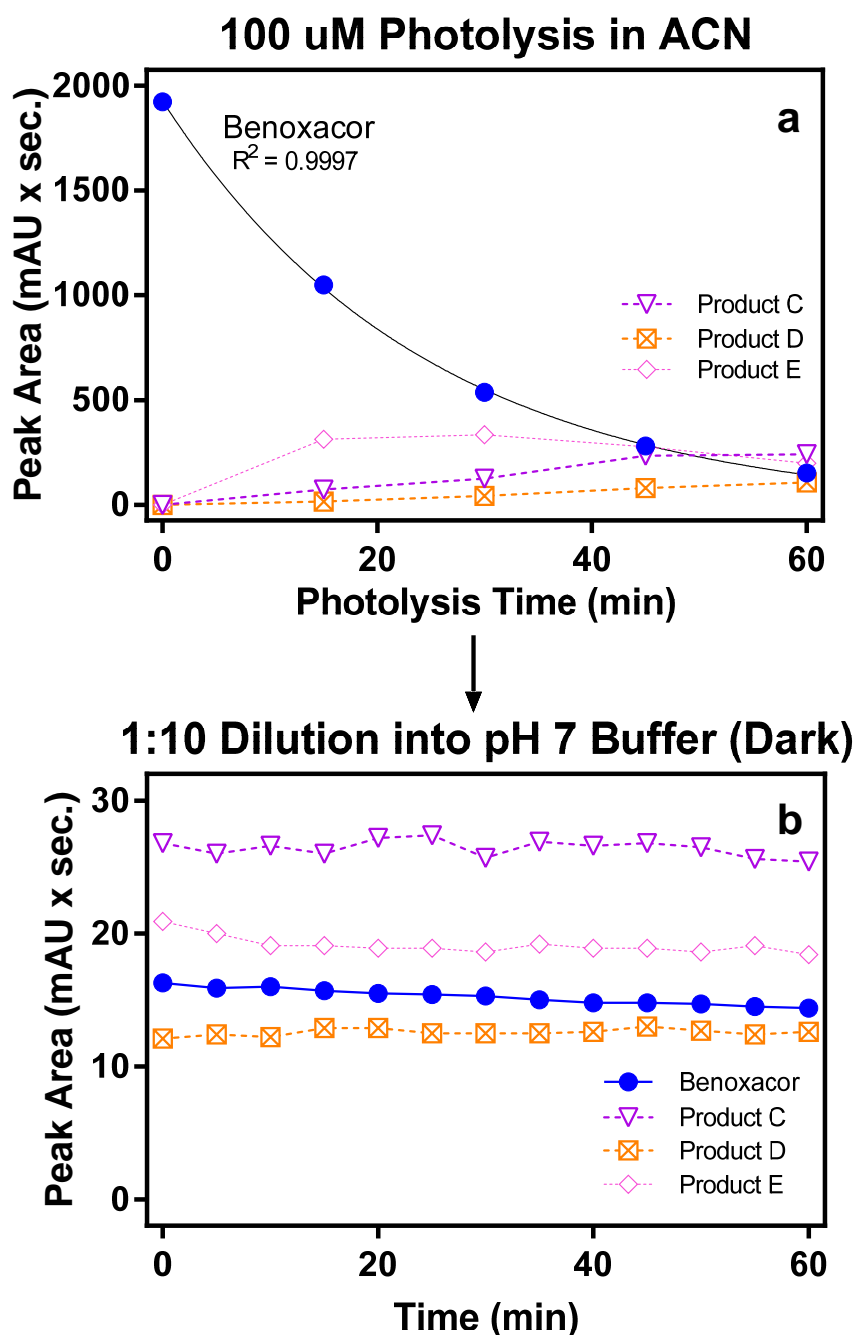


Figure 15 Benoxacor product yield plots in 0, 10, and 100 uM metolachlor.





**Figure 16** 500  $\mu$ M benoxacor photolysis in acetonitrile for 60 minutes. Subsequently, a 2 mL aliquot is spiked into pH 7 buffer where photolysis continued. Products C, D, and E accumulate in acetonitrile, but when photolysis is continued in water product E (pink diamonds) decays and products A and B (red squares and green triangles, respectively) begin to accumulate.



**Figure 17** 100  $\mu$ M benoxacor photolysis in acetonitrile for 60 minutes. Subsequently, a 2mL aliquot is spiked into 20 mL pH 7 buffer where the solution is placed in the dark and photolysis is stopped. Products C, D, and E are stable over this time period, as is the parent compound benoxacor. Formation of products A and B is not observed.

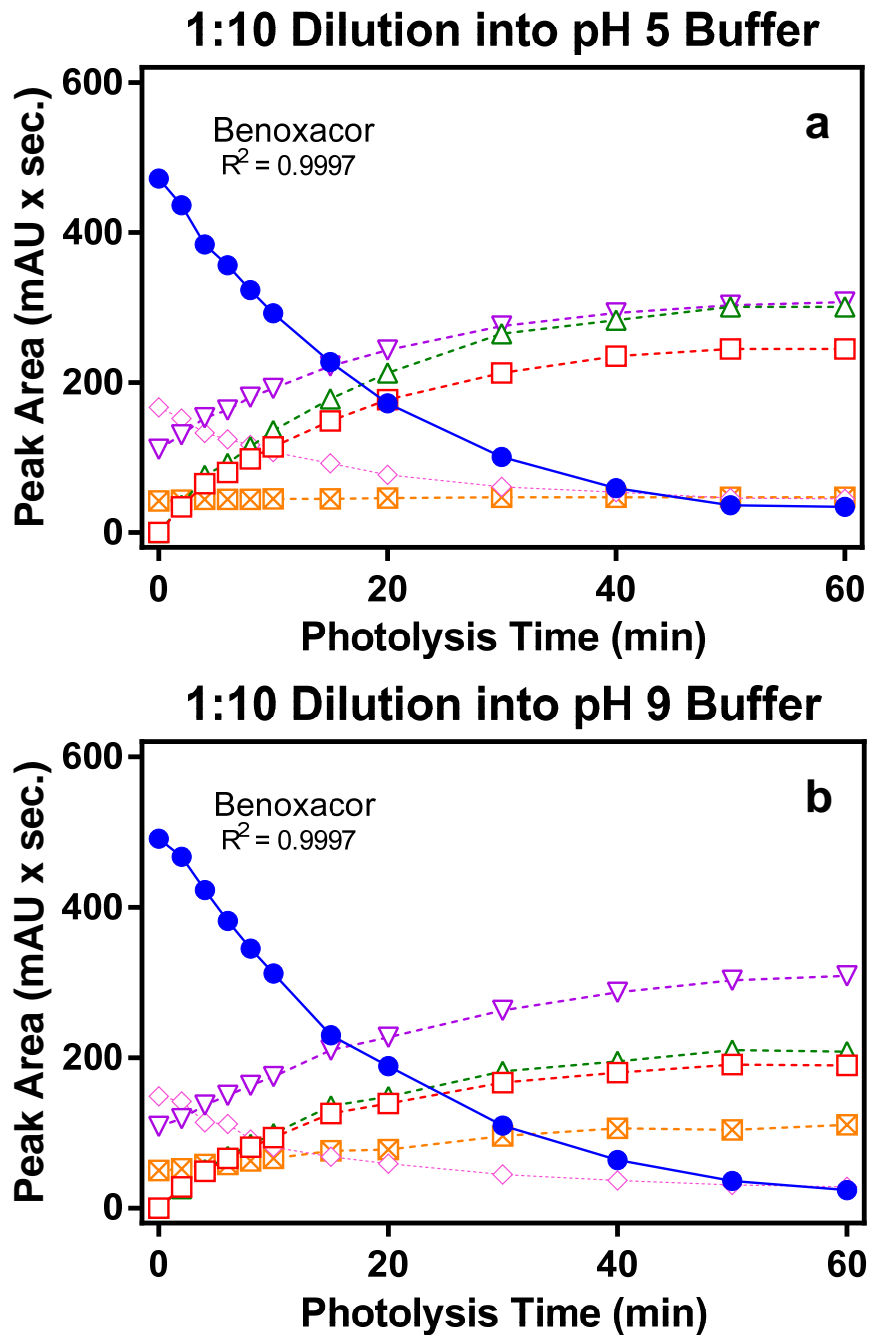


**Figure 18** Plots show continued photolysis of acetonitrile aliquots in pH 5 and pH 9 buffer (photolysis in acetonitrile not shown). Product E (orange squares) continues to accumulate during pH 9 photolysis. It does not continue to accumulate during pH 5 photolysis, however it also does not decay.

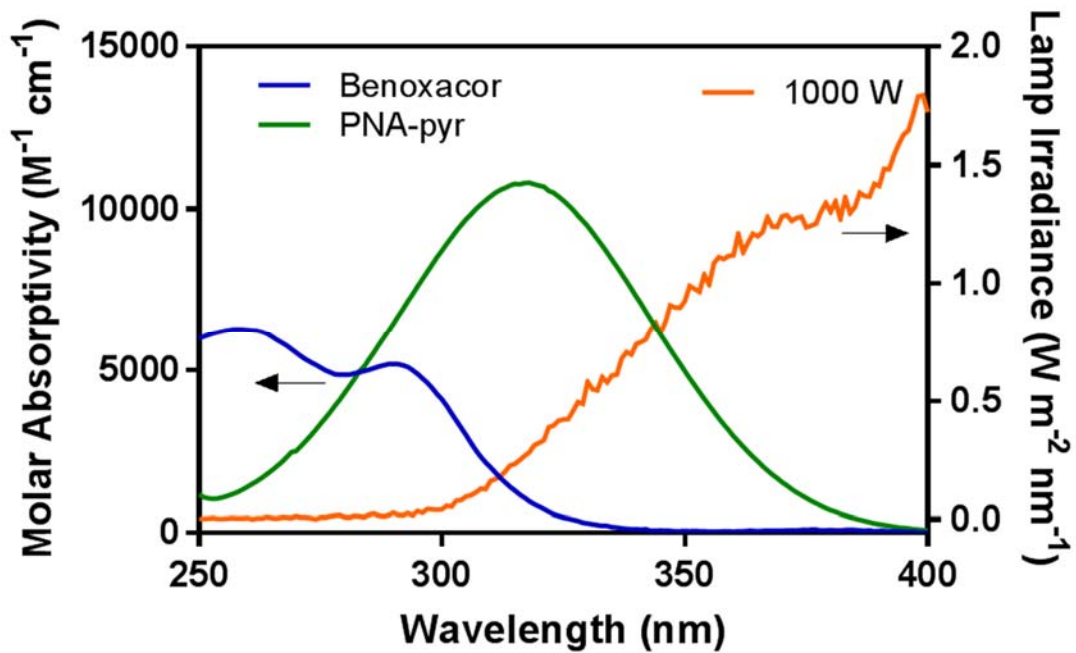


**Figure 19** PNA-pyr actinometer and benoxacor molar absorptivity compared to irradiance of 1000 W Xe lamp with 305 nm cut-on filter and AM 1.5 filter. Quantum yield was calculated between 300 and 400 nm.

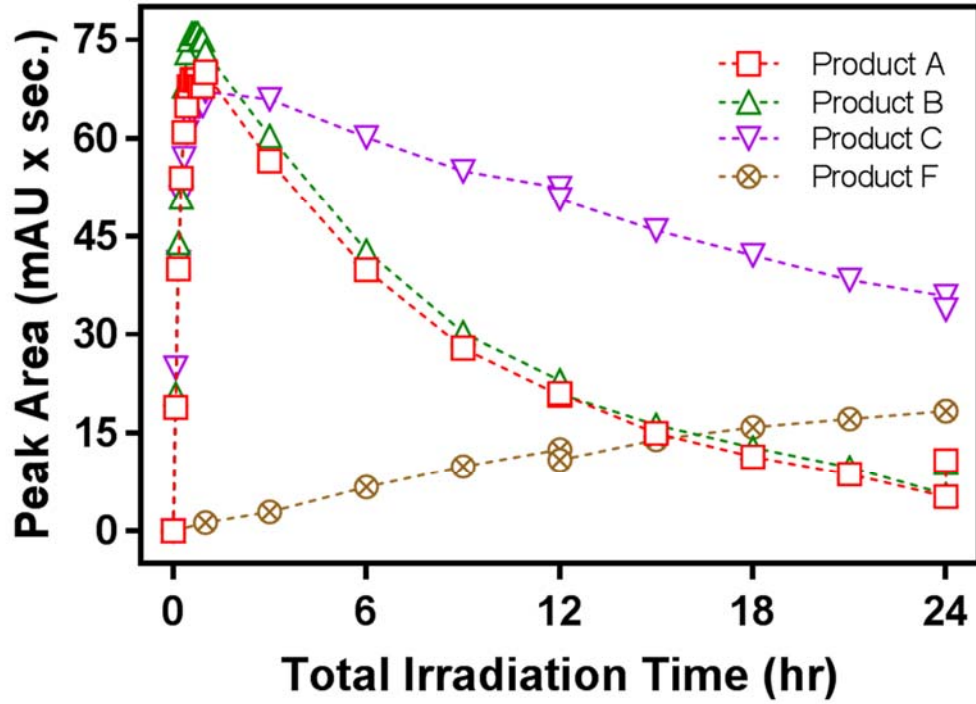


**Figure 20** Long-term photolysis of benoxacor reveals [PA] and [PB] are directly photolyzed and a sixth and significantly less polar major product, [PF], begins to accumulate.



**Figure 21** GC-MS spectrum of [PE].

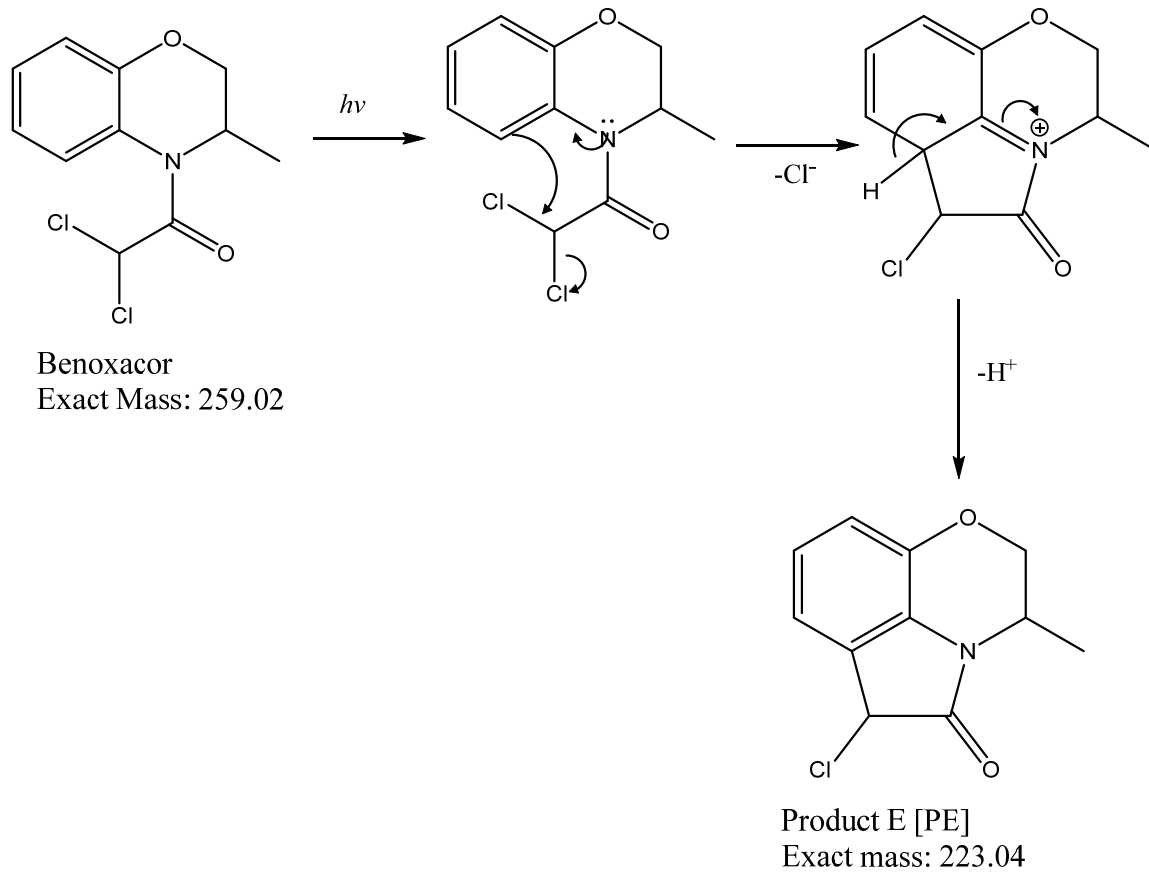


**Figure 22** Mechanism for the formation of [PE] via benoxacor direct photolysis.

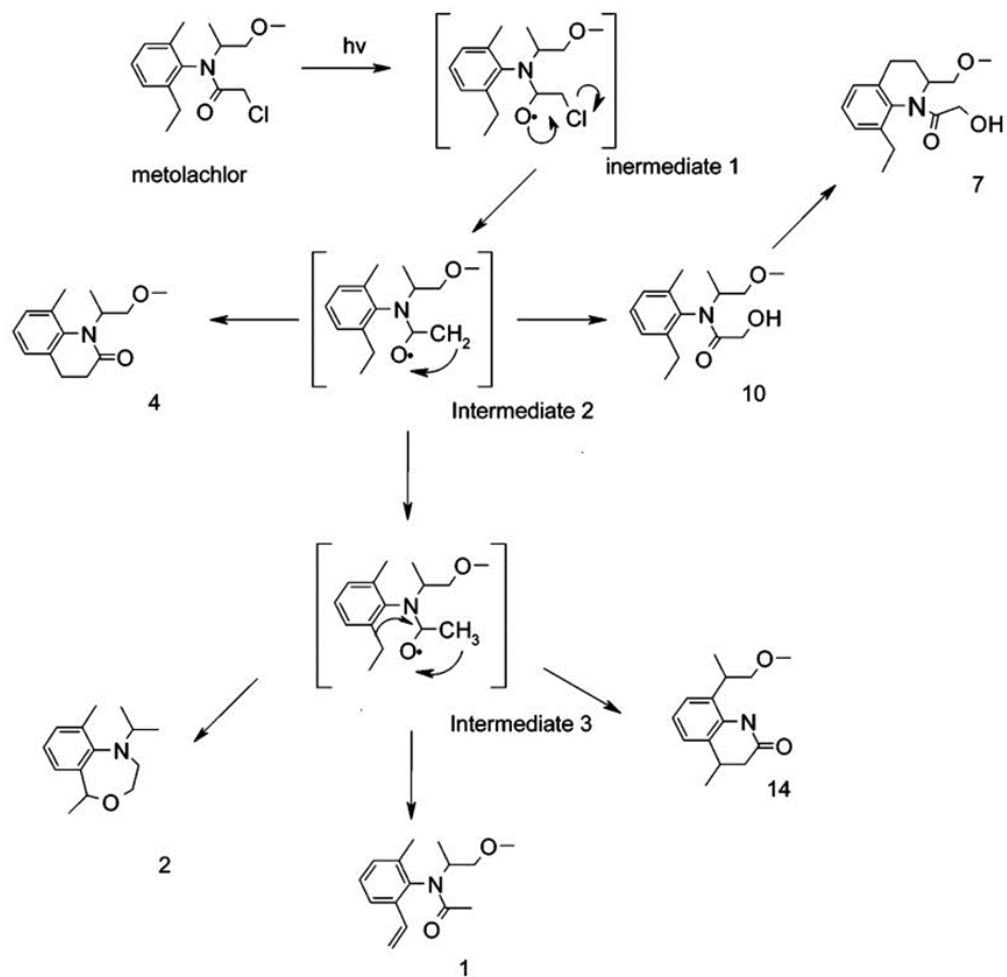


**Figure 23** Proposed mechanism for photolysis of metolachlor under UV light [6].



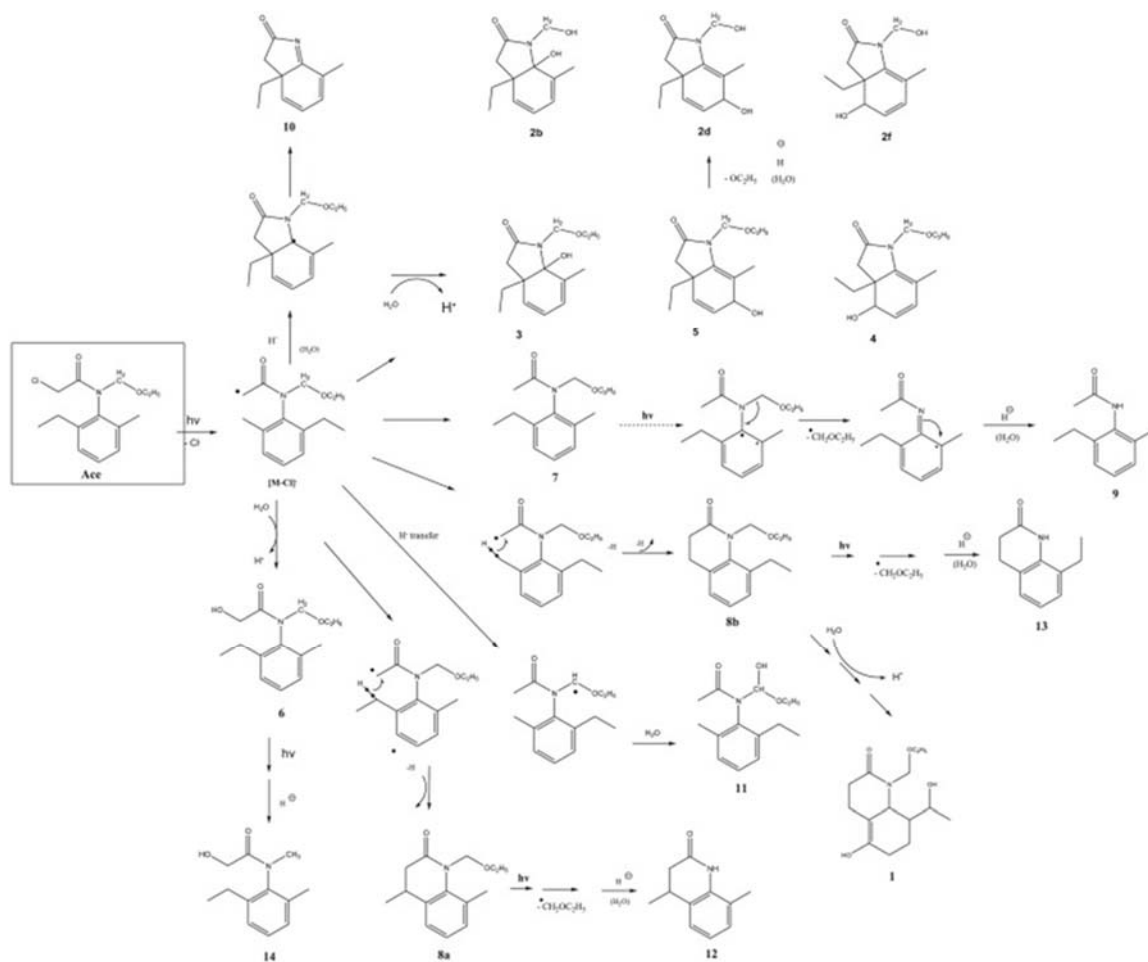


**Figure 24** Proposed mechanism for photolysis of acetochlor under UV light [9].

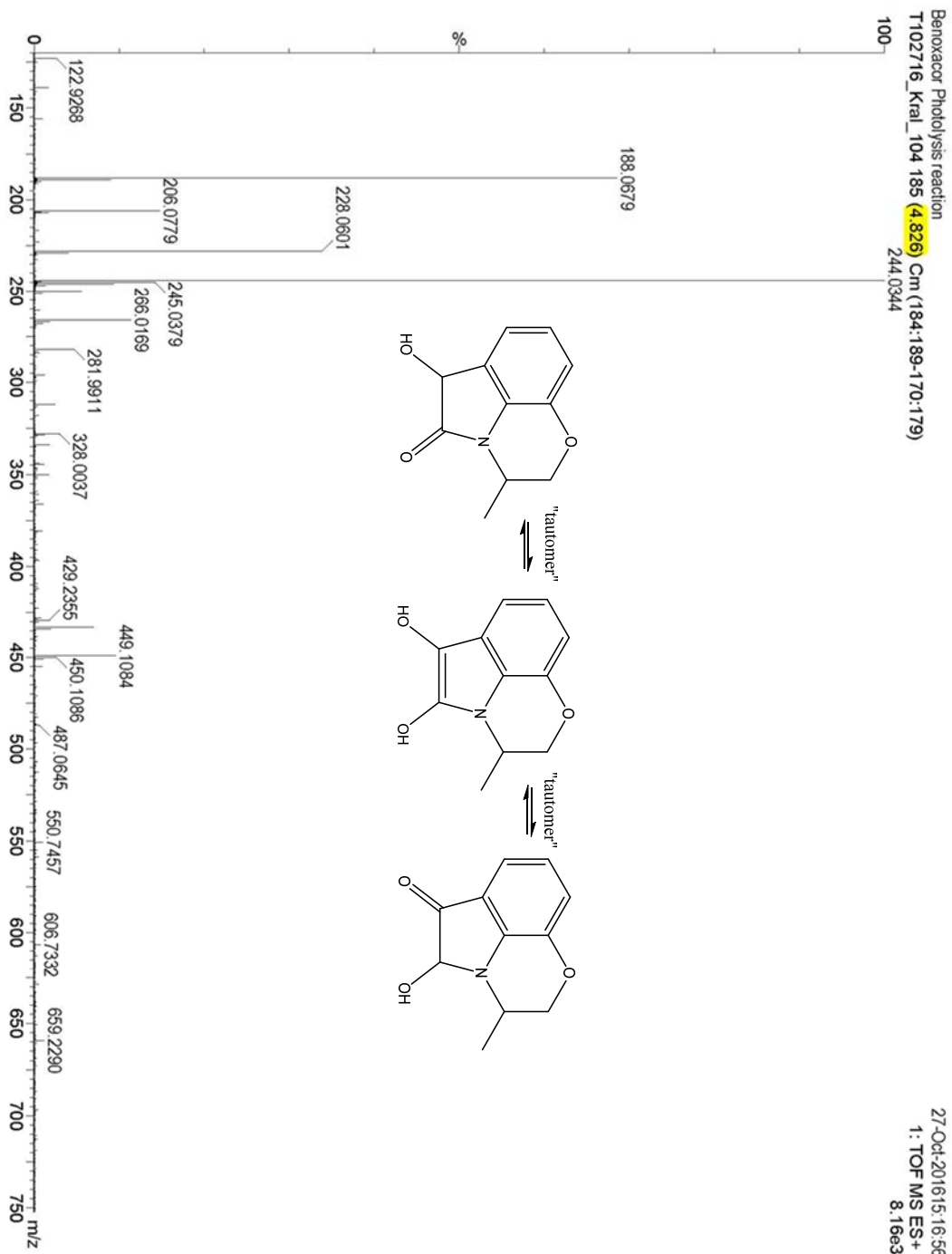


**Figure 25** High resolution mass spectrum of [PA] obtained through LC-HRMS.

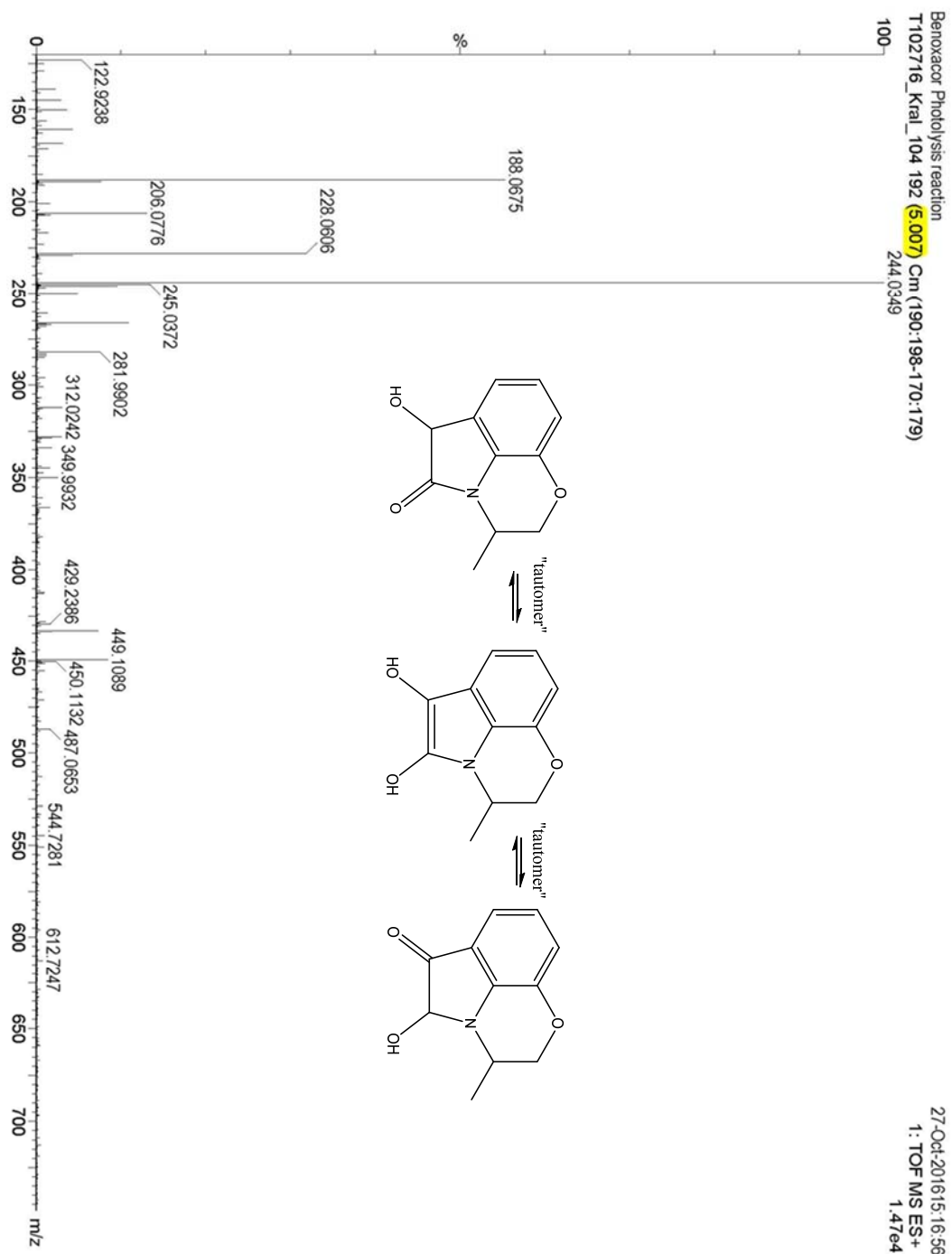


**Figure 26** High resolution mass spectrum of [PB] obtained through LC-HRMS.

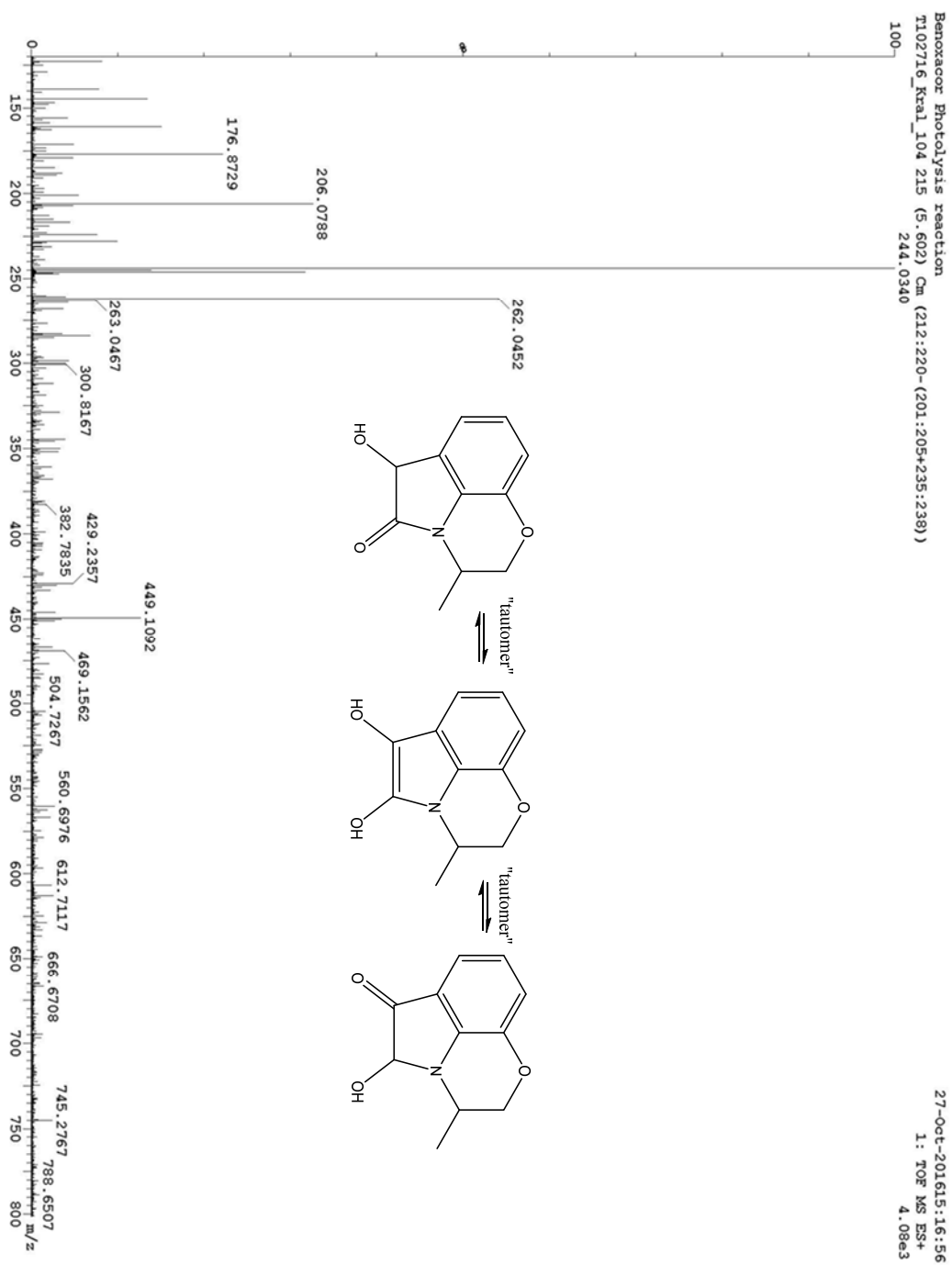


**Figure 27** High resolution mass spectrum of [PC] obtained through LC-HRMS.

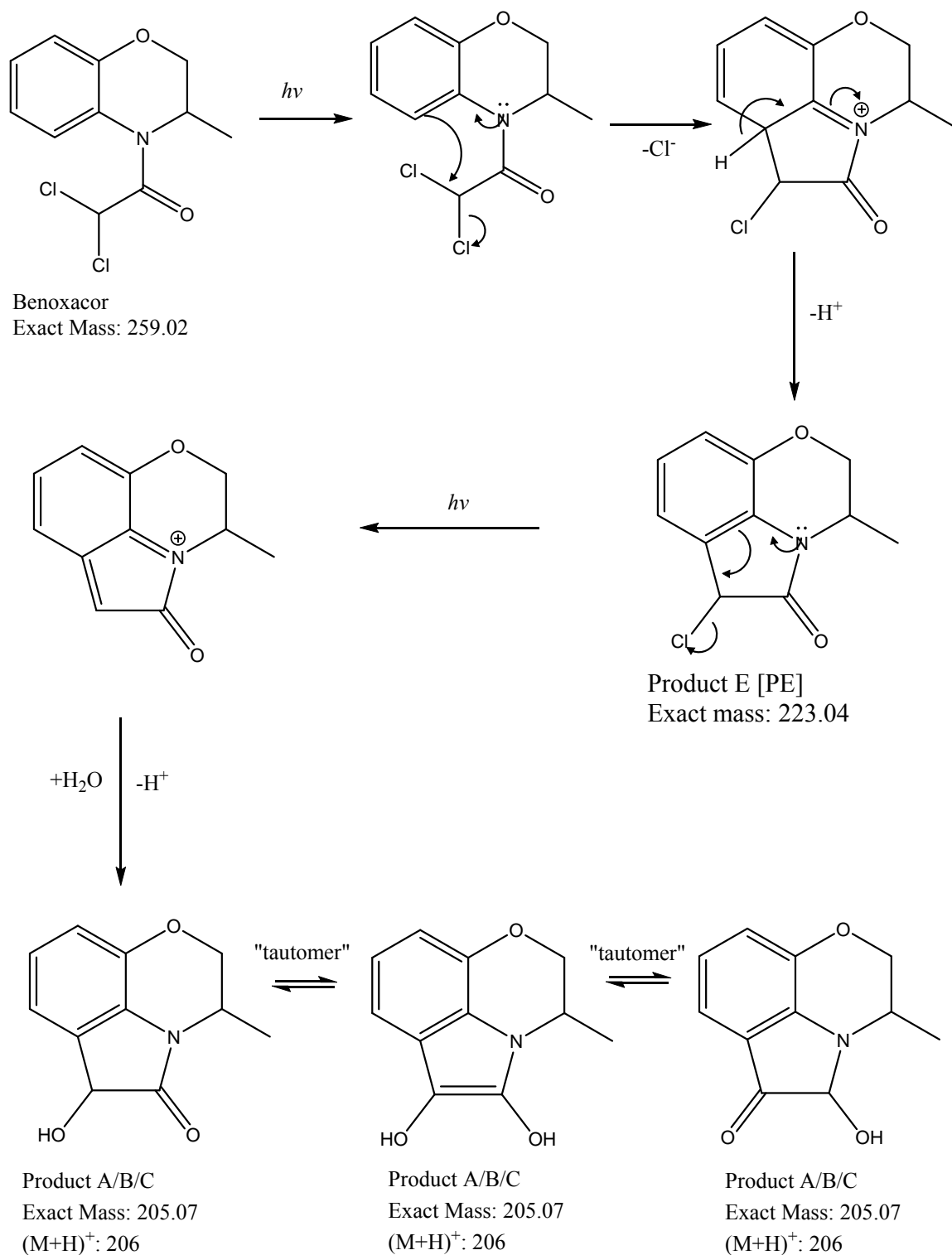


**Figure 28** Proposed mechanism for the formation of [PA], [PB], and [PC] from benoxacor and intermediate [PE] via direct photolysis.

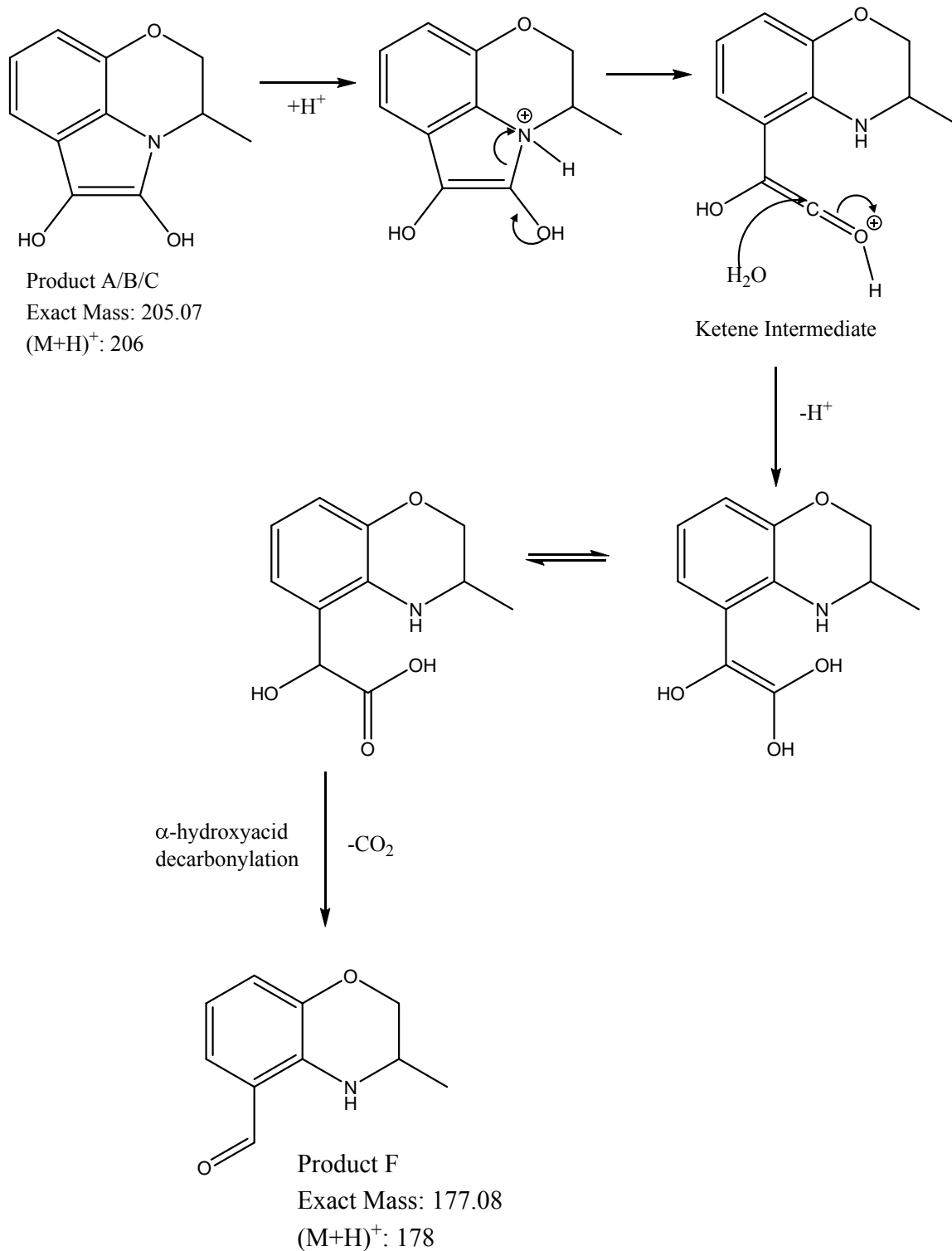


**Figure 29** Formation of [PF] during long-term benoxacor photolysis.

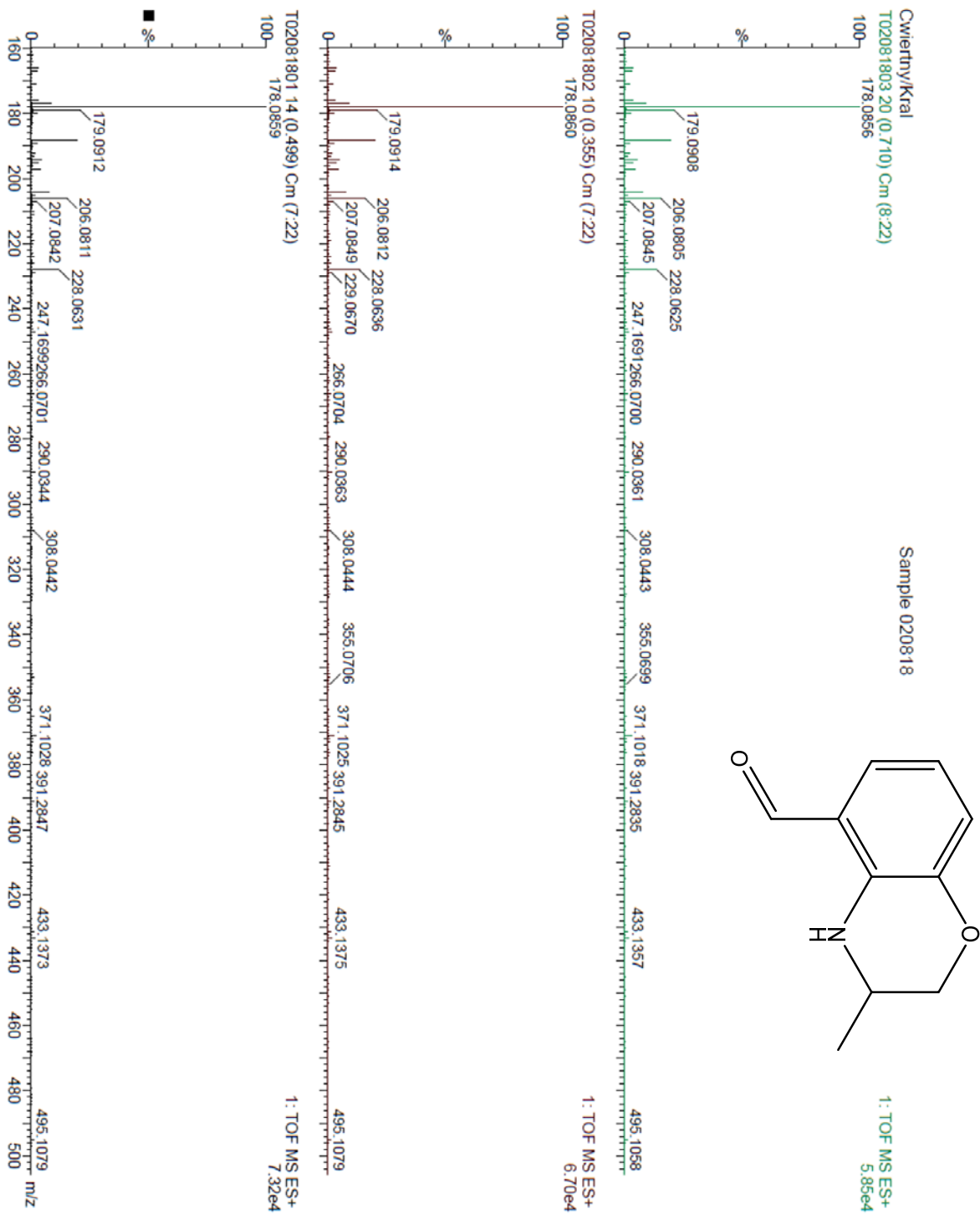


**Figure 30** Direct injection high resolution mass spectrometry results for [PF]. Parent mass  $[M+H]^+$  is shown at 178.1.

pH	$k_{obs}$ (minutes <sup>-1</sup> )	$t_{1/2}$ (min)
5	$0.086 \pm 0.0009$	$8.1 \pm 0.09$
7	$0.092 \pm 0.003$	$7.6 \pm 0.2$
9	$0.089 \pm 0.003$	$7.8 \pm 0.3$

**Table 3** Observed first order rate constants and half lives for benoxacor photolysis across pHs 5, 7, and 9.



Product ID	HPLC Retention Time (min)	$\lambda_{\max}$ (nm)
Product A	4.1	220, 250, 305
Product B	4.3	220, 250, 305
Product C	4.9	218, 250, 290
Product D	6.8	225, 245, 320
Product E	8.5	225, 320
Product F	9.3	198, 242, 278, 396
Benoxacor	10.7	216, 258, 290

**Table 4** The table shows product ID and corresponding HPLC retention time and absorbance maxima for major products of benoxacor photolysis.

## Chapter 4 Photolysis of AD-67, Dichlormid, and Furilazole

### 4.1. Introduction

The three other commonly used dichloroacetamide safeners—not including benoxacor—are AD-67, dichlormid, and furilazole (see Table 1). From a photochemical perspective, they differ from benoxacor in a significant way—they do not absorb light within the solar spectrum (i.e.,  $\lambda \geq 305$  nm) (see Figure 2). Accordingly, they will not be able to directly photolyze in sunlit surface waters [31]. For a photochemical reaction to occur within the solar spectrum for these three safeners, the photolysis reaction must be indirect, or sensitized (i.e., facilitated by a photoactive intermediate) [31].

Indirect photolysis is a common environmental fate pathway for many organic (micro)pollutants [31]. For indirect photolysis to occur, a compound other than the pollutant (i.e., the molecule of interest) must absorb light. As described in Chapter 3.1., when a compound directly absorbs light an electron is promoted from a non-bonding or bonding orbital into an anti-bonding orbital (e.g.,  $\pi \rightarrow \pi^*$  or  $n \rightarrow \pi^*$ ), entering an “excited state” [31]. For indirect photolysis, this excited state species can either (i) react directly with the pollutant of interest; (ii) produce a highly reactive intermediate species (usually from oxygen), which can then react with the pollutant; or (iii) transfer its absorbed energy to the pollutant (Figure 31) [31]. All three of these scenarios can induce a chemical change (e.g., bond breaking or bond formation) as a result of the photolysis of a different compound, typically called a photosensitizer, in the environment (see Figure 31) [31].

In natural aquatic systems, compounds that can serve this intermediate role or act as photosensitizers are abundant. For example, dissolved organic matter (DOM) is found in nearly all surface waters [31, 43]. DOM is formed during the decay and transformation

of plant and microbial remains [43]. DOM represents a wide array of heterogeneous organic compounds whose molecular weight can range from 100 to over 300,000 Daltons [43]. Many DOM compounds contain photoactive moieties (i.e., chromophores), and these chromophores are capable of producing several different reactive oxygen species (ROS) when they absorb light within the solar spectrum (i.e.,  $\lambda \geq 305$  nm). Common ROS include singlet oxygen ( $^1\text{O}_2$ ), alkoxy radical ( $\text{RO}^\bullet$ ), hydroperoxy radical ( $\text{HO}_2^\bullet$ ), superoxide ( $\text{O}_2^{\bullet-}$ ), and hydroxyl radical ( $\text{HO}^\bullet$ ) [31].

In addition, oxidized nitrogen species such as nitrate ( $\text{NO}_3^-$ ) and nitrite ( $\text{NO}_2^-$ ) can also be a major source of  $\text{HO}^\bullet$  (and other reactive species like nitrite radical ( $\text{NO}_2^\bullet$ ) and nitric oxide ( $\text{NO}^\bullet$ )) when they are photolyzed (Figure 32) [33]. In Iowa, nitrate contamination in natural aquatic systems is a highly publicized issue, with summertime concentrations often above  $10 \text{ mg L}^{-1}$  as N in many surface waters around the state [34]. As fertilizers (i.e., sources of nitrate and nitrite) are often applied during the same time of planting season as herbicides and safeners, it is likely AD-67, dichlormid, and furilazole could be exposed to  $\text{HO}^\bullet$  originating from nitrate and nitrite photolysis [1, 2, 34].

Beyond indirect photolysis, the only other scenario for the photolysis of these other safeners is via direct photolysis in engineered treatment systems that use lower wavelengths of light (i.e., higher energy light) not within the solar spectrum for disinfection (see Figure 2). For example, previous work has shown that dichlormid will photolyze with light at 254 nm, a wavelength commonly used for drinking water disinfection because DNA exhibits an absorption maximum at 260 nm [11]. Photolysis at  $\lambda \geq 250$  nm (i.e., UVC light) is a common germicidal method used by municipalities and private consumers to treat drinking water because of the damage it causes to DNA [32].

Not only are compounds like DNA transformed and degraded during photolysis at these wavelengths, but other pollutants can also undergo transformation. Notably, for engineered water treatment, mercury (Mg) lamps are often used for this purpose because they emit most of their light at 253.7 nm [32], and are therefore ideal for targeting pathogens.

Safeners have been reported in Iowa and Illinois surface waters [2], which are often used as a source for drinking water in adjacent communities. Safeners are also relatively polar and unlikely to be removed by standard drinking water treatment processes (e.g., solids removal and filtration). Thus, it is reasonable to suspect would persist through treatment and be exposed to disinfection processes, which are typically at the end of treatment process trains [32]. Further, it is anticipated that rural and small drinking water treatment systems will begin to adapt UVC disinfection to treat their drinking water as other forms of disinfection (i.e., chlorination) can produce harmful byproducts [32]. When exposed to UVC light in these systems, the stability of safeners remains largely unexplored, nor is it understood if safeners could yield photoproducts with altered environmental fate or augmented toxicity relative to their parent species [1].

In this study, we aim to understand the indirect photolysis and UVC photolysis (at  $\lambda \geq 250$  nm) of AD-67, dichlormid, and furilazole. For indirect photolysis, we examined the stability of AD-67, dichlormid, and furilazole in the presence of various photosensitizers including multiple forms of DOM,  $\text{NO}_3^-$ , and  $\text{NO}_2^-$  under a simulated solar spectrum generated from a SunTest CPS+ solar simulator with irradiance of  $750 \text{ W m}^{-2}$ . While this irradiance is approximately three times the irradiance of the sun at Earth's surface, it was necessary to facilitate indirect photolysis over timescales more readily

conducive to sample collection and analysis. To study photolysis in simulated UV disinfection systems, we photolyzed AD-67, dichlormid, and furilazole under a 200 W Mg(Xe) lamp with a 250 nm long-pass, cut-on filter. In both cases, reaction progress was monitored via HPLC analysis to observe decay of the parent compound and to monitor formation of any photoproducts generated from these possible photolysis reactions. Where possible, reaction mixtures were analyzed via high resolution electrospray ionization time-of-flight mass spectrometry (HR-ESI-TOFMS) in an attempt to structurally identify photoproduct species.

#### 4.2. Safener Photolysis in the Presence of Dissolved Organic Matter

To study if AD-67, dichlormid, and furilazole were susceptible to transformation due to DOM generated ROS, we photolyzed 10  $\mu\text{M}$  of each safener in pH 7 phosphate buffer (5 mM) in the presence of 5-10  $\text{mg L}^{-1}$  DOM. We considered two forms of model DOM: Suwanee River Humic Acid (SRHA; Hamilton County, FL) and Pahokee Peat Humic Acid (PPHA; Palm Beach County, FL), both of which were acquired from the International Humic Substances Society (IHSS). Humic acids represent the portion of fulvic acids (DOM) that precipitate below a pH value of 2 [43]. Given the diversity in origin and composition of DOM, we explored different sources of humic acid to explore the generality of safener stability in the presence of DOM generated ROS.

When photolyzed in 5  $\text{mg L}^{-1}$  SRHA and 10  $\text{mg L}^{-1}$  PPHA, only furilazole exhibited noticeable decay (Figure 33). Over 5 h of photolysis, furilazole decayed ~25% in 5  $\text{mg L}^{-1}$  SRHA and over 80% in 10  $\text{mg L}^{-1}$  PPHA (first order rate constants shown in Table 5). This suggests that furilazole is more susceptible to the ROS generated during humic acid photolysis (e.g.,  $^1\text{O}_2$ ,  $\text{RO}^\bullet$ ,  $\text{HO}^\bullet_2$ ,  $\text{O}_2^{\bullet-}$ ,  $\text{HO}^\bullet$ ) than AD-67 or dichlormid.

Furilazole, unlike AD-67 and dichlormid, has a furan moiety which is well described to be highly reactive with  $^1\text{O}_2$  [44-46], one of the chief ROS produced during DOM photolysis [31].

A product of furilazole transformation was observed in both SRHA and PPHA, and based on equivalent LC retention times we assume it is the same photoproduct in both systems (Figure 34). This product likely forms from an ROS found in both humic acid systems, like  $^1\text{O}_2$ . The product had a relatively uncharacteristic UV-Vis absorption spectrum (i.e., no clear maximum) (Figure 36)—similar to furilazole's absorbance spectrum (see Figure 2)—indicative of no chromophores.

To determine to what extent the role of  $^1\text{O}_2$  was in furilazole's indirect photolysis transformation, we photolyzed furilazole in  $10 \text{ mg L}^{-1}$  PPHA in the presence of  $10 \text{ mM}$  sodium azide, a known  $^1\text{O}_2$  quencher. The rate of furilazole decay was reduced, though noticeable decay was still observed (Figure 35), which suggests ROS other than  $^1\text{O}_2$  (e.g.,  $\text{RO}^\bullet$ ,  $\text{HO}_2^\bullet$ ,  $\text{O}_2^{\bullet-}$ ,  $\text{HO}^\bullet$ ) might also contribute to furilazole's decay in humic acids.

#### 4.3. Safener Photolysis in Nitrite and Nitrate

To explore the reactivity of AD-67, dichlormid, and furilazole with  $\text{HO}^\bullet$  generated from nitrite and nitrate photolysis—as well as other nitrogen radical species during nitrite photolysis (i.e.,  $\text{NO}_2^\bullet$  and  $\text{NO}^\bullet$ ) (see Figure 32) [33]—solutions of  $10 \mu\text{M}$  safeners were photolyzed in pH 7 phosphate buffer ( $5 \text{ mM}$ ) in  $10 \text{ mg L}^{-1}$   $\text{NO}_3^-$  or  $\text{NO}_2^-$  (as N).

Photolysis in nitrate resulted in decay for all three safeners (Figure 36, see Table 5). Once again, furilazole exhibited the most decay over five hours ( $\sim 30\%$ ) followed by dichlormid ( $\sim 20\%$ ) and AD-67 ( $\sim 10\%$ ). Nitrate photolysis is dominated by the ROS hydroxyl radical ( $\text{HO}^\bullet$ ) (see Figure 32) [31, 33]. Common reactions with  $\text{HO}^\bullet$  include

hydrogen abstraction and radical addition [31] which are often more reactive towards unsaturated bonds. Dichlormid and furilazole both have a greater number of unsaturated sites than AD-67, which might explain the relative reactivity trends observed in nitrate (i.e., AD-67 less reactive). The same polar furilazole photoproduct observed in SRHA and PPHA was also observed in nitrate (see Figure 34). This was the only product observed for all three safeners.

Photolysis in nitrite ( $\text{NO}_2^-$ ) resulted in the decay of all three safeners over five hours (Figure 37). Dichlormid and furilazole appeared most susceptible to the ROS and radicals generated during nitrite photolysis (see Figure 32) with nearly identical decay (~80-90%) and rate constants (see Figure 37, Table 5). Indeed, one photoproduct was observed accumulating over the course of five hours for both dichlormid and furilazole (Figure 38). While nitrite photolysis results in the production of many ROS, the chief species tend to be  $\text{HO}^\bullet$  and  $\text{NO}^\bullet$  [33]. Increases in decay of all three safeners could be due to the abundance and variety of nitrogen radical species like  $\text{NO}^\bullet$  which are less common in the nitrate system. As  $\text{HO}^\bullet$  is still present in nitrite but less abundant than in nitrate, this could explain the similar product observed for furilazole in both systems. In fact, the polar product observed during photoreaction in the presence of nitrite appears to be the same as that generated in humic acid systems (see Figure 34). This indicates a common ROS or oxidation route possible in humic acid, nitrate, and nitrite is likely responsible for its formation. Less decay was observed for AD-67 than for the other two safeners (~40%, see Figure 37, Table 5), likely indicative of the higher number of saturated moieties than dichlormid and AD-67, although AD-67 still appears to be more reactive in this system than in DOM (see Figure 33).

Radical quenching experiments were conducted for both  $\text{NO}_3^-$  and  $\text{NO}_2^-$  systems in the presence of 50 mM isopropyl alcohol (IPA). IPA is a well-known  $\text{HO}^\bullet$  quencher, but it is generally unselective and can quench other radical species (i.e.,  $\text{NO}^\bullet$ ) [31]. In these quenched systems, the rate of reaction for both furilazole and dichlormid was reduced dramatically (see Figure 35). The  $\text{NO}_2^-$  system still continued to show some decay, highlighting the more complex ROS environment created during  $\text{NO}_2^-$  photolysis [33] (see Figure 35).

#### 4.4. UVC Photolysis of AD-67, Dichlormid, and Furilazole

To explore how AD-67, dichlormid, and furilazole directly photolyzed in UVC wavelengths used for disinfection, we photolyzed solutions of 10  $\mu\text{M}$  of each safener in idealized pH 7 phosphate buffers (5 mM) free of any photosensitizers under a 200 W lamp with a 250 nm cut-on filter to simulate UV disinfection. Over the course of photolysis, all three safeners directly photolyzed at nearly identical rates (Figure 39). Assuming exponential decay, half-lives for AD-67, dichlormid, and furilazole during UVC photolysis are 87 min, 47 min, and 59 min respectively (Table 6).

Photolysis transformation products were detected via HPLC-DAD for all three compounds while monitoring at 220 nm. In solutions of AD-67 and furilazole, one transformation product was observed for each compound (Figure 40). For dichlormid, three transformation products were observed (Figure 40). This supports the findings of Abu-Qare *et al.* who also observed three photoproducts during photolysis of dichlormid at 254 nm, one of which was identified as the previously used herbicide CDAA, or N-N-diallyl-2-chloroacetamide (Figure 41) [11].



These solutions were analyzed using HR-ESI-TOFMS, but no product structures could be identified. As observed in previous experiments with benoxacor, this is likely due to poor ionizing capabilities of both the parent compounds and the transformation products. Based on the findings of Abu-Qare et al., one of the three products observed during dichlormid photolysis is potentially CDAA (see Figure 41). Based on the similarities in our results and the structures of these compounds (see Table 1), it is likely that AD-67 and furilazole follow one of the same transformation pathways reported for dichlormid in the literature: dechlorination, dealkylation, or loss of the  $-CHCl_2$  functional group all together (see Figure 41).

#### 4.5. Conclusions

Overall, furilazole showed the most pronounced and consistent decay in indirect photolysis systems (see Table 5), likely due to its furan moiety and other unsaturated moieties. The same polar product was observed in SRHA, PPHA, nitrite, and nitrate, suggesting  $HO^\bullet$  or a similar oxidation pathway plays a role in its formation (see Figure 34). Dichlormid and AD-67 showed decay in the complex nitrite photolysis system (see Figure 32, Figure 37) and in nitrate (dominated by  $HO^\bullet$  [31, 33]), although to a lesser extent. Both dichlormid and AD-67 showed minimal decay in humic acid systems (see Figure 33), suggesting the reactive intermediates produced during DOM photolysis don't play a large role in their indirect photolysis transformations. In several cases safener decayed occurred but no photoproducts were observed (i.e., dichlormid in nitrate and humic acid, AD-67 in all systems). This could be due to (i) lack of chromophores in photoproducts or (ii) the abundance of ROS which could generate highly polar compounds not observable by our analytical methods.

Indirect photolysis under simulated natural sunlight does not appear to be as significant an environmental pathway for these safeners as direct photolysis under natural sunlight was for benoxacor. However, direct photolysis under  $\lambda > 250$  nm did yield photoproducts for all three safeners. Thus, photolysis under drinking water UV disinfection conditions might pose an important transformation route for these widely used compounds in engineered systems, especially as UV disinfection of drinking water becomes a more popular option for rural communities [32].

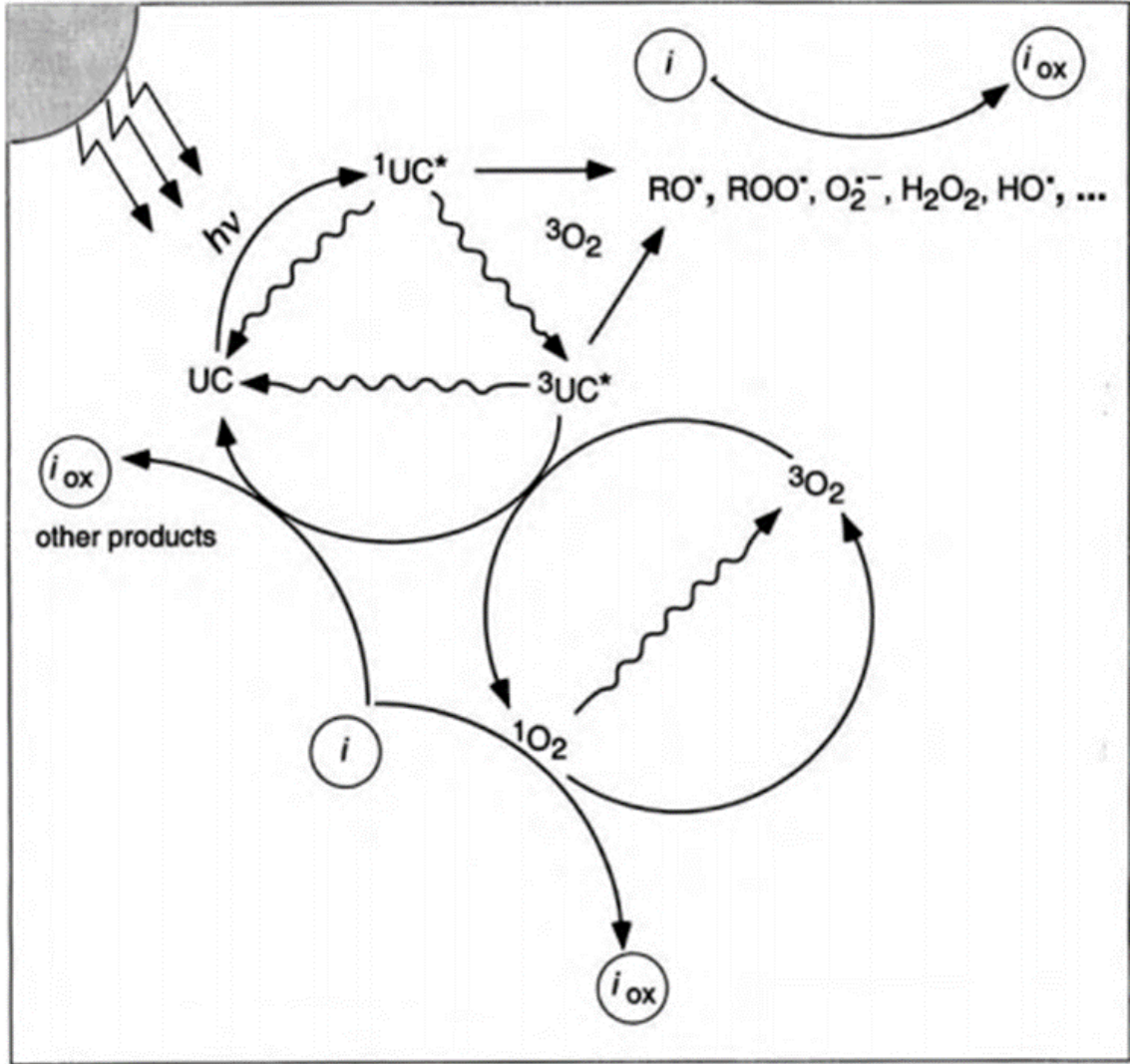
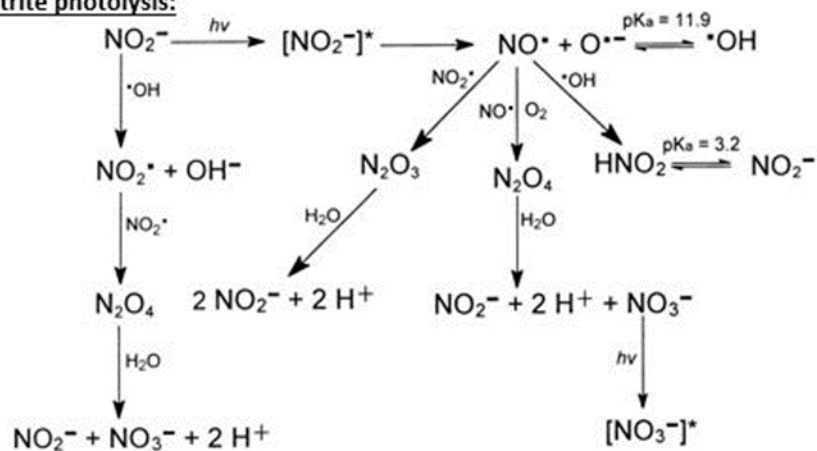


**Figure 31** Pathways for indirect photolysis, where  $i$  denotes the compound of interest (i.e., safener) and UC represents the photoactive compound.

**Nitrite photolysis:**



**Nitrate photolysis:**

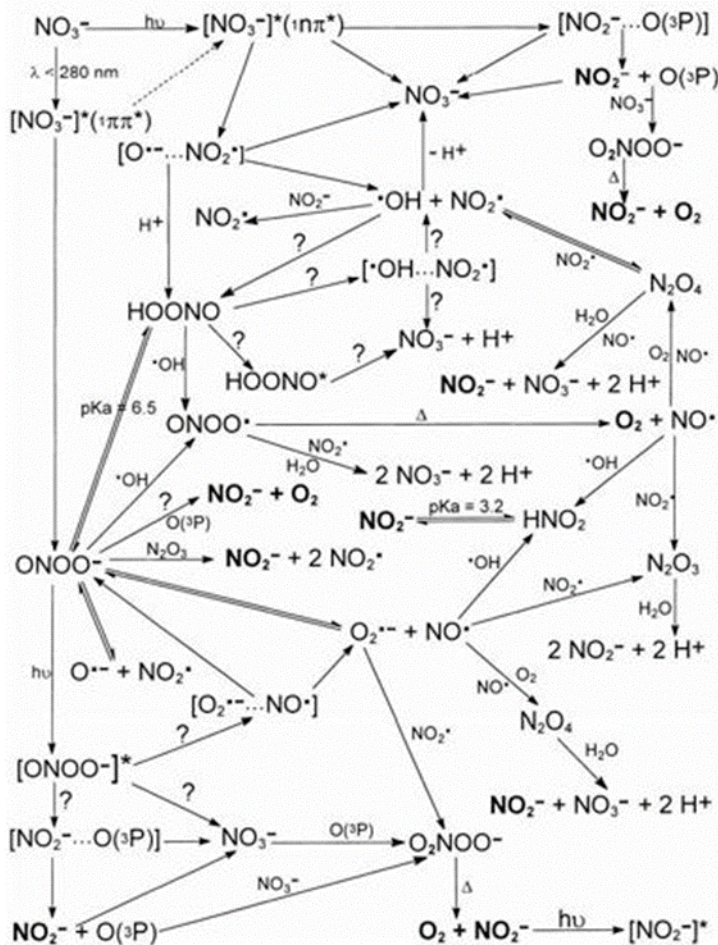


**Figure 32** Photolysis schemes for nitrite (above) and nitrate (below).

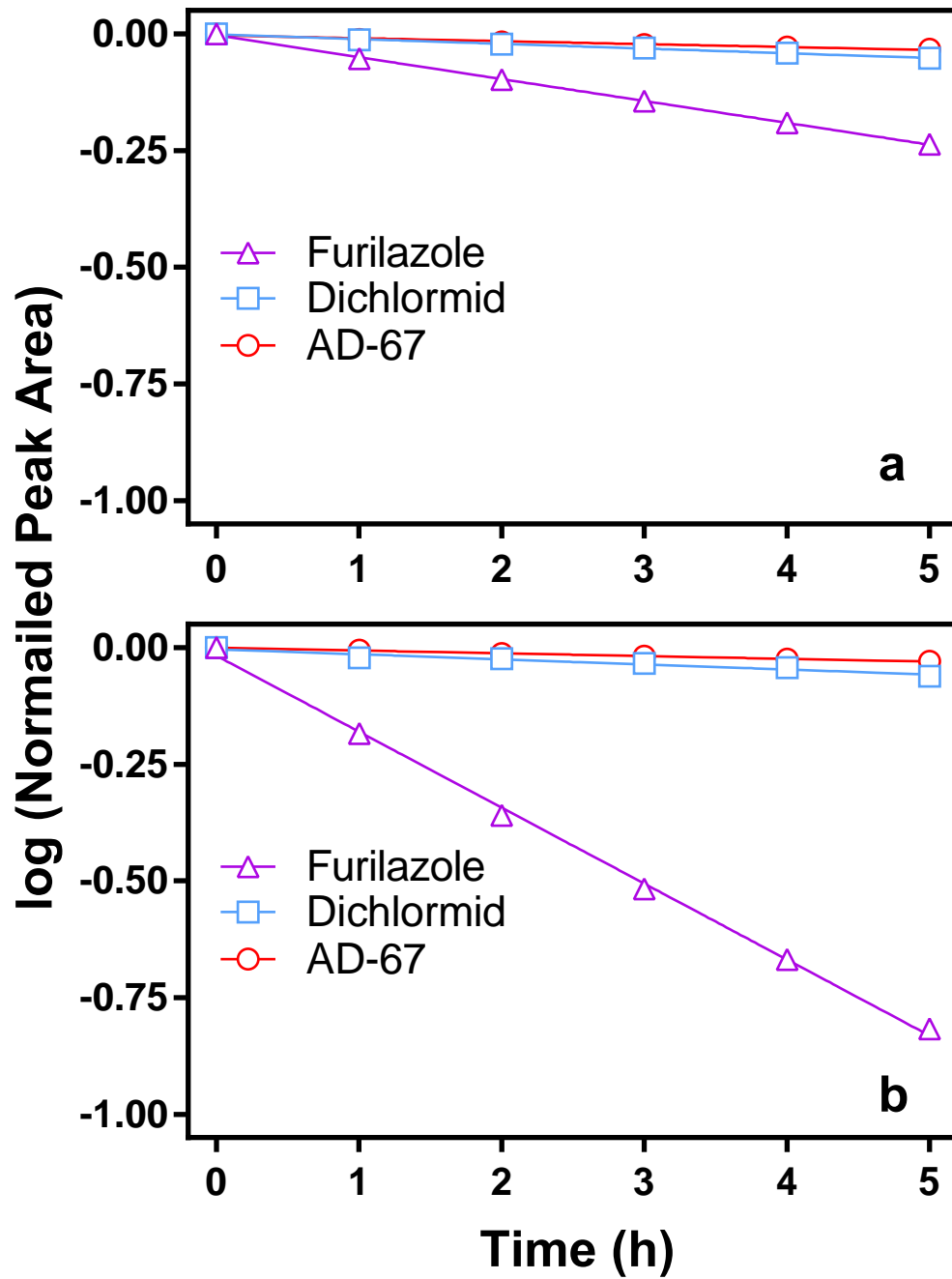


**Figure 33** Indirect photolysis of safeners in 5 mg L<sup>-1</sup> SRHA (a) and 10 mg L<sup>-1</sup> PPHA (b). Observed first order rate constants and half-lives are shown in Table 5.

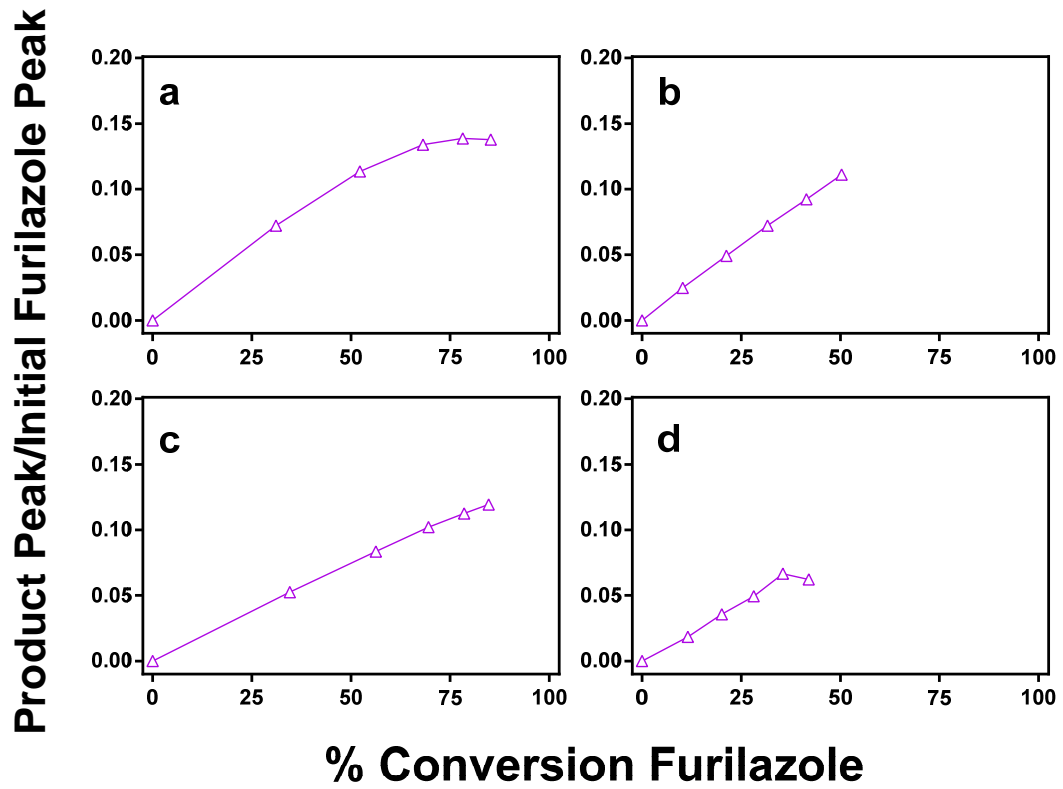


**Figure 34** Yield plots for the product observed during furilazole indirect photolysis in  $\text{NO}_2^-$  (a),  $\text{NO}_3^-$  (b), PPHA (c), and SRHA (d).

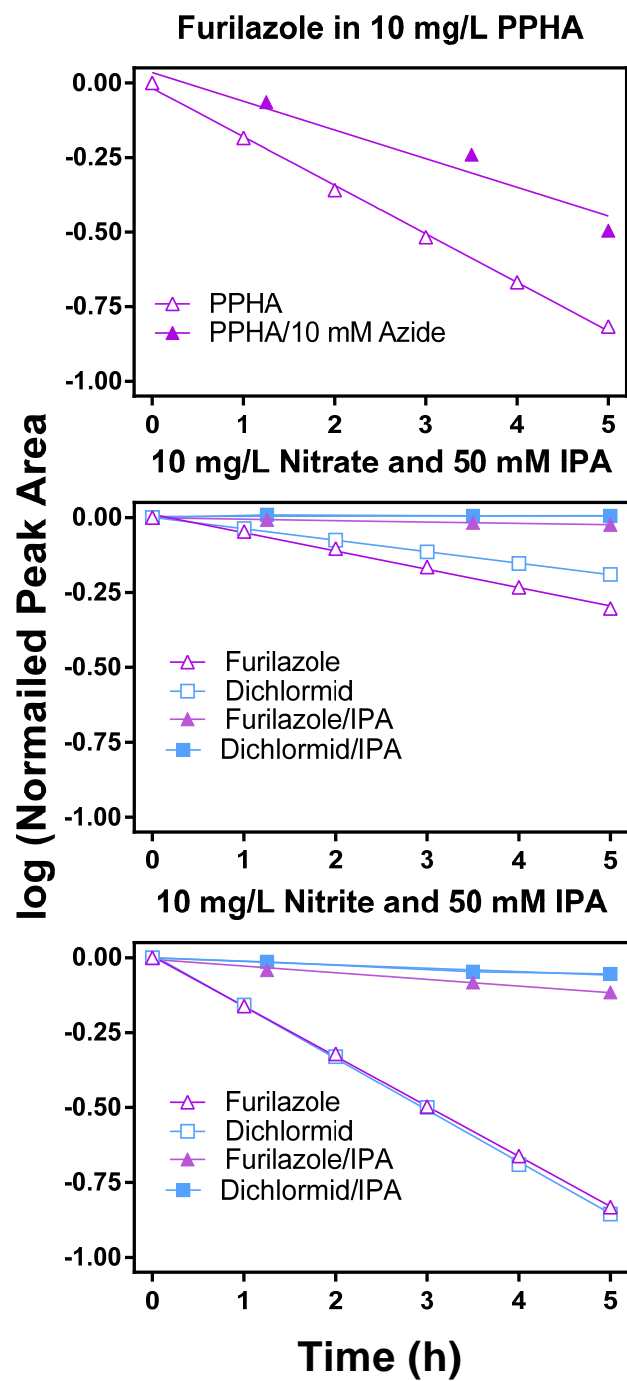


**Figure 35** Indirect photolysis quenching experiments were used to eliminate ROS like  $^1\text{O}_2$  (azide) and  $\bullet\text{OH}$  (isopropyl alcohol, or IPA) to probe their role in safener transformation.

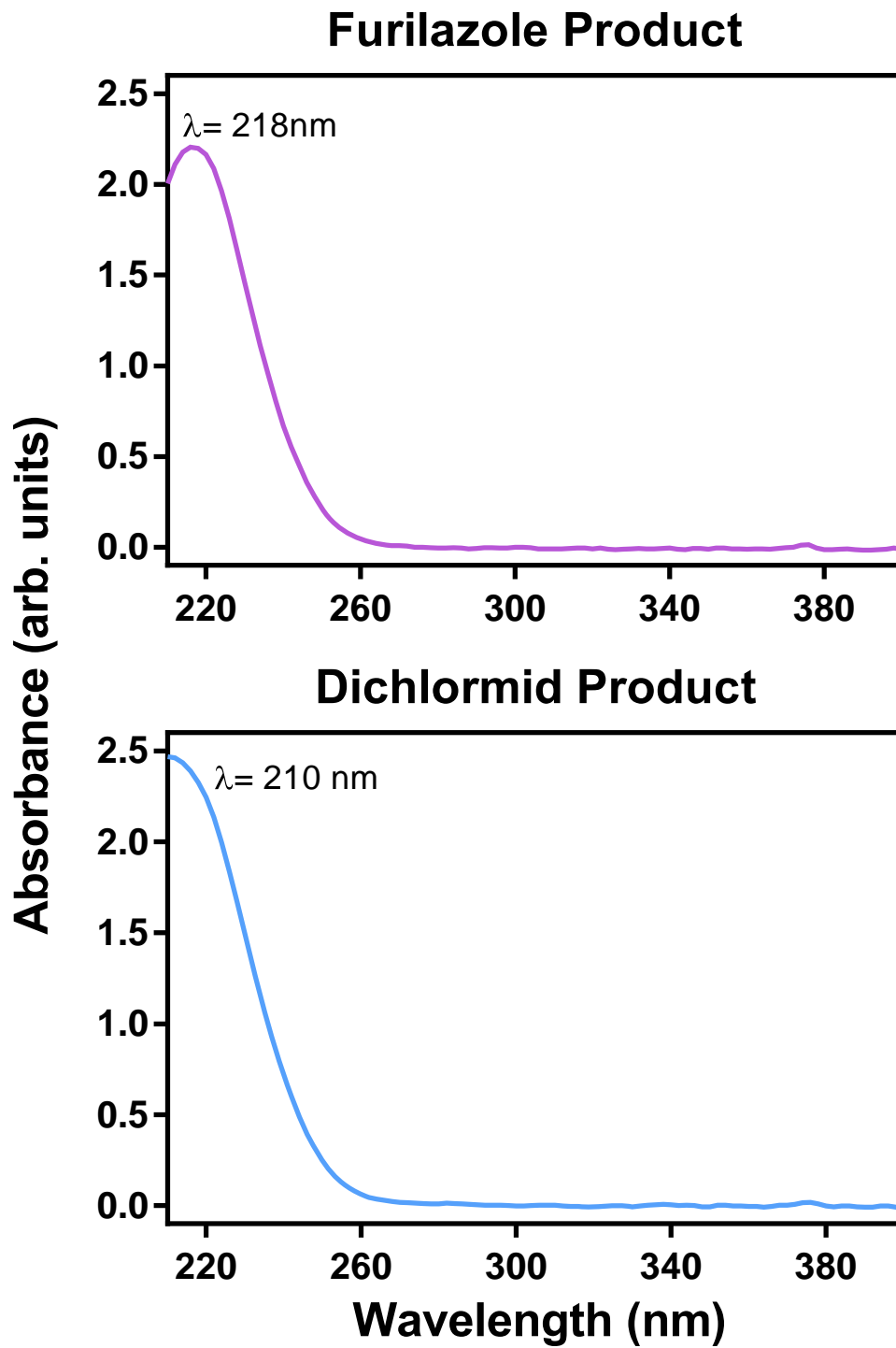


**Figure 36** Absorbance spectra for the products generated during furilazole and dichlormid indirect photolysis.



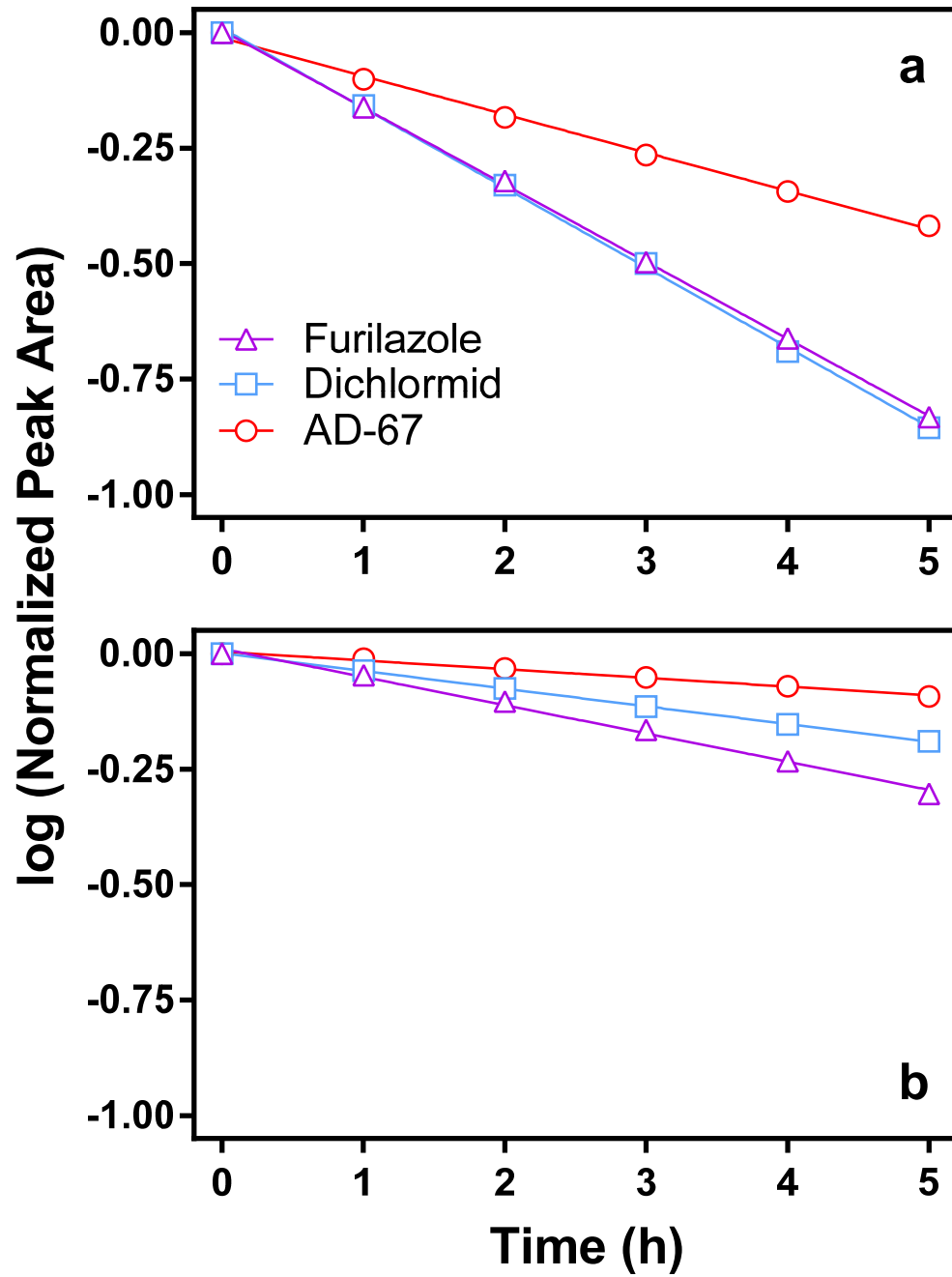


**Figure 37** Safener photolysis in nitrite (a) and nitrate (b). Observed first order rate constants and half-lives are shown in Table 5.

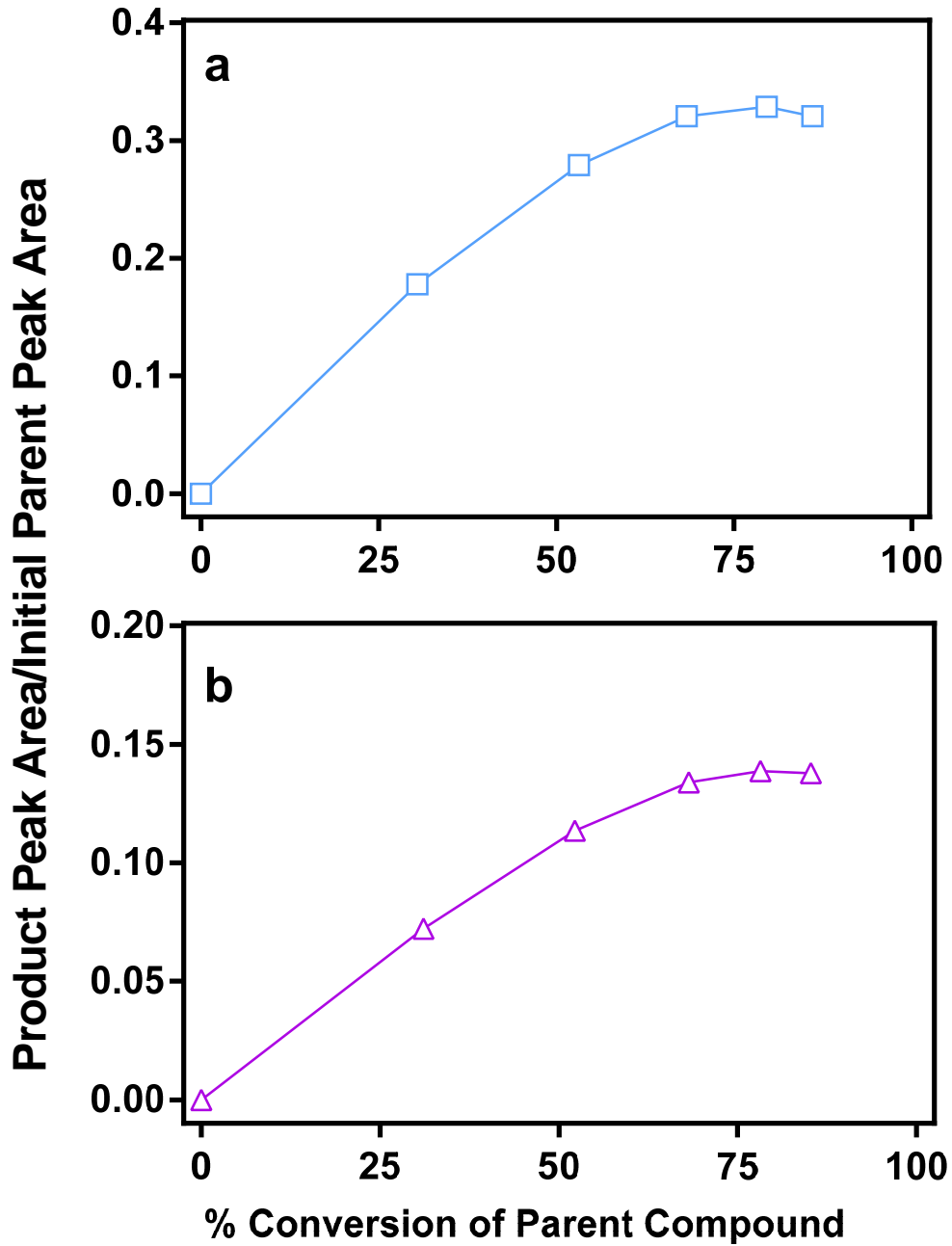


**Figure 38** Product conversion plots for indirect photolysis in nitrite of dichlormid photoproduct (a) and furilazole photoproduct (b).

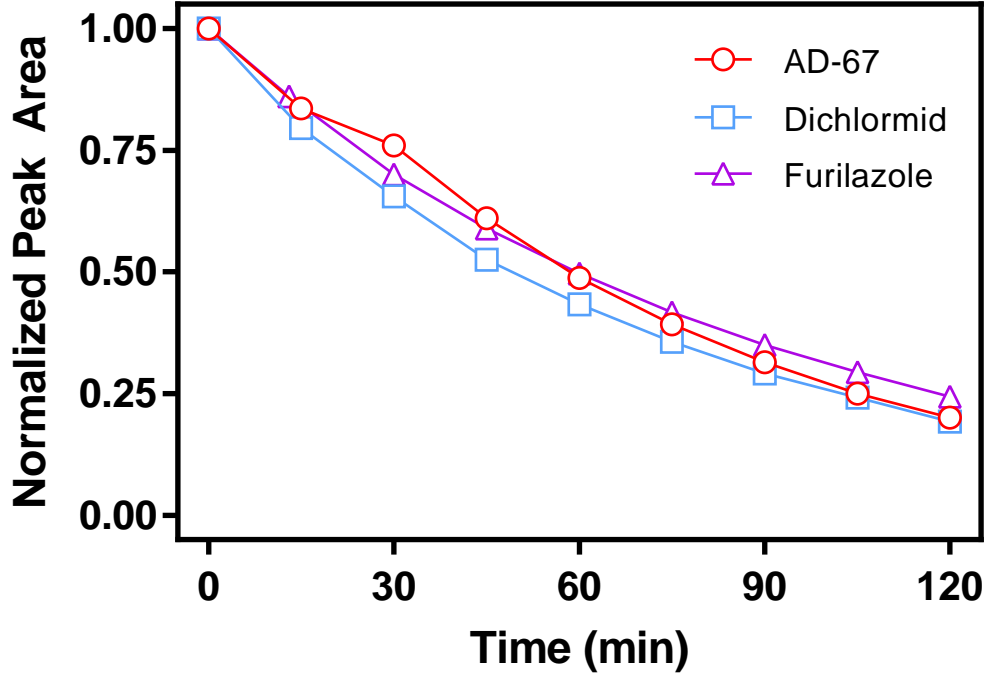


**Figure 39** Safeners photolyzed by  $\lambda \geq 250$  nm in pH 7 buffer free of photosensitizers. First order exponential decay constants, fits, and half-lives are shown below (see Table 6).

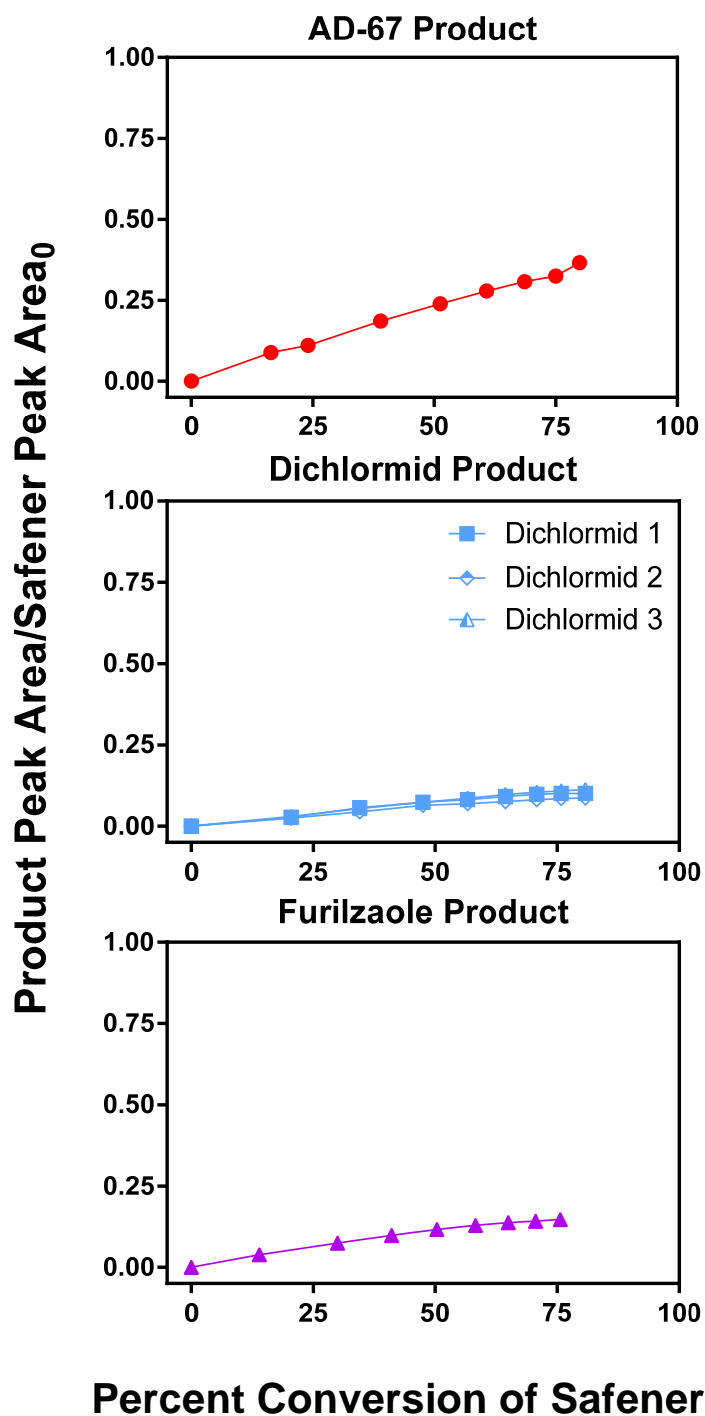


**Figure 40** Formation of photoproducts during safeners photolysis at  $\lambda \geq 250$  nm. While these products were observed via HPLC analysis, they were not observed during HR-ESI-TOFMS analysis.

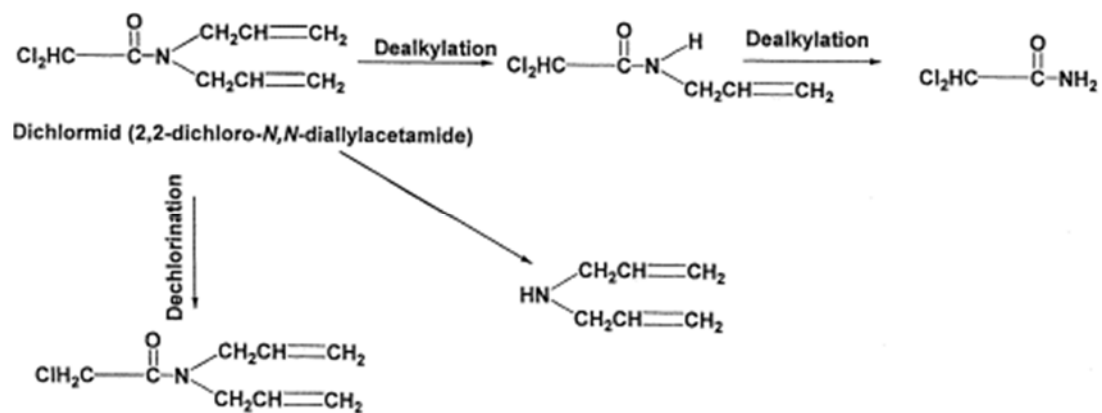


**Figure 41** Proposed photolysis pathway of dichlormid by Abu-Qare et al. under 254 nm light. Dechlorination product is CDAA, a formerly used herbicide.

Safener	System	$k_{obs}$ ( $h^{-1}$ )	$t_{1/2}$ (h)
AD-67	5 mg/L SRHA	0.01	48.1
	10 mg/L PPHA	0.01	50.3
	10 mg N/L $NO_2^-$	0.19	3.6
	10 mg N/L $NO_3^-$	0.04	16.0
Dichlormid	5 mg/L SRHA	0.02	29.8
	10 mg/L PPHA	0.02	27.8
	10 mg N/L $NO_2^-$	0.40	1.7
	10 mg N/L $NO_3^-$	0.09	7.9
Furilazole	5 mg/L SRHA	0.11	6.4
	10 mg/L PPHA	0.37	1.9
	10 mg N/L $NO_2^-$	0.38	1.8
	10 mg N/L $NO_3^-$	0.14	4.9

**Table 5** First order rate constants and half-lives for indirect photolysis systems.

Safeners	$k_{obs}$ (min <sup>-1</sup> )	R <sup>2</sup> first-order decay	$t_{1/2}$ (min)
AD-67	0.008	0.9960	87
Dichlormid	0.01	0.9996	47
Furilazole	0.01	0.9999	59

**Table 6** Safener photolysis at  $\lambda \geq 250$  nm and associated first order decay constants and half-lives.

## Chapter 5 Conclusions

In this work, we investigated the photochemical transformation of four commonly used dichloroacetamide safeners: AD-67, benoxacor, dichlormid, and furilazole. While these compounds are widely used ( $> 2 \times 10^6 \text{ kg yr}^{-1}$ ), they represent a class of understudied agrochemicals whose environmental fate and transformations are largely unknown. In this work, we focused on the photochemical transformations of these compounds (i.e., direct and indirect photolysis) to show that these pathways might be a major transformation route for these compounds in the environment.

In Chapter 3, we showed benoxacor rapidly photolyzed through direct absorption of light within the solar spectrum and produced several photoproducts. These products varied in number of chlorine atoms (e.g., monochlorinated and dechlorinated) and were all less polar than benoxacor—which has already been detected in natural surface waters [2]—suggesting that they will be highly mobile in aqueous as well. Most products formed after more than 5 minutes of benoxacor direct photolysis were fully dechlorinated, suggesting they will have different biochemical and toxicological properties than benoxacor. Although [PE]—the intermediate monochlorinated product of benoxacor direct photolysis—was short lived (i.e., decay began after  $\sim 5$  min of photolysis), in natural aquatic systems it might be generated from benoxacor and transported out of the photic zone where it could be more stable and persist. A monochlorinated species has potential for a great difference in bioactivity and toxicological fate, as shown in the differences between the active chloroacetamide herbicides and the inert dichloroacetamide safeners.



In Chapter 4, we indirectly photolyzed the safeners AD-67, dichlormid, and furilazole in solutions of DOM, nitrate, and nitrite. These safeners don't absorb light within the solar spectrum, thus in natural environments indirect photolysis would be the dominant photochemical transformation pathway. We showed furilazole was the most reactive compound across all three photosensitizers, likely due to its furan moiety which is known to be highly reactive with singlet oxygen ( $^1\text{O}_2$ ) and overall number of unsaturated moieties which are known to be highly reactive with ROS like  $^1\text{O}_2$  and  $\text{HO}^\bullet$ . One product was detected through all furilazole indirect photolysis systems which suggests a similar ROS in each system is involved in its formation, or at least a similar oxidation pathway. Dichlormid was the next most reactive compound, showing ~20 % decay in nitrate and ~80 % decay nitrite. It was followed by AD-67 which showed ~ 25 % decay in nitrite and less than ~ 10 % decay in nitrate. Neither dichlormid nor AD-67 showed noticeable decay in DOM whereas furilazole showed ~80 % decay in 10 mg L<sup>-1</sup> DOM—in which  $^1\text{O}_2$  is a chief ROS—highlighting further evidence that furilazole's furan moiety played a role in its relative reactivity. Overall, the relative reactivity of furilazole and dichlormid compared to AD-67 can be explained by AD-67's relative lack of unsaturated moieties which often react with ROS (like  $\text{HO}^\bullet$ , found to some extent in all of our systems) through pathways like hydrogen abstraction or radical addition.

In Chapter 4 we also showed AD-67, dichlormid, and furilazole are susceptible to direct photolysis at  $\lambda > 250$  nm which is commonly used in engineered systems to disinfect drinking water. One photoproduct was observed for AD-67 and furilazole, whereas three were observed for dichlormid as shown in previous work by Abu-Qare et al [11]. In their study, one of the compounds observed was the formerly used

chloroacetamide herbicide CDAA, suggesting that at least dichlormid has the potential to produce transformation products with herbicide-like toxicity under these lower wavelengths.

This study was the first comprehensive review of photochemical transformations for dichloroacetamide safeners. We showed direct photolysis will be an important fate pathway for benoxacor in the environment, one that produces several new transformation products—both chlorinated and fully dechlorinated. We showed indirect photolysis could be a significant environmental fate for furilazole and dichlormid, whereas the lack of unsaturated moieties on AD-67 suggest it will be relative stable when exposed to photochemical ROS. We also showed AD-67, dichlormid, and furilazole are susceptible to photolysis under UV light, suggesting that in engineered systems photochemical pathways are likely to transform these compounds into new, potentially monochlorinated compounds [11].

Future work on these compounds might include identifying other fate pathways (e.g., biotransformation) these four safeners could proceed through. As our work has already shown photolysis is likely a significant fate pathway—especially for benoxacor—understanding the toxicological properties of transformation products would be a useful study. Specifically, understanding how the monochlorinated products' toxicological properties differ from those of dichloroacetamides might suggest that these safeners are not as inert as their regulatory status may suggest.

## Literature Cited

1. Sivey, J.D., et al., *Environmental Fate and Effects of Dichloroacetamide Herbicide Safeners: "Inert" yet Biologically Active Agrochemical Ingredients*. Environmental Science & Technology Letters, 2015. **2**(10): p. 260-269.
2. Woodward, E.E., M.L. Hladik, and D.W. Kolpin, *Occurrence of Dichloroacetamide Herbicide Safeners and Co-Applied Herbicides in Midwestern U.S. Streams*. Environmental Science & Technology Letters, 2018. **5**(1): p. 3-8.
3. Gasnier, C., et al., *Glyphosate-based herbicides are toxic and endocrine disruptors in human cell lines*. Toxicology, 2009. **262**(3): p. 184-191.
4. Lerro, C.C., et al., *Use of acetochlor and cancer incidence in the Agricultural Health Study*. International Journal of Cancer, 2015. **137**(5): p. 1167-1175.
5. Sivey, J.D. and A.L. Roberts, *Abiotic Reduction Reactions of Dichloroacetamide Safeners: Transformations of "Inert" Agrochemical Constituents*. Environmental Science & Technology, 2012. **46**(4): p. 2187-2195.
6. Wu, C., H. Shemer, and K.G. Linden, *Photodegradation of Metolachlor Applying UV and UV/H<sub>2</sub>O<sub>2</sub>*. Journal of Agricultural and Food Chemistry, 2007. **55**(10): p. 4059-4065.
7. Dimou, A.D., V.A. Sakkas, and T.A. Albanis, *Metolachlor Photodegradation Study in Aqueous Media under Natural and Simulated Solar Irradiation*. Journal of Agricultural and Food Chemistry, 2005. **53**(3): p. 694-701.
8. Wilson, R.I. and S.A. Mabury, *Photodegradation of Metolachlor: Isolation, Identification, and Quantification of Monochloroacetic Acid*. Journal of Agricultural and Food Chemistry, 2000. **48**(3): p. 944-950.
9. Souissi, Y., et al., *Using mass spectrometry to highlight structures of degradation compounds obtained by photolysis of chloroacetamides: Case of acetochlor*. Journal of Chromatography A, 2013. **1310**: p. 98-112.
10. Tominack, R.L. and R. Tominack, *Herbicide Formulations*. Journal of Toxicology: Clinical Toxicology, 2000. **38**(2): p. 129-135.
11. Abu-Qare, A.W. and H.J. Duncan, *Photodegradation of the herbicide EPTC and the safener dichlormid, alone and in combination*. Chemosphere, 2002. **46**(8): p. 1183-1189.
12. Zhang, Q., et al., *Safeners coordinately induce the expression of multiple proteins and MRP transcripts involved in herbicide metabolism and detoxification in Triticum tauschii seedling tissues*. PROTEOMICS, 2007. **7**(8): p. 1261-1278.
13. Edwards, R., et al., *Differential Induction of Glutathione Transferases and Glucosyltransferases in Wheat, Maize and Arabidopsis thaliana by Herbicide Safeners*, in *Zeitschrift für Naturforschung C*. 2005. p. 307.
14. Cummins, I., D.N. Bryant, and R. Edwards, *Safener responsiveness and multiple herbicide resistance in the weed black-grass (Alopecurus myosuroides)*. Plant Biotechnology Journal, 2009. **7**(8): p. 807-820.
15. Davies, J. and J.C. Caseley, *Herbicide safeners: a review*. Pesticide Science, 1999. **55**(11): p. 1043-1058.
16. Bullock, D.S. and M. Desquilbet, *The economics of non-GMO segregation and identity preservation*. Food Policy, 2002. **27**(1): p. 81-99.

17. *Federal Insecticide, Fungicide, and Rodenticide Act. In Code of Federal Regulations: United States of America.* Government Printing Office: Washington, DC, 2012: p. Vol. 7, U.S.C. 136–136y.
18. EPA, U., *Inert Ingredients Overview and Guidance*; <https://www.epa.gov/pesticide-registration/inert-ingredients-overview-and-guidance>.
19. *U.S. EPA Benoxacor Pesticide Tolerances, Final Rule. In Federal Register.* Government Printing Office: Washington, DC, 1998: p. Government Printing Office: Washington, DC, 1998.
20. Organization, W.H., *Guideline for drinking-water quality, 2nd ed. Vol. 2.* Health Criteria and other supporting information, 1996: p. pp. 725-729.
21. Savoca, M.E., Eric M. Sadorf, S. Mike Linhart, and Kymm K.B. Akers, *Effects of land use and hydrogeology on the water quality of alluvial aquifers in Eastern Iowa and Southern Minnesota, 1997.* U.S. Geological Survey, Water-Resources Investigations Report 99-4246. Iowa City, IA., 2000.
22. Kalkhoff, S.J., and E.M. Thurman, *The occurrence of chloroacetanilide and triazine herbicide metabolites in streams in Eastern Iowa.* Abstracts of the Seventh Symposium on the Chemistry and Fate of Modern Pesticides, Lawrence, KS, September 14-16, 1999, 1999.
23. Hall, L.W.J., Ronald D. Anderson, Jay Kilian, and Dennis P. Tierney, *Concurrent exposure assessments of atrazine and metolachlor in the mainstem, major tributaries and small streams of the Chesapeake Bay Watershed: Indicators of ecological risk.* Environmental Monitoring and Assessment, 1999(59: 155-190).
24. Konda, L.N. and Z. Pásztor, *Environmental Distribution of Acetochlor, Atrazine, Chlorpyrifos, and Propisochlor under Field Conditions.* Journal of Agricultural and Food Chemistry, 2001. **49**(8): p. 3859-3863.
25. Liang, J. and Q. Zhou, [*Single and binary-combined toxicity of methamidophos, acetochlor and Cu on earthworm Eisenia foetida*]. Ying yong sheng tai xue bao = The journal of applied ecology, 2003. **14**(4): p. 593-596.
26. Carr, K.H., *Adsorption/desorption studies of MON 13909 and Aerobic Soil Metabolites.* Unpublished study performed and submitted by Monsanto Agriculture Company, Chesterfield, MO., 1990.
27. Subba-Rao, R.V., *R-25788: Adsorption and desorption in four soils.* Unpublished study performed and submitted by ICI Americas, Inc., Richmond, CA., 1990.
28. Liu, W., et al., *Structural Influences in Relative Sorptivity of Chloroacetanilide Herbicides on Soil.* Journal of Agricultural and Food Chemistry, 2000. **48**(9): p. 4320-4325.
29. Kochany, J. and R.J. Maguire, *Sunlight Photodegradation of Metolachlor in Water.* Journal of Agricultural and Food Chemistry, 1994. **42**(2): p. 406-412.
30. Philip, C.H., *Discovery, Development, and Current Status of the Chloroacetamide Herbicides.* Weed Science, 1974. **22**(6): p. 541-545.
31. Schwarzenbach, R.P., P.M. Gschwend, and D.M. Imboden, *Environmental organic chemistry.* 2003, Wiley,; Hoboken, N.J. p. 1 online resource (1329 p.).
32. Jones, C.H., et al., *Life Cycle Environmental Impacts of Disinfection Technologies Used in Small Drinking Water Systems.* Environmental Science & Technology, 2018. **52**(5): p. 2998-3007.

33. Mack, J. and J.R. Bolton, *Photochemistry of nitrite and nitrate in aqueous solution: a review*. Journal of Photochemistry and Photobiology A: Chemistry, 1999. **128**(1): p. 1-13.
34. Jaynes, D.B., J. Hatfield, and D. W. Meek, *Water Quality in Walnut Creek Watershed: Herbicides and Nitrate in Surface Waters*. Vol. 28. 1999.
35. USGS, *Estimated Annual Agricultural Pesticide Use; Pesticide Use Maps - Acetochlor*;  
[https://water.usgs.gov/nawqa/pnsp/usage/maps/show\\_map.php?year=2015&map=ACETOCHLOR&hilo=L&disp=Acetochlor](https://water.usgs.gov/nawqa/pnsp/usage/maps/show_map.php?year=2015&map=ACETOCHLOR&hilo=L&disp=Acetochlor). 2015.
36. USGS, *Estimated Annual Agricultural Pesticide Use; Pesticide Use Maps - Metolachlor-S*;  
[https://water.usgs.gov/nawqa/pnsp/usage/maps/show\\_map.php?year=2015&map=METOLACHLORS&hilo=L&disp=Metolachlor-S](https://water.usgs.gov/nawqa/pnsp/usage/maps/show_map.php?year=2015&map=METOLACHLORS&hilo=L&disp=Metolachlor-S). 2015.
37. Leifer, A., *The Kinetics of Environmental Aquatic Photochemistry: Theory and Practice*. American Chemical Society: Washington, DC, 1988.
38. Laszakovits, J.R., et al., *p-Nitroanisole/Pyridine and p-Nitroacetophenone/Pyridine Actinometers Revisited: Quantum Yield in Comparison to Ferrioxalate*. Environmental Science & Technology Letters, 2017. **4**(1): p. 11-14.
39. Pflug, N.C., et al., *Environmental photochemistry of dienogest: phototransformation to estrogenic products and increased environmental persistence via reversible photohydration*. Environmental Science: Processes & Impacts, 2017. **19**(11): p. 1414-1426.
40. Irzyk, G.P. and E.P. Fuerst, *Purification and Characterization of a Glutathione S-Transferase from Benoxacor-Treated Maize (Zea mays)*. Plant Physiology, 1993. **102**(3): p. 803-810.
41. Hutchinson, D., *Silurian-Devonian Aquifer*. Iowa Geological Survey, July 26th, 2017. <https://www.ihr.uiowa.edu/igs/silurian-devonian-aquifer/>.
42. Miller, K.D., et al., *Time Course of Benoxacor Metabolism and Identification of Benoxacor Metabolites Isolated from Suspension-Cultured Zea mays Cells 1 h after Treatment*. Journal of Agricultural and Food Chemistry, 1996. **44**(10): p. 3326-3334.
43. Mostofa, K.M.G., et al., *Dissolved Organic Matter in Natural Waters*, in *Photobiogeochemistry of Organic Matter: Principles and Practices in Water Environments*, K.M.G. Mostofa, et al., Editors. 2013, Springer Berlin Heidelberg: Berlin, Heidelberg. p. 1-137.
44. Lee, G.C.M., et al., *Singlet oxygen oxidation of substituted furans to 5-hydroxy-2(5H)-furanone*. The Journal of Organic Chemistry, 1991. **56**(25): p. 7007-7014.
45. Gollnick, K. and A. Griesbeck, *Singlet oxygen photooxygenation of furans: Isolation and reactions of (4+2)-cycloaddition products (unsaturated sec.-ozonides)*. Tetrahedron, 1985. **41**(11): p. 2057-2068.
46. Montagnon, T., et al., *Furans and singlet oxygen - why there is more to come from this powerful partnership*. Chemical Communications, 2014. **50**(98): p. 15480-15498.